EFFECT OF HIGH CHLORIDE CONCENTRATIONS ON CAST IRON CORROSION AND WATER QUALITY IN DRINKING WATER DISTRIBUTION SYSTEMS

by

Masoumeh Sharafimasooleh

Submitted in partial fulfilment of the requirements
for the degree of Doctor of Philosophy

at

Dalhousie University
Halifax, Nova Scotia
November 2016

I would like to dedicate my thesis to my beloved father and grandparents

Table of Contents

List of Tables

List of Figures

Abstract

Chloride can be present in drinking water from various sources including treatment practices for natural organic matter (NOM) removal, saltwater intrusion, run-off from deicing salt, and use of desalinated water. The purpose of this research was to examine the impacts of variable chloride concentrations on disinfection efficacy and microbial regrowth, iron corrosion and its release from iron surfaces, and effectiveness of different corrosion control strategies in chlorinated drinking water distribution systems. Additionally, the characteristics of resulting iron corrosion products and bacterial biofilm communities were investigated. Results showed that elevated chloride concentrations did not have a significant impact on microbial regrowth in terms of bulk or biofilm HPCs, and higher chlorine dosages were required to achieve target free chlorine residuals in high chloride systems. It was observed that in the presence of high chloride concentrations more crystalline and porous scales, which are less protective against corrosion, were formed on the surface of cast iron coupons that promoted the iron corrosion and release. Moreover, larger iron particles were formed, which can resuspend in flowing water and cause water discoloration. Investigations into the effect of variable chloride concentrations on effectiveness of different corrosion control strategies suggested that elevated chloride concentrations interfered with inhibiting action of the corrosion control strategies and reduced their effectiveness. Finally, results showed that bacterial biofilm population decreased with chlorination and increasing chloride concentrations, and were unlikely to contribute to the observed increased corrosion rates in cast iron systems under the conditions tested in this experiment.

List of Abbreviations and Symbols Used

°C	degree Celsius
AERs	anionic exchange resins
ANOVA	analysis of variance
AO	aesthetic objective
ARs	annular reactors
CFU	colony forming unit per
Cl^-	Chloride
Cl_2	Chlorine
cm	Centimeter
DOC	dissolved organic carbon
Fe^0	elemental iron
Fe^{2+}	ferrous ions
Fe^{3+}	ferric ions
GAC	granular activated carbon
h	Hour
HClO	hypochlorous acid
HPC	heterotrophic plate count
HRT	hydraulic retention time
ICP-MS	inductively coupled plasma-mass spectrometry
IOB	iron-oxidizing bacteria
IRB	iron-reducing bacteria
m/s	meter per second
MFI™	micro-flow imaging
mg/L	milligrams per liter
min	Minute
mL	Milliliter
mL/min	milliliter per minute
mm	Millimeter
mV	Millivolt

NaCl	sodium chloride
$NaHCO_3$	sodium bicarbonate
NaOCl	sodium hypochlorite
NaOH	sodium hydroxide
NOM	natural organic matter
NRB	nitrate-reducing bacteria
NTU	nephelometric turbidity units
OCl^-	hypochlorite ion
OTU	operational taxonomic units
PBS	phosphate buffered saline
PCoA	principal coordinate analysis
SEM	scanning electron microscope
SOB	sulfate-oxidizing bacteria
SRB	sulfate-reducing bacteria
TOC	total organic carbon
XRD	X-day diffractometer
USEPA	United States Environmental Protection Agency
WHO	World Health Organization
μm	Micrometer

Acknowledgements

Firstly, I would like to gratefully acknowledge the financial support of the National Sciences and Engineering Research Council of Canada (NSERC) and the A.D. Foulis Chair in Engineering program at Acadia University. I would also like to thank my supervisors, Dr. Margaret Walsh and Dr. Jennie Rand, for their support and advice over the years. To my committee members, Dr. Graham Gagnon and Dr. Lisbeth Truelstrup Hansen, thank you for your time and participation in my thesis development.

I would like to thank Heather Daurie, Elliot Wright, Andrew George and also Dalhousie technicians (Blair, Brian, Jesse and Dean) for assistance with laboratory work. This work would not be possible without their support. And a special thanks to June and Tarra for keeping paperwork and deadlines in check on stressful days.

Additionally, a big thank you to my lab mates and of course my friends Allison, Jess, Yannan, Wenwen, Monica, Lindsay, Ben, Yamuna, Amina, John Sarah Jane and Dallys who also helped me with the lab work and their advice, support and suggestions when requested.

I would also like to thank my sister for encouraging me to fulfill my dreams and cheering for me through my success. And last but certainly not least, to my mom, thank you so much for always supporting me and always being there for me. I would not be where I am today without your help and support.

Chapter 1 Introduction

1.1 Perspective

Cast iron corrosion in drinking water distribution systems is an important issue for many water utilities as iron corrosion is prevalent and can cause many problems such as water losses, increased headloss, leaks and deterioration in water quality, among other issues (McNeill and Edwards 2001). Iron pipes have been used for more than 500 years and account for a large percentage of current drinking water distribution system infrastructures and will be still in use for many years while utilities await costly upgrades (InfraGuide 2001). Moreover, other researchers (Deshommes et al. 2010, Trueman and Gagnon 2016) have shown that iron corrosion products are inextricably linked to lead in distribution systems, making this research even more important in the context of water utilities trying to prevent lead contamination of water supplies.

Changes in source water availability and treatment practices can lead to the presence of elevated levels of chloride in drinking water. This can occur due to removal of natural organic matter (NOM) through enhanced coagulation (Shi and Taylor 2007) or anionic exchange resins (Ishii and Boyer 2011, Willison and Boyer 2012), salt-water intrusion (Essink 2001), run-off from road application of deicing salts (Thunqvist 2004), or the use of desalinated source water (Greenlee et al. 2009). High levels of chloride in drinking water have been shown to increase corrosion of iron and its release to the water, and also to decrease disinfection efficacy leading to microbial regrowth. Previous research has shown that an increase in chloride concentration accelerates the corrosion of cast iron (Crittenden et al. 2012). As a result of the reactions between free chlorine and iron corrosion products in distribution systems, higher doses of free chlorine are required to maintain target free

chlorine residuals (Frateur et al. 1999, Hallam et al. 2002, Mutoti et al. 2007, Rand et al. 2013). Moreover, in the presence of high chloride concentrations, crystalline porous corrosion scales are formed, which are less corrosion protective and result in release of larger iron particles in the bulk water (Liu et al. 2013), resulting in colored water. The formation of iron oxides such as lepidocrocite, which are less stable against reduction (more prone to dissolution), has been shown to be promoted by chloride ions, thereby enhancing dissolution of the corrosion scale and leading to higher iron release (Taylor 1984, Sarin et al. 2004b, Liu et al. 2013).

In North America, drinking water is customarily chlorinated to control bacterial regrowth in drinking water distribution systems. It is widely accepted in the literature that chlorine disinfection residuals impact iron corrosion rates and the structure, composition and morphology of corrosion scales. When present in the bulk water, chlorine oxidizes the dissolved iron (Fe^{2+}) released to the water to ferric iron particles (Fe^{3+}), which impart color to the water and/or form corrosion scale (McNeill and Edwards 2001, Eisnor and Gagnon 2004, Wang et al. 2012). To the author's knowledge, to date, no research has been conducted to investigate the potential combined impacts of variable chloride concentrations and chlorine residuals on iron corrosion and the properties of the iron particles released to the bulk water. There is also a paucity of information in published literature that has examined the potential effects of high concentrations of chloride on disinfection efficacy to inactivate microorganisms and control biofilm formation, and also the effects on disinfection demand in the distribution system in presence of different pipe materials.

Colored water problems can be reduced by controlling corrosion, the properties of the iron particles and iron release from corrosion scales (Lytle et al. 2005). Corrosion and/or metal release in drinking water distribution systems may be controlled by common approaches: addition of a corrosion inhibitor, pH adjustment and alkalinity addition. Some researchers investigated the effects of control measures on iron release with blending of different water sources containing high chloride concentrations (Lytle et al. 2005, Alshehri et al. 2009, Zhang et al. 2014, Mi et al. 2016). However, little information is available about the mechanism of impact of variable chloride concentrations on effectiveness of the corrosion control practices. In addition, understanding of the mechanism of impact of corrosion inhibitors on the properties of the iron corrosion products and iron suspensions in presence of high chloride concentration is lacking.

Bacterial biofilm communities are widely found in drinking water distribution systems and their size and diversity depend on numerous factors including physiochemical properties of pipe materials, location and the water quality (nutrients, chlorine levels, pH, temperature, etc.) (Liu et al. 2012, Sun et al. 2014). Establishment of microbial biofilms has been shown to affect the corrosion of cast iron pipes in distribution systems (Teng et al. 2008, Zhu et al. 2014, Wang et al. 2015, Li et al. 2016). The role of microbes in corrosion processes is complex, because they can either enhance or inhibit corrosion (Sun et al. 2014, Zhu et al. 2014). To date, there have been no reports studying the potential for microbial biofilms contribute to the corrosion of cast iron in drinking water distribution systems exposed to elevated chloride levels and chlorination. In addition, there is a paucity of information in published literature on biofilm population responds to corrosion control

strategies, such as orthophosphate addition and pH adjustment, in the presence of variable chloride concentrations in chlorinated systems.

1.2 Research Hypotheses and Objectives

The main hypothesis of this research project was that elevated concentrations of chloride in drinking water distribution systems would increase corrosion and iron release in cast iron distribution systems, resulting in reduced disinfection efficacy in the distribution system, and interfere with inhibiting action of the corrosion control strategies, reducing their effectiveness. This hypothesis was tested through the completion of the objectives of this research project, which encompass areas of disinfection, microbial regrowth and corrosion of cast iron pipes in distribution systems, as outlined below.

1. To determine if elevated concentrations of chloride in finished water have negative effects on disinfection efficacy and microbial regrowth in drinking water distribution systems.
2. To examine the effect of variable chloride concentrations on iron corrosion and its release from corroding iron surfaces in chlorinated systems, and to investigate the structures and morphologies of resulting iron corrosion products.
3. To examine the size and characteristics of bacterial biofilm communities formed under different chloride and chlorine concentrations to determine if the microbes contributed to the corrosion of cast iron under the conditions tested in this research.
4. To evaluate the influence of common corrosion control strategies (orthophosphate addition and pH adjustment) on iron corrosion and release from cast iron surfaces in the presence of high chloride concentrations in chlorinated systems. An

additional goal was to investigate how biofilm population responds to these two corrosion control strategies in the presence of variable chloride concentrations in chlorinated systems.

5. To test whether common corrosion control strategies can counteract the possible corrosive effect of high chloride concentrations on iron release from corroded cast iron pipes in drinking water distribution systems.

1.3 Organization of Thesis

In order to present the research outcomes according to the five research objectives outlined above, the thesis was organized in the following chapters. The main chapters (Chapters 3 through 6) of this thesis are prearranged and formatted with the purpose of being submitted for possible publication in the refereed journals. Thus, these chapters contain their own abstract, introduction, materials and methods, results and discussion, and conclusion.

Chapter 1 describes the research perspective, research hypotheses and objectives, and the organization of the thesis. Background information on chemistry of corrosion, corrosion scale formation and structure, and factors influencing iron corrosion and release in distribution system can be found in Chapter 2. Chapter 3 outlines the results of annular reactor (AR) studies designed to identify the effects of variable concentrations of chloride on microbial regrowth, disinfection efficacy, and metal release in drinking water distribution systems. Chapter 4 reports the findings from an 8-week bench scale study examining the combined effect of high chloride concentrations and free chlorine residuals on iron corrosion and the release and characteristics of corrosion products from corroding iron surfaces. Chapter 5 details the results of an 8-week bench scale study that examined

the effectiveness of different corrosion control strategies on iron corrosion and release in chlorinated distribution systems in presence of variable chloride concentrations. Chapter 6 presents the results of a 4-month bench-scale study using a fill and dump procedure on the effectiveness of common corrosion control strategies on iron release from corroded cast iron pipes in presence of high concentrations of chloride. Chapter 7 summarizes the findings of this research, details the main conclusions of the thesis, and provides recommendations for future work.

Chapter 2 Review of the Literature

2.1 Iron Corrosion and Release in Water Distribution Systems

2.1.1 Changes to Iron Pipe

Cast iron corrosion in drinking water distribution systems can cause many problems including reduced lifetime of the pipe, leaks, catastrophic failure and scale buildup (McNeill and Edwards 2001, Sarin et al. 2004b, Benson et al. 2012). The formation of corrosion scale deposits can increase the head loss and reduce the hydraulic capacity of the pipe. As a result, a greater amount of energy is required to deliver water at a desired flow rate, resulting in higher pumping costs. Localized corrosion cause ruptures in the pipe, and can lead to losses in delivered water and pipe failure, which also requires costly pipe replacements.

2.1.2 Aesthetic Effects

Iron corrosion will deteriorate water quality during distribution (Zhang et al. 2014, Mi et al. 2016). The secondary drinking water guideline for iron is recommended as 0.3 mg/L by the U.S. Environmental Protection Agency (U.S. EPA 2008). The Canadian drinking water quality guideline for iron is an Aesthetic Objective (AO) of less than or equal to 0.3 mg/L (Health Canada 2014). Iron concentrations greater than 0.3 mg/L in drinking water can result in unpleasant metallic taste and rusty color. Water discoloration (red water) due to iron corrosion is the largest cause of consumer complaints (Husband and Boxall 2011). Red water events occur when iron corrosion particles are released to the bulk water. In addition to an unpleasant appearance, red water creates stains in sinks, fixtures, laundry and toilets.

2.1.3 Health Effects

The presence of iron in drinking water poses no direct threat to human health, so no primary drinking water standard has been established for iron in drinking water (Health Canada 2014). However, there are some significant health concerns that are related to iron corrosion in drinking water distribution systems. Iron corrosion has been shown to result in disinfectant loss (Al-Jasser 2007, Zhang et al. 2008, Sharafimasooleh et al. 2015) and promote harmful bacterial re-growth (McNeill and Edwards 2001, Chowdhury 2012). Additionally, corrosion of iron pipe can cause adsorption and release of toxic trace metals such as lead and arsenic, which can cause adverse health effects (Lytle et al. 2010, Peng and Korshin 2011, Trueman and Gagnon 2016).

Consequently, the use of cast iron pipes in drinking water distribution systems is prohibited in many developed countries. However, cast iron pipes have been used for more than 500 years to transport drinking water (Gedge 1993) and comprise a large percentage of current drinking water distribution system infrastructures. Cast iron and ductile iron pipes account for more than two-thirds of the existing water mains in use across Canada (InfraGuide 2001). Thus, iron pipes will still be in use for many years and research about associated corrosion and the physicochemical characteristics and performances of corrosion scales formed under different water quality conditions is of great importance.

2.2 Iron Corrosion

2.2.1 Iron Oxidation and Chemistry of Corrosion

Corrosion of cast iron in drinking water distribution systems is a complex phenomenon involving a series of electrochemical processes that results from chemistry at the interface between the water and the pipe wall, as well as the physical/mechanical characteristics of flow through the pipe. On the pipe surface, at an anodic site, the elemental iron (Fe^0) converts to ferrous iron (Fe^{2+}), releasing two electrons (oxidation), as shown in Equation 2.1.

$$Fe^0 \leftrightarrow Fe^{2+} + 2e^- \quad (2.1)$$

The released electrons travel through the internal circuit (pipe wall) to a site which acts as the cathode. At the cathode, the most common reaction in distribution systems is the acceptance of electrons by an electron acceptor (reduction). The most common electron acceptors are oxygen and chlorine in distribution systems. The typical reactions happening at the cathode are simply expressed in Equations 2.2 and 2.3.

$$\frac{1}{2}O_2 + 2H^+ + 2e^- \leftrightarrow H_2O \quad (2.2)$$

$$HClO + H^+ + 2e^- \leftrightarrow Cl^- + H_2O \quad (2.3)$$

The Fe^{2+} ions produced by the corrosion reaction are released to the water and are ready to react with the chemicals present in the water. A number of competing oxidation and precipitation reactions can occur with Fe^{2+} ions. The simplified overall redox reactions for

the conversion of Fe^{2+} to Fe^{3+} in presence of oxygen (Equation 2.4) and chlorine (Equation 2.5 and 2.6) are given below (McNeill and Edwards 2000, Lytle et al. 2004, Rahman and Gagnon 2014).

$$4Fe^{2+} + O_2 + 10H_2O \rightarrow 4Fe(OH)_3 + 8H^+ \quad (2.4)$$

$$2\mathrm{Fe}^{2+} + \mathrm{HClO} + 5H_2\mathrm{O} \rightarrow 2\mathrm{Fe}(OH)_3 + \mathrm{Cl}^- + 5H^+ \quad (2.5)$$

$$6\mathrm{Fe}^{2+} + 3\mathrm{ClO}^- + 3\mathrm{H_2O} \rightarrow 2\mathrm{Fe(OH)_3} + 4\mathrm{Fe}^{3+} + 3\mathrm{Cl}^- \quad (2.6)$$

The reaction of chlorine with Fe^{2+} is pH-dependent. Chlorine rapidly hydrolyzes in water to form hypochlorous acid (HClO), which in turn forms hypochlorite ion (OCl^-) (Droste 1997). Between pH 6.5 and 8.5, the dissociation reaction is incomplete, and both hypochlorous acid and hypochlorite ion are present as the primary oxidizing agents in water, although hypochlorite has a lower oxidizing potential. Below a pH of approximately 7.6, HClO dominates and at pH levels above 7.6, chlorine primarily occurs in the form of OCl^- (Water 2009).

Oxidized Fe^{2+} ions (Fe^{3+}) form particles because of their low solubility and subsequently contribute to color and turbidity in water. They may also deposit on the metal surface as corrosion scale. Iron corrosion scales may also dissolve and contribute to the amount of iron release (Sarin et al. 2004a, Lytle et al. 2004, Benson et al. 2012).

2.2.2 Iron Corrosion Scale Formation and Structure

Ferric particles resulting from oxidation of ferrous ions may deposit on the metal surface

as corrosion scale. The corrosion deposits may also dissolve and contribute to the amount of iron release (Sarin et al. 2004a, Lytle et al. 2004, Benson et al. 2012). It should be noted that exact composition and structure of iron corrosion scales in distribution system pipes depends on several factors including water quality parameters, fluctuations of water temperature in different seasons, and water flow patterns (McNeill and Edwards, 2001, Chun et al. 2005). According to previous studies, different corrosion products are formed on iron surfaces under different conditions. Typical iron corrosion products found in iron corrosion scales include goethite (α-FeOOH), lepidocrocite (γ-FeOOH), magnetite (Fe_3O_4), maghemite (α-Fe_2O_3), hematite (Fe_2O_3), ferrous hydroxide ($Fe(OH)_2$), ferric hydroxide ($Fe(OH)_3$), ferrihydrite ($5Fe_2O_3.9H_2O$), siderite ($FeCO_3$) and calcite ($CaCO_3$) (McNeill and Edwards 2001, Sarin et al. 2004b, Wang et al. 2012).

The iron corrosion scales formed on old iron surfaces have a complex morphology consisting of: (1) a corroded floor, (2) a porous interior, (3) a dense shell-like layer and (4) a top surface layer (Sarin et al. 2001, Sarin et al. 2004b, Lytle et al. 2005, Benson et al. 2012). The corroded floor is the corroded metal surface beneath the corrosion scale. This is the source of iron that is present in the corrosion scales. The porous interior of the scale is made up of different morphologies and structures. Study conducted by Sarin et al. (2001) showed the presence of a high concentration of ferrous iron in this region of the scale, which is present either as solids, or as dissolved iron in water inside the scale pores and cavities. As corrosion continues and scale is grown, a dense shell-like layer is covers the porous interior of the corrosion scale. Previous studies conducted by Sarin et al. (2001, 2004b) showed that the shell-like layer is predominantly composed of oxidized species

such as magnetite and goethite. This layer prevents flow of oxidants to the pipe surface, and separates them from the oxidizable ferrous ions and solids inside the scale. However, ions may continue to pass through the shell-like layer to maintain electroneutrality. On the top of shell-like layer (at the scale-water interface), particles are loosely held as a layer, which is in contact with the water and is greatly influenced by water quality. Portions of this layer can be transported to the bulk water by hydraulic and turbulent flows causing turbid and colored water. Iron oxides such as lepidocrocite and amorphous ferric hydroxide as well as the precipitates of silicates, phosphates and carbonates may be present in this layer (Sarin et al. 2001).

Although the formation of corrosion scale on the surface of the pipe can increase the corrosion resistance in the water distribution system by creating a barrier between the corrosive water and the metallic surface of the pipe, it serves as a reservoir for corrosion products that can be released into the bulk water. Therefore, it is important to understand the difference between the corrosion and the iron release in the water supply. Corrosion of iron is the conversion of "metallic iron" to an oxidized form, either soluble or an oxidized scale, which is usually measured as weight loss from metallic iron. However, iron release is the transport of iron, in soluble form or as a particle, from corrosion scale or metal to bulk water. In the absence of corrosion scales on the surface of the pipe (i.e. new pipes), corrosion of iron is the primary cause of iron release. However, with old corroded pipes, metal surfaces are covered with corrosion scales, which have an important impact on metal release. Factors influencing iron release are derived from a wide variety of issues

associated with water chemistry, biological processes, composition of pipe scale, and the hydraulic flow characteristics within the pipe.

2.3 Factors Influencing Iron Corrosion and Release

2.3.1 Water Quality Parameters

The following summarizes the impacts of different water chemistry parameters on iron corrosion and release that are relevant to this thesis.

2.3.1.1 Chloride Concentration

The presence of chloride in drinking water can be attributed to various sources including treatment practices for natural organic matter (NOM) removal, saltwater intrusion, run off from deicing salt, and use of desalinated water.

The presence of NOM in drinking water can cause color, taste, and odor issues as well as biological regrowth (Van der Kooij 2003), and formation of disinfection by-products (DBPs) in the presence of chlorine (Bursill 2001, Hwang et al. 2002). As a result, removing NOM from water is an important requirement to improve drinking water quality. Enhanced coagulation, which is used to remove turbidity and NOM from water, introduces chlorides and sulfates to the treated water. In their research, Shi and Taylor (2007) quantified chloride concentrations in the range of 37 to 69 mg/L in enhanced coagulation treated waters and concluded that the high corrosivity of the finished water could cause iron release and corrosion in a distribution system.

Ion exchange processes with anionic exchange resins (AERs) have also been demonstrated to be an effective treatment approach for removing NOM from surface water (Heijman et al. 1999, Bolto et al. 2002, Anderson and Walsh 2012). With AER processes, chloride (Cl^-) counter ions are displaced from the surface of AERs and exchange with anionic NOM species in the water to occupy the active site of the resin (Boyer and Singer 2007). As a result, the concentration of NOM decreases and the concentration of chloride increases in the treated water. Previous studies that have evaluated AER treatment have shown variable chloride concentrations in AER-treated waters. The final chloride concentration after AER treatment depends on many factors, such as the initial concentration of chloride and NOM in the raw water. Chloride concentrations of 50 mg/L (Willison and Boyer 2012) and 65 mg/L (Ishii and Boyer 2011) have been reported in studies of AER-treated water.

In coastal zones, freshwater aquifers are threatened by intrusion of saline water, which can lead to contamination of drinking water sources and increases in chloride concentration (Essink 2001). A geological survey in the U.S. state of Florida showed that resulting chloride concentrations from saltwater intrusion could range from 30 to 480 mg/L (Spechler 1994). Salt that is used to melt ice and snow on roadways can also contribute to increased chloride concentrations in ground and surface water through infiltration of runoff from roadways (Thunqvist 2004, Novotny et al. 2008, U.S. EPA 2010). The typical chloride concentrations resulting from deicing of roads have been reported in the range of 16 to 5,000 mg/L in different regions depending on the season.

Another source of high chloride concentration is the use of desalinated water. In some regions of the world, diminishing fresh water source supplies has increased the demand for development of saltwater desalination technology for potable water production. Desalination is the process of removing salt from water to produce fresh water containing less than 1,000 mg/L of salts (Reuter 2000, Greenlee et al. 2009).

The aesthetic objective (AO) for chloride concentrations outlined in the Canadian Drinking Water Quality Guidelines (Health Canada 2014) is 250 mg/L. Chloride concentrations can influence corrosion and chemical composition and structure of iron corrosion scales. Previous studies have shown that an increase in the concentration of chloride accelerates the corrosion of cast iron and its release to the water (Shi and Taylor 2007, Crittenden et al. 2012, Willison and Boyer 2012, Sharafimasooleh et al. 2015). Shi and Taylor (2007) investigated the potential impacts of adopting enhanced coagulation on water quality in distribution systems through a field investigation using pilot-scale water treatment and distribution systems. That study found higher iron release in finished waters with higher chloride concentrations (e.g., 68.5 mg/L). A study conducted by Willison and Boyer (2012) indicated that changes in chloride, sulfate, and NOM concentrations could impact the corrosion of water distribution systems that are dominated by iron-based pipes and corrosion scales. However, the main focus of that study was on lead release from pipes in the distribution system. A recent study by Liu et al. (2013) investigated the effects of blending desalinated water (chloride concentration = 157 mg/L) with conventionally-treated surface water on iron corrosion. The authors concluded that higher blend fractions

of desalinated water were associated with more fragile corroding surfaces, lower retention of iron oxidation products, and release of larger iron particles in the bulk water.

In the presence of high chloride concentrations, porous corrosion scales with more crystalline morphology are formed, which are less corrosion protective and result in increasing release of larger iron particles in the bulk water (Liu et al. 2013). In addition, chloride ions promote formation of iron oxides (i.e., lepidocrocite) that are less stable against reduction, thereby promoting dissolution of the corrosion scale and higher iron release (Taylor 1984, Sarin et al. 2004b, Liu et al. 2013). High concentrations of chloride could diffuse and damage the dense shell-like layer of iron scale on old pipes, thereby increase the iron release. The porous interior of the corrosion scale serves as a reservoir for ferrous iron ions, which attract negative ions of chloride (Cl^-) from the bulk water to maintain electroneutrality and to complete the electrical circuit of the corrosion cell (Burlingame et al. 2006). Therefore, the rate of chloride diffusion to the porous interior increases with an increase in chloride concentration, resulting in an increase in acidity of the solution inside the porous interior that promotes ferrous iron production and its release. On the other hand, an increase in ferrous iron in the porous interior will drive the penetration of iron from the pipe surface into the bulk water and break down the dense shell-like layer, thereby resulting in an increase in iron release.

2.3.1.2 Free Chlorine

Chlorine is the most commonly used disinfectant in North America to control bacterial regrowth in drinking water distribution systems. Free chlorine concentrations in most

Canadian drinking water distribution systems range from 0.04 to 2.0 mg/L (Health Canada, 2014). It is well established that due to the reaction of free chlorine with iron corrosion products in distribution systems, higher doses of free chlorine are required to maintain target free chlorine residuals (Frateur et al. 1999, Hallam et al. 2002, Sarin et. al. 2004 a, b, Mutoti et al. 2007, Rand et al. 2013, Sharafimasooleh et al. 2015).

Generally, disinfectant residuals increase corrosion rates (McNeill and Edwards 2001). As highly electron acceptors (oxidizing agents), disinfectant residuals react with the iron surface and accelerate the corrosion rate. The rate of this reaction may also be increased by the presence of chloride ion (Le Puil et al.). Eisnor and Gagnon (2004) examined the impact of secondary disinfection on corrosion using free chlorine, chloramine, chlorine dioxide and chlorite. The results of their research suggested that chlorite had the lowest corrosion rate followed by chlorine dioxide, free chlorine and monochloramine. However, the effects of adding chlorine does not always result in increased corrosion. Zhang and Edwards (2007) showed that the presence of free chlorine decreased iron release to water and corrosion rate relative to the same condition without disinfectant. Wang et al. (2012) concluded that formation of a dense oxide layer on the surface of iron coupons inhibited iron corrosion, causing stable lower chlorine decay. In corroded iron pipes (when corrosion scales are present), chlorine oxidizes the dissolved iron (Fe^{2+}) content of the scale to less soluble Fe^{3+} forms and precipitates the ferric phases within the scale. This in turn makes the scales denser and less permeable to Fe^{2+} diffusion. However, the effect of chlorine on corrosion of pipe metal or the iron release rate will depend on the corrosion scale characteristics. A highly porous scale would be least protective towards corrosion of the

underlying pipe metal, and at higher concentrations of chlorine, higher iron release may be observed. In agreement with the model proposed by Sarin et al. (2004b), the migration of negative ions of chloride (Cl^-) from bulk water to maintain electroneutrality, which was discussed earlier, increases the porosity of the corrosion scale. As a result, it would be easier for chlorine to diffuse to the metal surface, thereby promoting dissolution of the metal and higher corrosion rates. It should be mentioned that stagnation of water leads to rapid depletion of oxidants next to the scale and produces reducing conditions at the outer layer of the scale, favoring dissolution of the outer scale layer and formation of soluble ferrous species. This provides for greater opportunity for iron release (Sarin et al. 2004a, Burlingame et al. 2006).

2.3.1.3 Dissolved Oxygen (DO)

The effect of dissolved oxygen on iron corrosion and release depends on the characteristics of the iron corrosion scale formed. If scale is highly porous, dissolved oxygen would readily react with metal iron causing the release of ferrous ions into solution. However, if the scale is dense, oxygen is consumed both in the corrosion reaction of the iron metal and in the oxidation of the Fe^{2+} into Fe^{3+} that may then precipitate and make the scale denser and less permeable to ferrous iron diffusion. Then, higher dissolved oxygen concentrations supplied by flowing water may decrease iron release in old established scales compared to stagnant conditions.

2.3.1.3 pH

Raising the water pH protects pipes by decreasing the solubility of pipe materials and

corrosion products, thereby decreasing the corrosion rate and metal concentrations at the tap (Maddison et al. 2001, Zhang et al. 2014, Mi et al. 2016). Previous studies (Lasheen et al. 2008) showed that in pH values less than 5 iron corrodes rapidly, while pH values higher than 9 may decrease corrosion rates. Sarin et al. (2003) reported that increasing pH from 7.6 to 9.5 could reduce the amount of iron released to water from more than 1.5 mg/L to less than 0.3 mg/L over a period of few months. They suggested that an increase in pH decreases the solubility of ferrous solids (ferrous hydroxide and siderite) in the scale, thereby reducing the amount of iron release. It has also been proposed that more porous ferrous phases form at lower pH, whereas a higher pH results in formation of denser ferric phases, which are less likely to dissolve, and if precipitated in the scale can make the scale less porous. Formation of a denser scale structure limits the rate of migration of ions through the scales, and thereby lowers the corrosion rate and iron release rate (Sarin et al. 2003, Sarin et al. 2004b).

Investigation of the effect of pH adjustment on iron release and properties of the iron suspensions revealed that stability of the iron suspensions increased as pH of the solutions increased (Lytle et al. 2004).

2.3.1.4 Alkalinity

Increasing alkalinity generally decreases iron corrosion and release. Experiments conducted by Imran et al. (2005) at a pilot water distribution system in Tampa, Florida, revealed that alkalinity has a strong negative correlation to increase in iron release in old iron pipes. This study concluded that maintaining the alkalinity concentration above 80

mg/L as $CaCO_3$ is the most important individual parameter for preventing the release of metal ions to the water. Another study (Sarin et al. 2003) revealed that decreasing the alkalinity from 30–35 mg/L as $CaCO_3$ to 10–15 mg/L as $CaCO_3$ under constant pH led to an immediate increase in iron release (50-250%). Iron release decreased back to original values upon raising alkalinity to initial values. It is suggested that the link between alkalinity and iron release is related to the dissolution of carbonate containing iron phases such as siderite ($FeCO_3$) within the scale. Lower iron corrosion rates and iron concentrations in distribution systems have been associated with higher alkalinity due to the formation of the less soluble siderite species (Sarin et al., 2003).

Higher alkalinity in the water also may minimize pH variations due to its higher buffer capacity. Minimization of local pH variations has been shown to promote formation of a denser scale structure on the surface of the pipe, thereby decreasing the release of iron and the chance for red water events to occur (Sarin et al. 2004b, Imran et al. 2005).

2.3.2 Phosphate-Based Corrosion Inhibitors

The addition of phosphate-based chemicals has been reported to be effective in controlling iron corrosion and release. Phosphate-based corrosion inhibitors can be dosed as either orthophosphoric acid, combinations of orthophosphoric acid and zinc orthophosphate, polyphosphates, or blends of orthophosphoric acid and polyphosphate. Orthophosphate inhibitors promote the formation of a protective impervious layer on the surface of cast iron, thereby making it more difficult for ferrous iron species to diffuse out of the scale and for anions (e.g. chloride ions) to diffuse into the core of the scale in order to maintain

electroneutrality. In addition, orthophosphate likely plays a secondary role as an anodic inhibitor by inducing formation of iron phosphate solids that precipitate and cover the corrosive sites in the iron oxide film, thereby reducing corrosion and iron release (Maddison et al. 2001, Lytle and Snoeyink 2002, Sarin et al. 2003, Lytle et al. 2005, Alshehri et al. 2009, Mi et al. 2016). Formation of iron phosphate precipitates can also decrease the permeability of the scale and reduce the solubility of ferrous iron, and thus decrease iron release (Singley 1994, Sarin et al. 2004b, Ebrahimi Mehr et al. 2004, Lytle et al. 2005, Zhang et al. 2014). However, there are contradictory results of research efforts. Studies conducted by McNeill and Edwards (2000), and Zhang and Andrews (2011) showed that addition of phosphate-based corrosion inhibitors has no effect or a detrimental effect on iron release under stagnant and low flow conditions. However, polyphosphates have a different mode of action. Polyphosphates are strong chelating agents which actually reduce scaling and have been shown to be effective in sequestrating Fe^{2+} ions to treat "red water" (Maddison et al. 2001).

Previous studies (Lytle and Snoeyink 2002, Lytle et al. 2005, Rahman and Gagnon 2014) also evaluated the effects of phosphate-based corrosion inhibitors on iron release and properties of the iron suspensions. They concluded that phosphate changed the properties of iron particles and reduced color and turbidity of the resulting iron suspensions.

2.3.3 Microbial Induced Corrosion

Bacterial biofilm communities are widely found in drinking water distribution systems, where the size and diversity of the microbial community depend on numerous factors

including physiochemical properties of pipe materials, location and the water quality (nutrients, chlorine levels, temperature, etc.) (Liu et al. 2012, Sun et al. 2014). Establishment of microbial biofilms has been shown to affect the corrosion of cast iron pipes in distribution systems (Teng et al. 2008, Zhu et al. 2014, Wang et al. 2015, Li et al. 2016). The role of microbes in corrosion processes is complex, because they can either enhance or inhibit corrosion by influencing the chemical cathodic and/or anodic corrosion reactions and thereby modifying the corrosion products (Sun et al. 2014, Zhu et al. 2014). Microbes can enhance corrosion by two main processes. Firstly, their growth on the surface of the pipe can create regions of differing dissolved oxygen, hydrogen ion, and metal ion concentrations, which leads to localized concentration cell corrosion. Moreover, microbes can be responsible for redox reactions that directly affect corrosion. Microorganisms affecting iron corrosion include sulfate-reducing bacteria (SRB), sulfur-oxidizing bacteria (SOB), iron-reducing bacteria (IRB), iron-oxidizing bacteria (IOB), nitrate-reducing bacteria (NRB), and bacteria producing organic acids and slime (Wang et al. 2012, Sun et al. 2014, Zhu et al. 2014). These microorganisms affect corrosion reactions and corrosion scale formation directly or indirectly by converting Fe^{2+} to Fe^{3+}, Fe^{3+} to Fe^{2+}, sulfate to sulfite, sulfite to thiosulfate, thiosulfate to sulfide, sulfite to sulfate, and also nitrification and denitrification.

2.3.4 Hydraulics

The flow regime within a pipe affects iron release under either stagnant or turbulent flow. Low flow, dead-end, and stagnant conditions lead to rapid depletion of oxidants (e.g. oxygen and free chlorine) in the bulk water and next to the scale, which produce reducing

conditions at the outer layer of the scale and favor formation of ferrous species. This provides greater opportunity for iron release via dissolution of the outer layer of the corrosion scale. In addition, the lack of a dense layer on the corrosion scale provides no barrier for the migration of ferrous species from the porous core of the scale to the bulk water (Sarin et al. 2004b, Lytle et al. 2005, Burlingame et al. 2006, Benson et al. 2012). The ferrous species can be oxidized if mixed with oxidant-rich waters and result in red water. Under flow conditions with maintained dissolved oxygen or chlorine residual, the released ferrous species from the interior of the scale are oxidized and form the denser layer at the surface of the scale. High flow conditions may increase the corrosion rate of pipes by continually supplying oxidants to the pipe surface; however, after a mature scale is developed on the surface of the pipe, the constant supply of oxidants enhances the formation and development of denser protective scale. If the flow is very high, the water can scour away the protective scale (McNeill and Edwards 2001, Benson et al. 2012).

Chapter 3 Effect of High Chloride Concentrations on Microbial Regrowth in Drinking Water Distribution Systems

3.1 Abstract

High levels of chloride can be present in drinking water from various sources, while some potential downstream consequences may be unknown. This study was designed to identify the effects of variable concentrations of chloride on microbial regrowth, disinfection efficacy, and metal release in drinking water distribution systems. Annular reactors (ARs) containing cast iron or polycarbonate coupons were operated in this research to simulate distribution systems. Experiments were conducted with test water containing chloride concentrations of 10 and 75 mg/L. Chlorine disinfection was applied to achieve 0.2 and 1.0 mg/L free chlorine residuals. Another experiment was repeated with ARs containing cast iron coupons at chloride concentration of 250 mg/L. Results showed that the ARs operated with chloride concentration of 75 mg/L were not significantly different from the ARs operated with chloride concentration of 10 mg/L in terms of microbial regrowth. Higher chlorine doses were required to achieve goal residuals for those ARs with chloride concentration of 75 mg/L compared to ARs with chloride concentration of 10 mg/L in cast iron systems. However, in polycarbonate systems, similar doses of chlorine were required to achieve the target free chlorine residual in ARs operated with either chloride concentration. The results also showed that higher total iron concentration spikes were observed in the cast iron ARs receiving chloride concentration of 75 mg/L after chlorine disinfection was initiated compared to 10 mg/L chloride. However, total iron concentrations decreased back to the initial levels after a few days. Comparing the results of the

experiments with 75 and 250 mg/L chloride concentrations showed that in the presence of higher chloride concentrations, there was higher iron release in the effluent of the ARs that persisted. Further, more iron release was observed in these ARs at 1.0 mg/L compared to 0.2 mg/L chlorine residual

Keywords: Water distribution, Cast iron, Chlorine disinfection, Iron release, Chloride.

3.2 Introduction

The presence of chloride in drinking water can be attributed to various sources including treatment practices for natural organic matter (NOM) removal, saltwater intrusion, run off from deicing salt, and use of desalinated water.

The presence of NOM in drinking water can cause color, taste, and odor issues as well as biological regrowth (Van der Kooij 2003), and formation of disinfection by-products (DBPs) in presence of chlorine (Bursill 2001, Hwang et al. 2002). As a result, removing NOM from water is an important requirement to improve drinking water quality. Enhanced coagulation, which is used to remove turbidity and NOM from water, introduces chlorides and sulfates to the treated water. In their research, Shi and Taylor (2007) quantified chloride concentrations in the range of 37–69 mg/L in enhanced coagulation treated waters and concluded that the high corrosivity of the finished water could cause iron release and corrosion in a distribution system. Ion exchange processes with anionic exchange resins (AERs) have also been demonstrated to be an effective treatment approach for removing NOM from surface water (Heijman et al. 1999, Bolto et al. 2002, Anderson and Walsh 2012). With AER processes, chloride (Cl^-) counter ions are displaced from the surface of AERs and exchange with anionic NOM species in the water to occupy the active side of

the resin (Boyer and Singer 2007). As a result, the concentration of NOM decreases and the concentration of chloride increases in the treated water. Previous studies that have evaluated AER treatment have shown variable chloride concentrations in AER-treated waters, and the final chloride concentration after AER treatment depends on many factors, such as the initial concentration of chloride and NOM in the raw water. Chloride concentrations of 50 mg/L (Willison and Boyer 2012) and 65 mg/L (Ishii and Boyer 2011) have been reported in studies of AER-treated water. In coastal zones, freshwater aquifers are threatened by intrusion of saline water, which can lead to contamination of drinking water sources and increases in chloride concentration (Essink 2001). A geological survey in the U.S. state of Florida showed that resulting chloride concentrations from saltwater intrusion could range from 30 to 480 mg/L (Spechler 1994). Salt that is used to melt ice and snow on roadways can also contribute to increased chloride concentrations in ground and surface water through infiltration of runoff from roadways (Thunqvist 2004, Novotny et al. 2008, U.S. EPA 2010). The typical chloride concentrations resulting from deicing of roads have been reported in the range of 16–5,000 mg/L in different regions depending on the season. Another source of high chloride concentration is the use of desalinated water. In some regions of the world, diminishing fresh water source supplies has increased the demand for development of saltwater desalination technology for potable water production. Desalination is the process of removing salt from water to produce fresh water containing less than 1,000 mg/L of salts (Reuter 2000, Greenlee et al. 2009). Desalinated water is usually blended with conventionally treated surface water.

In considering the potential for high chloride concentrations from a variety of sources in drinking water, it is important to explore how variable chloride concentrations may impact

disinfection efficacy, microbial regrowth, and chemical water quality in drinking water distribution systems. Previous research has shown that an increase in chloride concentration accelerates the corrosion of cast iron (Crittenden et al. 2012). As a result of the reactions between free chlorine and iron corrosion products in distribution systems, higher doses of free chlorine are required to maintain target free chlorine residuals (Frateur et al. 1999, Hallam et al. 2002, Mutoti et al. 2007, Rand et al. 2013). Shi and Taylor (2007) investigated the potential impacts of adopting enhanced coagulation on water quality in distribution systems through a field investigation using pilot-scale water treatment and distribution systems. That study found higher iron release in finished waters with higher chloride concentrations (e.g., 68.5 mg/L). A study by Willison and Boyer (2012) indicated that changes in chloride, sulfate, and NOM concentrations could impact the corrosion of water distribution systems that are dominated by iron-based pipes and corrosion scales. However, the main focus of that study was on lead release from pipes in the distribution system. A recent study by Liu et al. (2013) investigated the effects of blending desalinated water (chloride concentration = 157 mg/L) with conventionally-treated surface water on iron corrosion. The authors concluded that higher blend fractions of desalinated water were associated with more fragile corroding surfaces, lower retention of iron oxidation products, and release of larger iron particles in the bulk water.

The purpose of this study was to determine if elevated concentrations of chloride in finished water have negative effects on disinfection efficacy, microbial regrowth, and metal release in drinking water distribution systems. Bench-scale annular reactors (ARs) were used to simulate drinking water distribution systems containing cast iron or polycarbonate pipe materials. Microbial regrowth was monitored in each system by collecting bulk and

biofilm heterotrophic plate counts (HPCs) as an indicator of drinking water microbiological quality (U.S. EPA 1989, WHO 2011). HPC constitutes a standard indicator that is easily and widely used by many utilities (Allen et al. 2004, Pavlov et al. 2004). High HPC may indicate some failure in the treatment process (Sartory 2004). Chlorine residual, total iron concentrations, and other standard water-quality parameters (pH, temperature, TOC, alkalinity, and hardness) were also measured in the effluent of each AR on a regular basis.

3.3 Materials and Methods

3.3.1 Model Distribution System

Bench-scale ARs (Model 1120 LS, BioSurface Technologies, Bozeman, Montana) were used as the model distribution system to study disinfection efficacy and microbial regrowth in the presence of elevated chloride concentrations. ARs have been widely used for drinking water research (Camper 1996, Sharp et al. 2001, Ollos et al. 2003, Gagnon et al. 2005, Cantwell 2005, Rand et al. 2007, Wang et al. 2012, Rand et al. 2013, Zhu et al. 2014). Each AR consists of an outer glass cylinder that enfolds an inner rotating drum, with a variable speed motor located above the reactor that controls the speed. The drum embeds 20 removable coupons. The total working volume in each reactor is approximately 950 mL. A 2-h hydraulic retention time (HRT) was controlled by the volumetric flow rate of the influent water (e.g., 8.33 mL/min) entering the ARs. Each AR was set at a rotational speed of 50 rpm, which results in the shear stress of 0.25 N/m^2 at the outer wall (Camper 1995). This shear stress approximately corresponds to a flow of 0.30 m/s in a smooth pipe with diameter of 100 mm. It is also similar to the shear conditions of other pilot-scale and bench-scale investigations (Camper 1996, Sharp et al. 2001, Gagnon et al. 2005). All non-

opaque surfaces were covered with aluminum foil to reduce phototrophic growth and all experiments were run at room temperature (21.0±1.0 °C).

3.3.2 Experimental Design

Two sets of experiments with four ARs in each were operated in parallel. ARs containing cast iron or polycarbonate coupons were used in the first and second set of experiments, respectively. In each study, two ARs were operated with a chloride concentration of 10 mg/L, and two additional ARs were operated with a chloride concentration (75 mg/L). Chloride concentrations of 10 mg/L represented natural chloride present in the tap water used in this study. The chloride concentration of 75 mg/L was used to represent typical concentrations of chloride in drinking water distribution systems resulting from treatment practices such as enhanced coagulation, ion exchange, and use of desalinated water. Additionally, a separate cast iron study was repeated operating at chloride concentration of 250 mg/L to represent the aesthetic objective (AO) for chloride concentrations outlined in the Canadian Drinking Water Quality Guidelines (Health Canada 2014).

The ARs were operated for a period of 4 weeks to establish biofilm and attain pseudosteady state (determined through weekly HPC sampling). This is a common acclimation period used by previous AR studies (Hallam et al. 2001, Gagnon et al. 2005, Cantwell 2005, Dykstra et al. 2007, Rand et al. 2007, Murphy et al. 2008, Rand et al. 2013). After the four-week acclimation period, one AR with chloride concentration of 10 mg/L and one AR with chloride concentration of 75 mg/L in each experiment was disinfected with chlorine to a target of 0.2 mg/L for 6 weeks, followed by a six-week operating period with a higher free

chlorine residual concentration of 1.0 mg/L. The water feed to the ARs in both studies was tap water, which was passed through a granular activated carbon (GAC) filter to remove free chlorine residuals. Similar results were observed for TOC concentrations before and after GAC filtration (Figure 3.1). Table 3.1 summarizes the characteristics of the water that was fed to the ARs during the study.

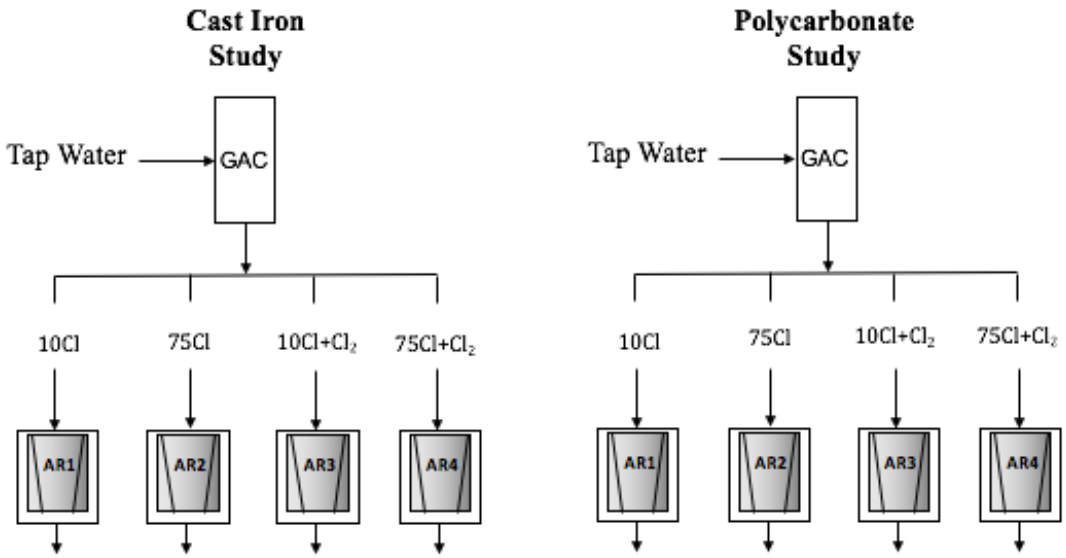

Figure 3.1 Schematic of experimental design.

Table 3.1 Characteristics of the feed water

Water Quality Parameter	Value
Temperature (°C)	20 ± 0.2
pH	6.7±0.3
Chloride (mg/L)	9.5±1.5
Sulfate (mg/L)	8.5±2.0
Alkalinity (mg/L as $CaCO_3$)	16.5±0.2
TOC (mg/L)	2.1±0.2

Stock chlorine feed bottles were prepared in demand-free 4-L amber glass bottles using a 6% solution of sodium hypochlorite (NaOCl) and applied to the chlorinated ARs at a rate of 0.45 mL/min. To increase the chlorine residual at the second stage of chlorination (1.0 mg/L), the concentration of the stock chlorine bottles was increased to the point that the desired chlorine residual was achieved. Stock chloride feed bottles were prepared at a concentration of approximately 1,388 mg/L Cl^- using sodium chloride (NaCl) salt and were applied at a flow rate of 0.45 mL/min. The solutions were kept in demand-free 4-L amber glass bottles and pumped into two ARs in order to achieve a target chloride concentration of 75 mg/L.

3.3.3 Analytical Methods

Sampling and testing methods were performed as outlined in the *Standard Methods for the Examination of Water and Wastewater, 22nd Ed.* (APHA 2012). Samples for water quality analysis were collected from the effluent of each AR. Free chlorine residual concentrations and flow rates were measured three times per week. Free chlorine was measured using the DPD colorimetric method and a UV-VIS spectrophotometer (DR5000, HACH, Loveland, Colorado). Total iron concentrations and microbiological parameters were monitored on a weekly basis throughout the experiment. The concentration of total iron was measured using an inductively coupled plasma-mass spectroscopy (ICP-MS) instrument (Thermo Fisher Scientific, Waltham, Massachusetts). Two drops of concentrated nitric acid were added and the samples were refrigerated at 4°C until an analysis was performed.

Bulk HPC bacteria samples were taken from the effluent of each AR and collected in sterile 50 mL test tubes. For biofilm HPCs, the AR test coupons were removed aseptically in

sequence from the ARs. The attached cells were manually scraped into a sterile 50-mL tube containing 25 mL of autoclaved phosphate buffered saline (PBS) using a 70% ethanol-sterilized and flame-sterilized utility knife. Sterile glass tubes containing 9 mL PBS solution were used to prepare dilutions depending on concentration. Dilutions were used to target a microbial yield of 30–300 colonies per plate per 1 mL of sample. HPC counts were conducted using a standard spread plate technique as described in Standard Methods for the *Examination of Water and Wastewater, 22nd Ed.* (APHA 2012) on R2A agar (Difco Laboratories, Detroit, Michigan). The plates were then incubated in dark for 7 days at room temperature (21.0±1.0 °C) and colonies were counted using a dark-field colony counter.

General water quality parameters including TOC, hardness, alkalinity, pH, and temperature were also measured on a weekly basis. TOC was analyzed using a TOC-V CHP analyzer (Shimadzu Corporation, Kyoto, Japan). pH and temperature of samples were measured using a pH meter (CyberScan pH 6000, Eutech). Alkalinity and hardness were measured using Standard Methods 2320 B.4d Titration method for low alkalinity and 2340 B, respectively (APHA 2012).

3.3.4 Data Analysis

Statistical analysis was conducted to determine if significant differences existed in microbiological growth in the ARs. In addition, statistical tests were used to identify any significant differences between the average influent and effluent values for the water quality parameters measured. Statistical procedures followed an analysis of variance (ANOVA) test at a significance level of 95%, using Minitab version 16. Error bars included

in figures represent a 95% confidence interval. In addition; values throughout represent one standard deviation.

3.4 Results and Discussion

As expected, general water quality data collected throughout all of the experiments showed that there was not a significant difference (p-values>0.05) between the individual ARs in terms of pH (6.7±0.3), temperature (21.0±1.0 °C), hardness (13.5±0.5 mg/L), phosphate (0.5± 0.05 mg/L PO_4^{3-}) and alkalinity (17.3±1.5 mg/L as $CaCO_3$). These data confirm that the ARs were operating under similar conditions over the course of the experiment. The average TOC concentrations were not significantly different in the effluents of the individual ARs in either cast iron or polycarbonate study (p-values>0.05). However, average TOC concentrations were 1.3±0.5 and 1.9±0.2 mg/L in cast iron and polycarbonate ARs, respectively. Statistical analysis showed that these average values were significantly different (p-values<0.05).

3.4.1 Bulk and Biofilm Heterotrophic Bacteria Counts

After the acclimation period and prior to disinfection in the polycarbonate study, the average number of bulk heterotrophic bacteria between all of the ARs was $1.09 \times 10^5 \pm 2.4 \times 10^4$ CFU/mL. The average concentration of biofilm heterotrophic bacteria between all of the ARs was $2.8 \times 10^5 \pm 3.3 \times 10^4$ CFU/cm^2. In the study with cast iron coupons, the overall average number of bulk and biofilm heterotrophic bacteria between all of the ARs was $9.02 \times 10^4 \pm 2.75 \times 10^4$ CFU/mL and $1.8 \times 10^7 \pm 6.6 \times 10^6$ CFU/cm^2, respectively.

Statistical analysis of the data collected during the four-week acclimation period showed that the average bulk and biofilm HPC bacteria were statistically similar for all ARs in each study (p-values>0.05). There was not a significant difference between the two studies in terms of bulk HPC bacteria (p-value=0.17 and 0.38 for 10Cl+Cl_2 and 75Cl+Cl_2 ARs, respectively). However, there was a statistically significant difference between the two studies in terms of biofilm HPC bacteria (p-value=4.45E-11 and 1.42E-5 for 10Cl+Cl_2 and 75Cl+Cl_2 ARs, respectively). Rough surfaces of corroding iron act as substrates for bacteria regrowth and have higher potential for bacteria regrowth. As a result, in cast iron systems, significant differences will only be observed in attached HPC bacteria. However, this might not be observed in different water-quality conditions.

After the four-week acclimation period, one AR with chloride concentration of 10 mg/L and one AR with chloride concentration of 75 mg/L (10Cl+Cl_2 and 75Cl+Cl_2) in each study were disinfected with chlorine. The two remaining ARs were not treated with chlorine and continued operation as experimental controls (10Cl and 75Cl). The four ARs in each experiment were monitored for bulk and biofilm HPC bacteria while disinfection was applied at a target free chlorine residual of 0.2 mg/L followed by1.0 mg/L, each for a six-week period.

Figure 3.2 shows the results of bulk HPCs in the 10Cl+Cl_2 and 75Cl+Cl_2 ARs in polycarbonate and cast iron studies. The ARs treated at the target free chlorine residual of 0.2 mg/L had lower bulk HPCs after disinfection with chlorine was initiated compared to ARs with no chlorination. Log reductions were also calculated using average bulk and biofilm HPC data from the acclimation and two disinfection phases in each AR. Results showed that applying chlorine to achieve a 0.2 mg/L free chlorine residual in the

polycarbonate study resulted in a 2.6-log reduction in bulk HPC in both 10Cl+Cl_2 and 75Cl+Cl_2 ARs. However, in the cast iron study, bulk HPCs in 10Cl+Cl_2 and 75Cl+Cl_2 ARs were only reduced by 1.4-log and 1.3-log, respectively, from acclimation HPC levels after chlorine was dosed at a free chlorine residual target of 0.2 mg/L.

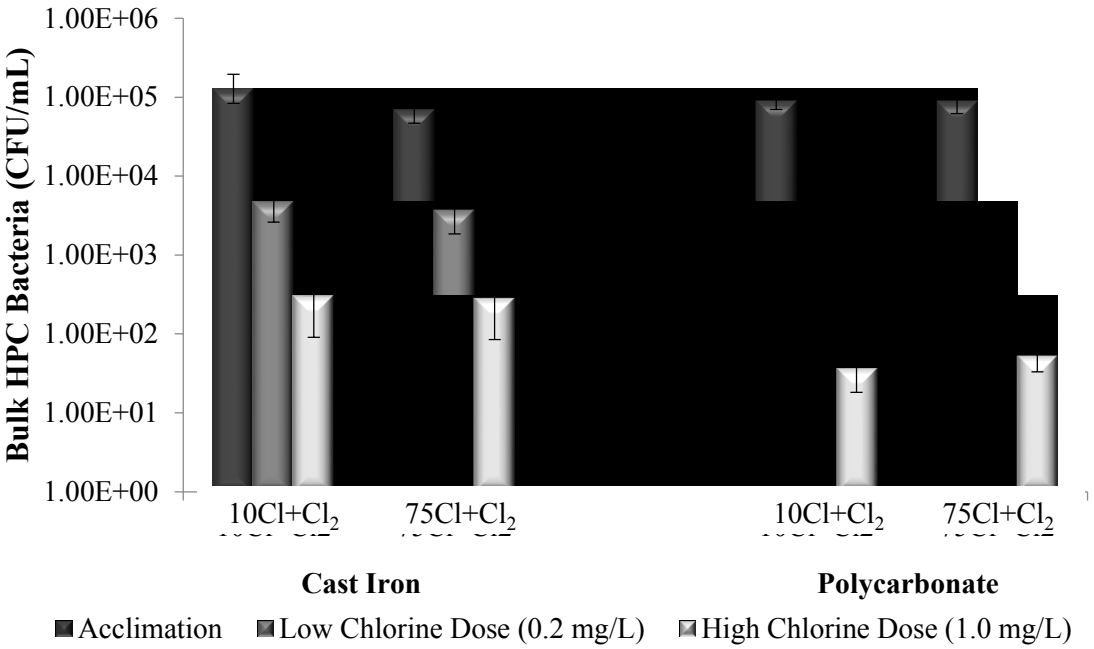

Figure 3.2 Average bulk heterotrophic bacteria in acclimation (n=4) and different stages of chlorination (n=8 for each) in both studies

In the polycarbonate study, after increasing the free chlorine residual to 1.0 mg/L, there was a 3.4-log and 3.2-log reduction in bulk HPC from the acclimation phase in 10Cl+Cl_2 and 75Cl+Cl_2 ARs, respectively. In presence of cast iron coupons, increasing the free chlorine residual to 1.0 mg/L reduced bulk HPCs by 2.6-log and 2.4-log from the acclimation phase in 10Cl+Cl_2 and 75Cl+Cl_2 ARs, respectively.

In comparing pipe materials, results of this study showed that bulk HPCs in the ARs containing cast iron coupons were much more resistant to chlorine disinfection than those

containing polycarbonate coupons. This finding is similar to results of other studies (LeChevallier et al. 1988, Gagnon et al. 2004).

Statistical analysis of the bulk HPC data collected from 10Cl+Cl_2 and 75Cl+Cl_2 ARs in polycarbonate study did not show a significant difference in bulk HPCs at either 0.2 (p-value =0.96) or 1.0 mg/L (p-value=0.41) free chlorine residual disinfection targets. Similarly, there was no significant differences between the bulk HPC data collected from 10Cl+Cl_2 and 75Cl+Cl_2 ARs in cast iron study at either 0.2 (p-value =0.59) or 1.0 mg/L (p-value=0.94) free chlorine residual disinfection targets. These results demonstrate that the elevated concentration of chloride evaluated in these two studies (i.e., 75 mg/L) in treated water does not have a significant effect on disinfection efficacy of chlorine in terms of bulk HPC bacteria in either polycarbonate or cast iron systems compared to low chloride concentration.

Figure 3.3 shows the results of biofilm HPC concentrations in 10Cl+Cl_2 and 75Cl+Cl_2 ARs of both studies. In the polycarbonate study, there was a 0.5-log and 0.4-log reduction post-disinfection with the free chlorine residual target of 0.2 mg/L in 10Cl+Cl_2 and 75Cl+Cl_2 ARs, respectively. At the higher free chlorine residual target of 1.0 mg/L, biofilm HPC bacteria were reduced by 1.5-log and 1.3-log from the acclimation phase in 10Cl+Cl_2 and 75Cl+Cl_2 ARs, respectively. In the cast iron study, at the free chlorine residual targets of 0.2 and 1.0 mg/L, there was not a significant (p-values>0.05) reduction in biofilm HPC bacteria in either 10Cl+Cl_2 or 75Cl+Cl_2 ARs. These results demonstrate that biofilm HPCs are more resistant to chlorine disinfection on cast iron compared to polycarbonate surfaces, which has also been reported in other studies (Murphy et al. 2008, Wang et al. 2012, Rand et al. 2013). Similar to the bulk HPC results, a significant difference between 10Cl+Cl_2 and

75Cl+Cl_2 ARs was not found for biofilm HPC concentrations at both chlorine disinfection targets (p-value=0.89 and 0.23 for 0.2 and 1.0 mg/L free chlorine residual in polycarbonate study, respectively; p-value=0.58 and 0.84 for 0.2 and 1.0 mg/L free chlorine residual in cast iron study). These results again demonstrate that the elevated concentration of chloride (75 mg/L) evaluated in this study did not have a significant effect on disinfection efficacy of chlorine in terms of biofilm HPCs.

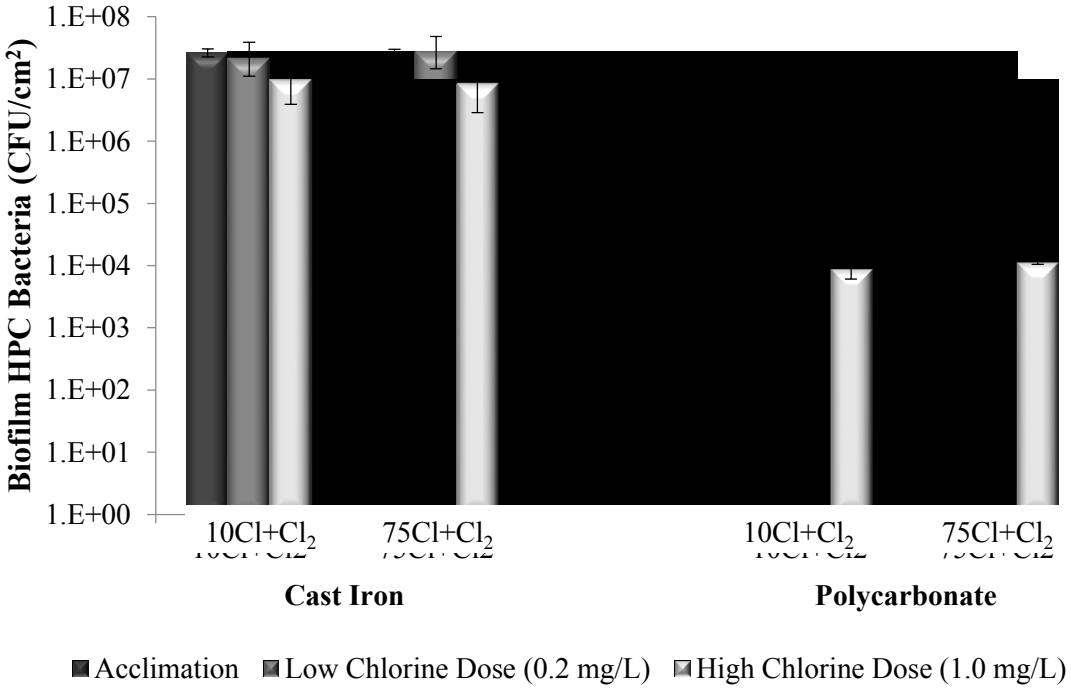

Figure 3.3 Average biofilm heterotrophic bacteria in acclimation (n=4) and different stages of chlorination (n=8 for each) in both studies.

In comparing the results of the polycarbonate and cast iron studies, the average biofilm HPC concentrations were found to be approximately 2-log higher in the cast iron systems compared to the polycarbonate systems during acclimation or two stages of disinfection. Other researchers have concluded that the corroding surfaces of cast iron coupons support

considerably higher amount of biofilm than polycarbonate coupons (Camper et al. 2003, Ollos et al. 2003, Murphy et al. 2008). Previous studies have also suggested that in the presence of NOM, the increased formation of biofilm HPC in cast iron systems is due to the adsorption of higher amounts of carbon on the iron surface and subsequent utilization and growth by bacteria (Niquette et al. 2000, Camper 2003). This may be applicable to the current study as the average TOC concentrations in the effluents of the ARs containing cast iron and polycarbonate coupons were 1.3±0.5 and 1.9±0.2 mg/L, respectively (p-value=0.0002), despite having the same TOC levels in the influent of all ARs (2.1±0.2 mg/L).

3.4.2 Chlorine Disinfection

As previously mentioned, following the acclimation period in each study, one AR with chloride concentration of 10 mg/L and one AR with chloride concentration of 75 mg/L (10Cl+Cl_2 and 75Cl+Cl_2) were dosed with chlorine to yield 0.2 mg/L free chlorine residual for 6 weeks, followed by 1.0 mg/L free chlorine residual in the effluents. Results of the free chlorine residual measurements and the chlorine doses required to achieve residual targets in both sets of experiments are presented in Table 3.2. The target free chlorine residual concentrations of 0.2 and 1.0 mg/L were achieved over the experimental period in both studies. However, maintaining consistent free chlorine residual was more challenging in the ARs equipped with cast iron coupons. From Table 3.2 it can be seen that in the cast iron study, a higher amount of chlorine was required to achieve the free chlorine residual targets in 75Cl+Cl_2 AR than 10Cl+Cl_2 AR. In the experiment with polycarbonate coupons, similar doses of chlorine were required to achieve the free chlorine residual targets in

10Cl+Cl_2 and 75Cl+Cl_2 ARs. Statistical analysis showed that in presence of cast iron coupons, significantly higher chlorine dose was required to achieve the free chlorine residual targets in 75Cl+Cl_2 AR than 10Cl+Cl_2 AR (p-value=0.003). However, in the experiments with polycarbonate coupons, the required chlorine dose to achieve the target free chlorine residual was not significantly different between 10Cl+Cl_2 and 75Cl+Cl_2 ARs (p-value=0.996).

Table 3.2 Free chlorine residual and dosages during the disinfection stage

	Cast Iron Study				**Polycarbonate Study**			
	Target Residual = 0.2 mg/L		**Target Residual = 1.0 mg/L**		**Target Residual = 0.2 mg/L**		**Target Residual = 1.0 mg/L**	
	Residual	**Dose**	**Residual**	**Dose**	**Residual**	**Dose**	**Residual**	**Dose**
10Cl+Cl_2 AR	0.2±0.06	2.3±0.90	1.0±0.14	4.7±1.02	0.2±0.04	0.4±0.04	1.0±0.02	1.1±0.02
75Cl+Cl_2 AR	0.2±0.14	3.4±1.03	1.1±0.14	5.8±0.42	0.2±0.03	0.4±0.04	1.0±0.06	1.1±0.01

Note: Results demonstrate average chlorine concentration ± standard deviation

Chloride, as an aggressive ion, accelerates the corrosion of cast iron (Crittenden et al. 2012). Studies have also reported that the reactions between free chlorine and iron corrosion scales results in the loss of free chlorine in the distribution system (Sarin et al. 2004a, b). The iron corrosion scale formed on the surface of iron generally contains reduced iron that reacts with disinfectants. Specifically, chlorine reacts with ferrous iron (Fe^{2+}) from pipe material and oxidizes Fe^{2+} into ferric iron (Fe^{3+}). These reactions cause free chlorine loss in the distribution system and higher doses of free chlorine are required to maintain target free chlorine residuals. This could be a possible explanation for the fact that the higher chlorine doses were required to achieve free chlorine residual targets in ARs

receiving water with higher concentrations of chloride (75Cl+Cl_2 AR) in cast iron study and also higher chlorine demand in the cast iron study compared to the polycarbonate study. These results are in accordance with other studies, which reported a higher chlorine demand in presence of cast iron pipe material (Frateur et al. 1999, Hallam et al. 2002, Mutoti et al. 2007, Rand et al. 2013).

3.4.3 Iron Release

The effluents of the ARs were sampled on a weekly basis for measurement of total iron concentrations. Iron concentrations in the polycarbonate study were found to be below the detection limit and data is not presented.

Figure 3.4 shows the iron concentrations measured in 10Cl+Cl_2 and 75Cl+Cl_2 ARs over the course of the experiment. As can be seen, the total iron concentration increased to 3.4 mg/L in 75Cl+Cl_2 AR after chlorine disinfection was initiated at 0.2 mg/L free chlorine residual target. The next sample taken 7 days later showed that the total iron concentrations decreased to about 0.8 mg/L and finally to within the initial levels of iron concentrations (i.e., 0.3±0.1 mg/L) after 14 days and remained at relatively constant levels in the presence of a continuous free chlorine residual concentration of 0.2 mg/L. A similar trend was observed at the initiation of the higher free chlorine residual target of 1.0 mg/L. The total iron concentration increased to 6.3 mg/L and then decreased to 4.4 mg/L after 3 days and finally to the initial iron concentration level of 0.3±0.1 mg/L after 7 days. The effluent iron concentration spike observed with the 1.0 mg/L of free chlorine trial was higher than that observed with the 0.2 mg/L free chlorine target experiment. In contrast, only a small

increase in total iron concentrations was observed in 10Cl+Cl_2 AR with the 0.2 and 1.0 mg/L free chlorine disinfection target trials.

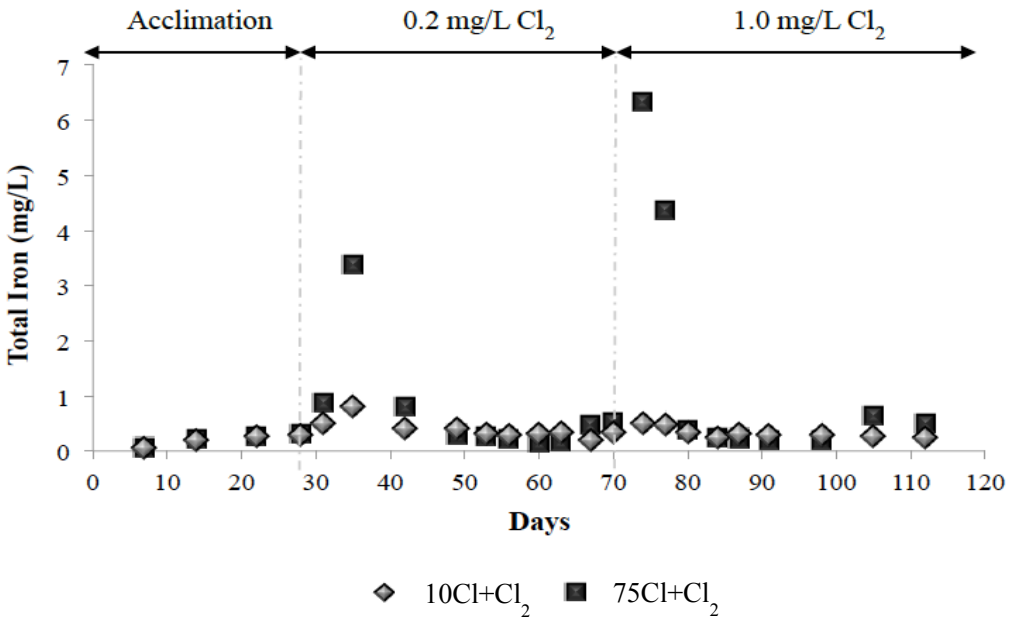

Figure 3.4 Total Iron concentration in cast iron ARs (chloride concentration of 75 mg/L).

These results led the authors to investigate through further AR experiments with a higher chloride concentration of 250 mg/L in the treated water to represent the aesthetic objective (AO) for chloride concentrations outlined in the Canadian Drinking Water Quality Guidelines (Health Canada 2014). Although it would be rare to see chloride concentrations at this level in drinking water distribution systems, experiments were conducted at this AO concentration to model worst-case scenario water quality conditions in terms of elevated chloride concentrations in cast iron systems given current regulatory guidelines.

Results of these experiments showed that the effluent total iron concentrations increased to 2.5 mg/L in the AR containing 250 mg/L chloride (250Cl+Cl_2) after chlorine disinfection was initiated at 0.2 mg/L (Figure 3.5). This spike in the effluent iron concentration remained constant through the 0.2 mg/L free chlorine disinfection stage. An increase in the

chlorine dose to achieve a 1.0 mg/L free chlorine residual resulted in gradual increase in total iron concentrations to approximately 12 mg/L measured in the effluent of 250Cl+Cl_2 AR. Similar to the previous experiments running at a chloride concentration of 75 mg/L, there was not a significant increase in total iron concentrations in the effluent of 10Cl+Cl_2 AR during the two stages of chlorination, with iron remaining relatively constant at concentrations of 0.6±0.1 mg/L.

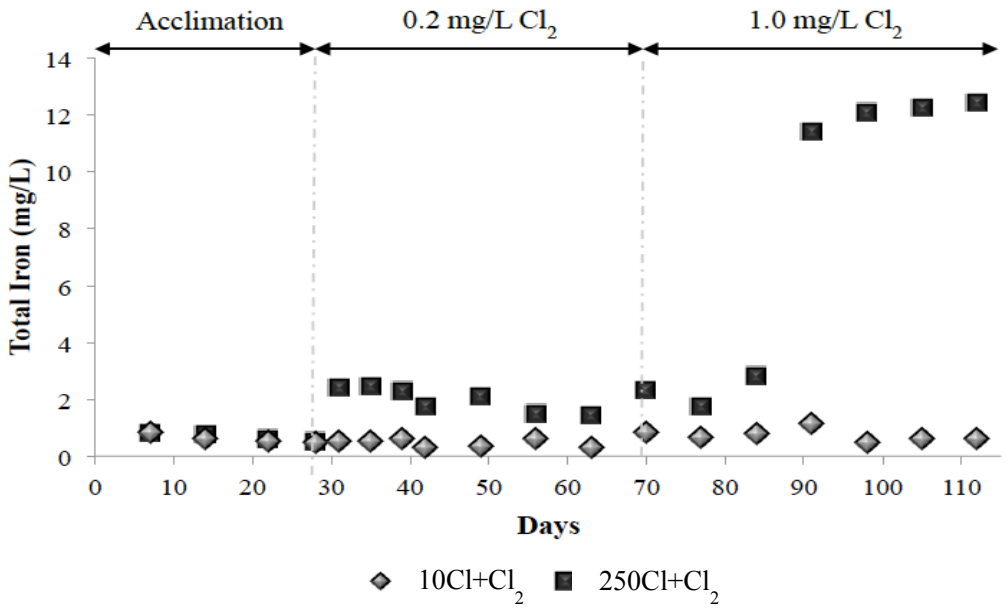

Figure 3.5 Total Iron concentration in cast iron ARs (chloride concentration of 250 mg/L).

It can be concluded that the observed changes of iron release from the surface of the cast iron coupons in this study can be attributed to presence of elevated chloride concentrations in the AR feed waters. Specifically, the presence of elevated chloride concentrations is believed to have an impact on the morphology and characteristics of the oxide layer formed on the surface of the cast iron coupons. Chloride affects the formation of Fe-O-Fe linkages during the formation of iron oxide layer and promotes the formation of lepidocrocite (γ-

FeOOH) crystal structure, which is known to be relatively less protective against corrosion than other iron corrosion products such as siderite and magnetite (Sarin et al. 2004a, b, Liu et al. 2013). It is also widely accepted in the literature that disinfectant residuals as strong oxidizing agents increase corrosion rates and can oxidize soluble ferrous ions into particulate ferric ions (AWWA 1999, McNeill and Edwards 2001). It is hypothesized that the spike in iron concentrations observed during chlorination in the cast iron ARs was due to the presence of loose and non-protective oxide layers on the surface of the cast iron coupons. In the 75 mg/L chloride test ARs, it is hypothesized that this oxide layer inhibited further corrosion, which resulted in total iron concentrations in the AR effluents decreasing back to levels observed prior to disinfection. In the AR experiments run at 250 mg/L chloride concentrations, it is believed that corrosion was not inhibited and iron concentrations remained at elevated levels through this set of disinfection trials. The theory behind this fact is that high concentrations of chloride can degrade the oxide film formed on the surface of cast iron and interfere with its ability to reform a dense and protective oxide layer against corrosion.

3.5 Conclusions

The objective of this study was to investigate the potential impact of elevated chloride concentrations in finished water on disinfection efficacy, microbial regrowth and metal release in drinking water distribution systems. The results of this study found that

1. Elevated chloride concentrations (i.e., 75 mg/L) in treated water did not have a significant effect on disinfection efficacy of chlorine in controlling bulk and biofilm HPC bacteria.

2. Elevated chloride concentrations (i.e., 75 mg/L) did not have a significant impact on microbial regrowth in terms of bulk or biofilm HPCs in either the polycarbonate or cast iron ARs.
3. Higher chlorine dosages were required to achieve target free chlorine residuals in 75Cl+Cl_2 ARs compared to 10Cl+Cl_2 ones in the cast iron systems. However, in polycarbonate systems, similar doses of chlorine were required to achieve the target free chlorine residual in both 10Cl+Cl_2 and 75Cl+Cl_2 ARs.
4. Higher total iron concentration spikes were observed in the cast iron ARs receiving chloride concentration of 75 mg/L after chlorine disinfection was initiated compared to 10 mg/L chloride. However, total iron concentrations decreased back to the initial levels after a few days.
5. Comparing the results of the experiments with 75 and 250 mg/L chloride concentrations showed that in presence of higher chloride concentrations, there was higher iron release in the effluent of the ARs that persisted. The results indicate that in the presence of high chloride concentration of 250 mg/L, the oxide layer formed on the surface of the cast iron coupons was less corrosion-protective and was not able to inhibit further iron release, therefore iron concentrations remained at elevated levels through disinfection trials.
6. The results of this study showed that high concentrations of chloride paired with chlorination could be very detrimental in distribution systems containing cast iron and might result in increased iron release. However, more research is required on different test waters to determine if other water quality variables would impact the results found in this study.

Chapter 4 Effect of High Chloride Concentrations and Chlorine Disinfection on Iron Corrosion Products and Water Quality in Distribution Systems

4.1 Abstract

"Red water" resulting from release of suspended iron particles is a major concern in drinking water distribution systems. The objective of this study was to evaluate the effect of water chloride content on iron corrosion products and water quality in chlorine-disinfected drinking water distribution systems. A secondary objective was to determine if the microbes contribute to the corrosion of cast iron under the experimental conditions. An 8-week bench-scale fill and dump experiment was conducted with cast iron coupons placed in 1-L bottles containing model water with variable chloride concentrations (10, 75 and 250 mg/L) with and without a maintained chlorine residual (0.2-1 mg/L). Chlorination of water containing 250 mg/L chloride caused the average size of the iron particles released from cast iron coupons to increase from 30.2 μm to 65.5 μm. Moreover, this chloride concentration coupled with chlorine disinfection led to higher iron release and corrosion rates, and enhanced formation of crystalline and porous scales. While the biofilm contained bacteria with possible impacts on corrosion, the community size shrank to levels as low as 3.1 Log_{10} *16S rRNA* copies/cm^2 in the chlorinated water with 250 mg/L chloride, rendering it unlikely that the microbes caused the observed corrosion. It was determined that increase in water chloride concentration combined with chlorine disinfection significantly enhanced corrosion and iron release from the model cast iron pipes, pointing to the risk of development of red water in distribution systems with elevated chloride concentrations.

Keywords: Drinking water, cast iron pipes, corrosion scale, chloride concentration, iron release, chlorine disinfection, iron corrosion particles, biofilm.

4.2 Introduction

Cast iron corrosion in drinking water distribution systems can cause many problems including reduced lifetime of the pipe, leaks, catastrophic failure and scale buildup (McNeill and Edwards 2001). The formation of corrosion scale deposits can increase the head loss and reduce the hydraulic capacity of the pipe. As a result, a greater amount of energy is required to deliver water at a desired flow rate (Sarin et al. 2004b). In addition, iron corrosion will deteriorate water quality during distribution (Zhang et al. 2014, Mi et al. 2016), cause disinfectant loss (Al-Jasser 2007, Zhang et al. 2008, Sharafimasooleh et al. 2015), promote bacterial re-growth (McNeill and Edwards 2001, Chowdhury 2012), and cause adsorption and release of toxic trace metals (Lytle et al. 2010, Peng and Korshin 2011). Water discoloration due to iron corrosion is the largest cause of consumer complaints (Husband and Boxall 2011). Consequently, the use of cast iron pipes in drinking water distribution systems is prohibited in many developed countries. However, cast iron pipes have been used for more than 500 years to transport drinking water (Gedge 1993) and comprise a large percentage of current drinking water distribution system infrastructures. According to InfraGuide (2001), cast iron and ductile iron pipes account for more than two-thirds of the existing water mains in use across Canada. Thus, iron pipes will still be in use for many years.

Corrosion of cast iron in drinking water distribution systems is a complex phenomenon involving a series of electrochemical processes that results from chemistry at the interface

between the water and the pipe wall, as well as the physical/mechanical characteristics of flow through the pipe. On the pipe surface, at an anodic site, the elemental iron (Fe^0) converts to ferrous iron (Fe^{2+}), releasing two electrons (oxidation). The released electrons travel through the internal circuit (pipe wall) to a site which acts as the cathode. At the cathode, the most common reaction in distribution systems is the acceptance of electrons by oxygen and/or by chlorine (reduction). The Fe^{2+} ions produced by the corrosion reaction either dissolve in the water or deposit on the metal surface as corrosion scale (Lytle et al. 2004, Sarin et al. 2004a, Benson et al. 2012).

Different iron corrosion products have been shown to form under different conditions, and the exact composition and structure of iron corrosion scales and the rates of iron release strongly depends on the water quality as well as the flow conditions (Sarin et al. 2004b, Chun et al. 2005, Wang et al. 2012). Chloride concentrations and free chlorine residuals are two water quality parameters that influence corrosion, and chemical composition and structure of iron corrosion scales (Wang et al 2012, Liu et al. 2013, Zhu et al. 2014). Chloride can be present in drinking water from various sources including treatment practices for natural organic matter (NOM) removal such as enhanced coagulation (Shi and Taylor 2007) and anionic exchange resins (AERs) (Ishii and Boyer 2011, Willison and Boyer 2012), salt-water intrusion (Essink 2001), run-off from deicing salt (Thunqvist 2004), and use of desalinated water (Greenlee et al. 2009, Liu et al. 2013). Previous studies have shown that an increase in the concentration of chloride accelerates the corrosion of cast iron and its release to the water (Shi and Taylor 2007, Crittenden et al. 2012, Willison and Boyer 2012, Sharafimasooleh et al. 2015). In the presence of high chloride concentrations, porous corrosion scales with more crystalline morphology are formed,

which are less corrosion protective and result in increasing release of larger iron particles in the bulk water (Liu et al. 2013). In addition, chloride ions promote formation of iron oxides (i.e., lepidocrocite) that are less stable against reduction, thereby promoting dissolution of the corrosion scale and higher iron release (Taylor 1984, Sarin et al. 2004b, Liu et al. 2013).

Chlorine is the most commonly used disinfectant in North America to control bacterial regrowth in drinking water distribution systems. It is widely accepted that chlorine disinfectant residuals as electron acceptors (oxidizing agents) react with the iron surface and accelerate the corrosion rates. The rate of this reaction may also be increased by the presence of chloride ion (Le Puil et al.). When present in the bulk water, chlorine oxidizes the dissolved iron (Fe^{2+}) released to the water to ferric iron particles (Fe^{3+}), which impart color to the water and/or form corrosion scale. Chlorine residuals also impact the structure, composition and morphology of corrosion scales (McNeill and Edwards 2001, Eisnor and Gagnon 2004, Wang et al. 2012).

Bacterial biofilm communities are widely found in drinking water distribution systems, where the size and diversity of the microbial community depends on physiochemical properties of pipe materials, location and the water quality (nutrients, chlorine levels, temperature, etc.) (Liu et al. 2012, Sun et al. 2014). Establishment of microbial biofilms has been shown to affect the corrosion of cast iron pipes in distribution systems (Teng et al. 2008, Zhu et al. 2014, Wang et al. 2015, Li et al. 2016). The role of microbes in corrosion processes is complex, because they can either enhance or inhibit corrosion by influencing the chemical cathodic and/or anodic corrosion reactions and thereby modifying the corrosion products (Sun et al. 2014, Zhu et al. 2014). Microorganisms affecting iron

corrosion include sulfate-reducing bacteria (SRB), sulfur-oxidizing bacteria (SOB), iron-reducing bacteria (IRB), iron-oxidizing bacteria (IOB), nitrate-reducing bacteria (NRB), and bacteria producing organic acids and slime (Wang et al. 2012, Sun et al. 2014, Zhu et al. 2014). At this time, it is not known if microbial biofilms contribute to the corrosion of cast iron in drinking water distribution systems exposed to elevated chloride levels and chlorination.

Previous studies dealt separately with effects of either variable chloride concentrations or chlorine disinfection on iron corrosion and release. Therefore, the objective of this study was to examine the combined effect of variable chloride concentrations and free chlorine residuals on iron corrosion and its release from corroding iron surfaces under stagnant conditions, and to investigate the structures and morphologies of resulting iron corrosion products. An additional goal of this study was to quantify the size and concentration of iron corrosion particles released from corroding cast iron surfaces. Moreover, the size and characteristics of bacterial biofilm communities were investigated to determine if the microbes contributed to the corrosion of cast iron under the experimental conditions.

4.3 Materials and Methods

4.3.1 Experimental Design

An 8-week bench-scale fill-and-dump experiment was conducted to examine iron release from cast iron coupons in model water with chloride concentrations of 10, 75 and 250 mg/L, with (10Cl+Cl_2, 75Cl+Cl_2 and 250Cl+Cl_2) and without (10Cl, 75Cl and 250Cl) maintained chlorine residual between 0.2 and 1.0 mg/L. This big range of target free chlorine residual was chosen because previous studies (Rand et al. 2013, Sharafimasooleh

et al. 2015) showed that in the presence of cast iron, free chlorine residuals varied greatly making frequent adjustments necessary to maintain consistent free chlorine residuals that met Health Canada's Guidelines for Canadian Drinking Water Quality (≥ 0.2 mg/L) (Health Canada 2014). Chloride concentrations of 10 mg/L represented the indigenous content in the tap water used in this study, while the concentration of 75 mg/L represented typical concentrations of chloride found in drinking water distribution systems due to treatment practices such as enhanced coagulation, ion exchange and use of desalinated water (Shi and Taylor 2007, Ishii and Boyer 2011, Willison and Boyer 2012, Liu et al. 2013). Lastly, a concentration of 250 mg/L chloride was used to represent the upper limit for the aesthetic objective (AO) for chloride concentrations outlined in the *Canadian Drinking Water Quality Guidelines* (Health Canada 2014), and thus to model worst-case scenario in terms of elevated chloride concentrations in cast iron systems.

Tap water was passed through a granular activated carbon (GAC) filter for de-chlorination. Parameters measured every week for the source water (GAC-filtered tap water) during the study were as follows: temperature 18.0 ± 0.5 °C, pH 6.7 ± 0.3, alkalinity 16.5 ± 0.2 mg/L as $CaCO_3$, total iron <0.01 mg/L, phosphate 0.5 ± 0.02 mg/L PO_4^{3-}, dissolved organic carbon (DOC) 1.4 ± 0.06 mg/L, chloride 9.5 ± 1.5 mg/L and sulfate 8.5 ± 0.2 mg/L. The source water was then spiked to yield the different water quality characteristics in terms of chloride concentrations and free chlorine residuals of the test water in each bottle (Table 4.1).

Table 4.1 Test bottle water quality characteristics

	Chloride Concentration (mg/L)	Chlorine Residual Concentration (mg/L)
10Cl	10	0
75Cl	75	0
250Cl	250	0
10Cl+Cl_2	10	0.2-1.0
75Cl+Cl_2	75	0.2-1.0
250Cl+Cl_2	250	0.2-1.0

The experiments were conducted using six 1-L amber glass bottles in parallel with an additional 6 bottles run in parallel as duplicates. The bottles were made chlorine demand-free before use by soaking in a concentrated sodium hypochlorite solution (~300 mg/L NaOCl) for at least 24 hours prior to the test, rinsed three times with deionized water and dried in the oven at 100 °C. Three of the test bottles in each series were chlorinated to obtain an initial chlorine residual of 1 mg/L, using a chlorine stock solution of 1,000 mg/L prepared by diluting an aqueous sodium hypochlorite (NaOCl) solution (Fisher Scientific, USA). Based on preliminary chlorine demand analyses conducted with the test water, the free chlorine residual decreased from the initial value of 1 mg/L to 0.27 mg/L after 24 hours. As a result, free chlorine residuals were monitored daily and chlorine boosting was performed whenever the free chlorine residual decreased below 0.5 mg/L to maintain residuals between 0.2 and 1 mg/L throughout the 8-week study period. The three other test bottles in each series were not dosed with chlorine and represented the unchlorinated controls in the experiments.

Two virgin cast iron coupons (1.0 cm x 1.0 cm x 0.5 cm), one with a predetermined weight

for corrosion rate determination and the other designated for biofilm and morphological analyses, were suspended in the bulk water of each test bottle using nylon lines. The test bottles were kept in the dark to simulate the distribution system environment and preclude algal growth. The test bottles were kept at room temperature (20-22 °C) and gently mixed with 5 manual rotations on a daily basis after addition of chlorine, and then allowed to sit for a 24-hour stagnant period. At the end of each week, all of the water in the test bottles was decanted and replaced with 1.0 L of fresh model water to simulate the intermittent water flow environment in an actual water distribution system (Teng et al. 2008). Before decanting, water samples were withdrawn and prepared for analysis of total and dissolved iron concentrations, DOC, pH, temperature, apparent color and turbidity.

Size analysis and images of settled iron particles were analyzed using a Micro-Flow Imaging (MFI™) system (Brightwell Technologies Inc., Ottawa, ON). To collect settled iron particles, bottles were inverted gently two times and a 30 mL sample was collected using a wide mouth pipette and resuspended in 40-mL glass vials.

4.3.2 Determination of Rate and Characteristics of Corrosion of the Cast Iron

At the end of Week 8, the two iron coupons were removed from each bottle. The biofilm was harvested from one side of one of the coupons (see section 4.3.4) and then the coupons were dried under vacuum condition for one day at room temperature. The vacuum condition was chosen to avoid altering the crystalline composition of corrosion scales. The test coupons with predetermined weights were placed in 0.01 M phosphoric acid and sonicated for 10 minutes to remove oxidation products from the surface of the coupons. These coupons were then rinsed with deionized water, wiped, air-dried for a day and

weighed to determine the weight loss and corrosion rate over the experiment following methodology presented by Liu et al. 2013.

To calculate the corrosion rate from metal weight loss, Equation 4.1 (ASTM G31-72) was used:

$$mm/y = 87.6 \times (W / DAT) \quad (4.1)$$

where:

- W = weight loss in milligrams ($W_{loss}=W_{initial}-W_{final}$)

  $W_{initial}$= initial weight of coupon

  W_{final}= weight of coupon after the corrosion scales were removed
- D = metal density in g/cm^3
- A = area of sample in cm^2
- T = time of exposure of the metal sample in hours

The corrosion scales were scraped from the surface of the second test coupon from each bottle with a clean utility knife and analyzed with Scanning Electron Microscopy (SEM, Hitachi S-4700, Japan) and X-ray diffraction (XRD, Siemens D500) to examine the morphology and composition of corrosion products. XRD analysis used Cu$K\alpha$ radiation (λ=1.54 Å) at a scanning range of 2θ=10-70º, tube voltage of 35 kV, and tube current of 30 mA.

Total amount of particulate iron released from cast iron coupons exposed to different conditions was also calculated. Total particulate iron release is defined as the summation of the concentration of suspended iron particles in solution, and the settleable iron particles. The mass of settled iron particles (Equation 4.2) was calculated using average particle size

and their concentration obtained from MFI™ analysis. It was assumed that all particles were spherical and composed of ferric hydroxide with the density of 4.25 g/cm^3.

$$\text{Settled iron particles concentration} = n \times V \times \rho \qquad (4.2)$$

where:

- n = particle concentration
- V = particle volume ($4/3\pi r^3$)

  r = particle radius
- ρ = particle density

4.3.3 Water Quality Analysis

Free chlorine was measured on a daily basis using the DPD colorimetric method at a wavelength of 530 nm using a DR5000 UV-Visible spectrophotometer (HACH Co., Loveland, Colorado). Total suspended and dissolved iron (samples passed through a 0.45 μm pore size polysulfone membrane filter) concentrations were measured using an Inductively Coupled Plasma-Mass Spectroscopy (ICP-MS) instrument (Thermo Fisher Scientific, MA, USA). Two drops of concentrated nitric acid were added and the samples were refrigerated at 4 ºC until analysis was performed. Samples for DOC analysis were passed through a 0.45-μm polysulfone membrane filter and analyzed using a TOC-V CHP analyzer (Shimadzu Corporation, Kyoto, Japan). pH and temperature of samples were measured using a pH meter (CyberScan pH 6000). A HACH 2100 AN Turbidimeter was used to measure the turbidity in water samples.

4.3.4 Extraction of DNA from Coupon Biofilms

At the end of Week 8, the biofilm formed by the naturally occurring microbiota on one coupon from each treatment was harvested by scraping with a sterile spatula and transferred into 10 mL of sterile phosphate-buffered saline (pH 7.0) in a 50 mL sterile test tube. Following centrifugation at 3200 x *g* for 15 minutes, the supernatant was discarded. The resulting cell pellet was resuspended using the residual liquid (250 µL) and subjected to genomic DNA extraction using the MO BIO PowerSoil DNA isolation kit (MO BIO Laboratories, Carlsbad, CA, USA) according to manufacturer's instructions. DNA concentrations were then quantified with a QuantiFluor@ ds DNA kit (Promega Corporation, Madison, WI, USA) and a Quantus Fluorometer (Promega) and ranged from 0.02-0.15 ng/µL. All DNA samples were stored at -20°C until further analysis.

4.3.5 *16S rRNA* Copy Number in Biofilms

To determine the size of biofilm communities, the copy numbers of bacterial *16S rRNA* genes were detected using a quantitative polymerase chain reaction (qPCR) assay with primer set BACT 2 (Suzuki et al. 2000). The qPCR amplification was conducted on a Bio-Rad CFX96 Touch Real-Time PCR system (Bio-Rad, Hercules, CA, USA) in 20-µL total reaction volumes consisting of 4.0 µL of template DNA, 4.4 µL of sterile and nuclease-free water (Fisher Scientific), 0.8 µL of each primer (10 µM), and 10 µL of Power SYBR Green PCR master mix (Applied Biosystems, Life Technologies, Canada) using the following thermocycler program: 10 minutes initial denaturation at 95 °C, followed by 40 cycles of 15 seconds (s) denaturation at 94 °C, 30 s annealing at 55 °C, and 30 s extension at 72 °C. Melt curve analysis was also performed to confirm presence of the *16S rRNA*

gene PCR amplicon with a melting temperature of 80.7 °C ± 0.4 °C.

A plasmid construct containing the partial region of bacterial *16S rRNA* gene was a generous gift from Dr. Yost (University of Regina, personal communication) and used to create a standard curve (10-fold serial dilutions, 10^1 to 10^8 copies/µL) to enable quantification of *16S rRNA*. Two technical replicates were run for all standards, samples, and non-template controls and the difference of the threshold cycle (Ct) value between the replicates was less than 0.5. The qPCR assay efficiency was 102%, with an R^2 value of 0.999. The limit of detection (LOD) is 10^3 copies/cm^2 coupon. The limit of quantification (LOQ) for the *16S rRNA* gene is 10^2 copies/µL. The quantity of *16S rRNA* gene numbers was reported as $\log_{10}$ gene copies/cm^2 of cast iron coupon area.

4.3.6 Biofilm Diversity

The diversity in biofilm microbial communities were elucidated by sequencing of bacterial *16S rRNA* PCR amplicons (V6-V8 region) on the Illumina Miseq system. Details of the protocol are available on the Integrated Microbiome Resource (IMR) website (http://cgeb-imr.ca/protocols.html) at the Center for Comparative Genomics and Evolutionary Biology (CGEB) at Dalhousie University, Halifax, NS, Canada and are also described elsewhere (Comeau et al. 2011). Raw paired-end MiSeq sequencing reads in de-multiplexed fastq format were processed in PEAR (Zhu et al. 2014) to stitch paired-end reads together followed by removal of low quality reads (<400 bp, low quality scores, contained "Ns"). The final high quality sequences in the fast format were then clustered into Operational Taxonomic Units (OTUs) at an identity level of ≥97% using the UPARSE-OTU algorithm in the USEARCH pipeline (Edgar 2013). In the UPARSE-OTU algorithm, chimeric

sequences are removed. Subsequent analyses were carried out using the Quantitative Insights Into Microbial Ecology (QIIME) pipeline (Caporaso et al. 2010b). Representative sequences from each of the OTUs (from UPARSE) were classified with the Ribosome Database Project (RDP) classifier v2.2 (Wang et al. 2007). The cut-off value to define a sequence's taxonomy was set at 60% to provide at least 95% accurate taxonomy assignment at the genus level (Claesson et al. 2009). Representative OTU sequences were then aligned using the default and template guided alignment method (PyNAST) (Caporaso et al. 2010a). This alignment was used to build a phylogenetic tree in FastTree (Price et al. 2010). The final output from the QIIME pipeline consisted of a rarefied OTU table containing the counts and associated taxonomic classification of each OTU in each sample. This table was used to summarize relative OTU abundance and calculate phylogenetic β-diversity quantitatively using the weighted unifrac metric to indicate whether different treatments caused the abundance of taxonomic groups to change. An exploratory multivariate statistics method, principal coordinate analysis (PCoA), was then performed on the weighted unifrac β-diversity metric to identify trends between different treatments.

4.3.7 Data Analysis

Statistical analysis was conducted to identify any significant differences between the average values for the water quality parameters measured. Statistical procedures followed an analysis of variance (ANOVA) test at a significance level of 95%, using Minitab version 16 (MINITAB, State College, PA). Error bars included in figures, and ± values throughout the manuscript represent one standard deviation.

4.4 Results and Discussion

4.4.1 General Water Quality

General water quality data collected from the bottles throughout the experiment showed that there were no significant differences (p-values>0.05) between the bottles receiving the different chloride and chlorine treatments in terms of pH (6.7±0.1), temperature (18.0±0.1 ºC) and DOC (1.4±0.06 mg/L).

Similar to previous works (Zhang et al. 2008, Sharafimasooleh et al. 2015), presence of increasing chloride concentrations caused higher chlorine doses to be required to maintain the target free chlorine residual in the bulk water. Hence, the average of total weekly chlorine dosages added to each bottle from exposure weeks 5 to 8 were 2.49±0.23, 3.28±0.09 and 3.76±0.22 mg/L at chloride concentrations of 10, 75 and 250 mg/L, respectively. It appeared that increasing chloride concentrations enhanced the corrosion, which in combination with the previously established oxidizing effect of chlorine on the iron corrosion products (Sarin et al. 2004a, Sarin et al, 2004b), resulted in free chlorine loss in the model distribution system and higher doses of free chlorine were required to maintain target free chlorine residuals.

4.4.2 Iron Release

Averaged dissolved iron and total suspended iron concentrations released from the test coupons from exposure weeks 5-8 are presented in Figure 4.1, because iron levels were stable in most experimental conditions after 4 weeks of exposure. Results showed that the total and dissolved iron concentrations released from the test coupons into the bulk water decreased with increasing chloride concentrations in both the non-chlorinated and chlorine-

disinfected test bottles. In the non-chlorinated bottles, total suspended iron concentrations were found to be 4.36±0.38 mg/L in 10Cl test bottles, while 250Cl test bottles contained a significantly (p-value<0.001) lower concentration of 1.38±0.45 mg/L. Measurement of dissolved iron concentrations showed the same trend. The 10Cl test bottles were found to have 0.09±0.02 mg/L dissolved iron concentration compared to <0.01±0.01 mg/L (p-value=0.006) found in the 250Cl test bottles.

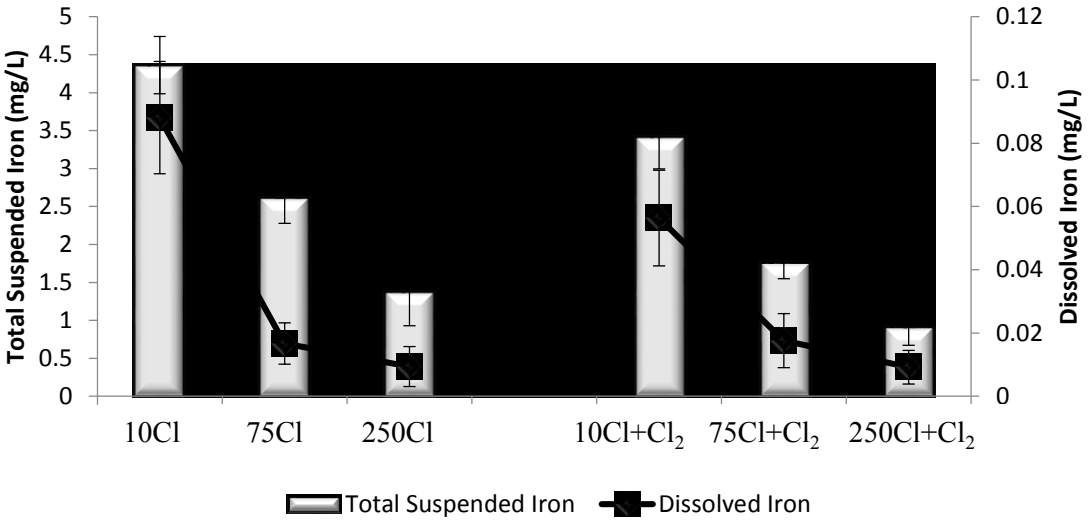

Figure 4.1 Effect of chloride concentration and chlorine disinfection on dissolved iron and total suspended iron released from corroding iron coupons (n=8).

It was hypothesized that the higher chloride concentration in the non-chlorinated test water led to the formation of large iron particles released from the surface of coupons, which settled more rapidly under stagnant conditions and resulted in lower iron concentration in the bulk water compared to the iron particles formed and released in the lower chloride concentration test bottles. The results of turbidity and apparent color measurements (Figure 4.2) supported this hypothesis, and showed a similar trend of lower turbidity and apparent

color measurements (average from exposure weeks 5-8) in the non-chlorinated test bottles operating at higher chloride concentrations.

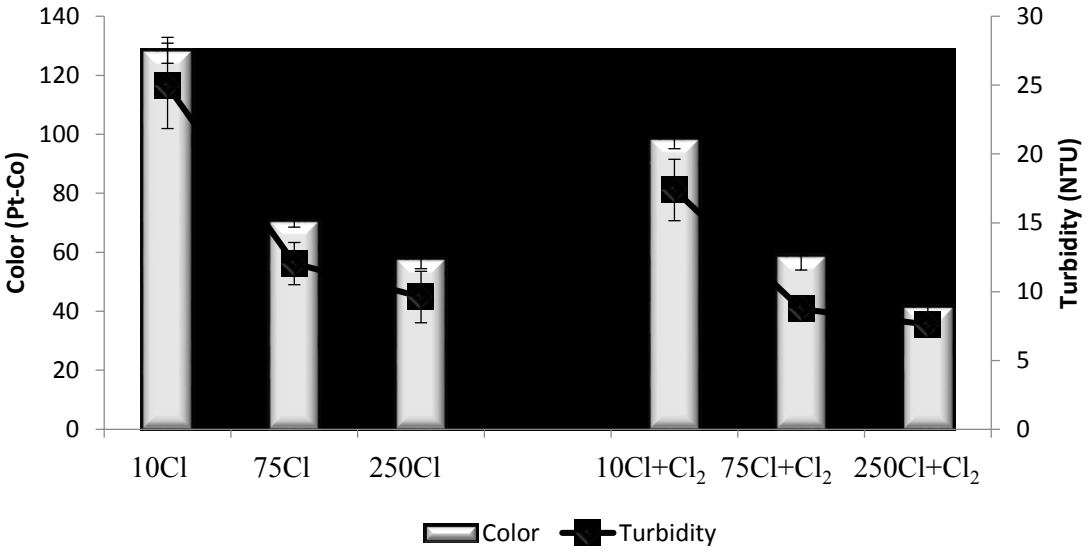

Figure 4.2 Effect of chloride concentration and chlorine disinfection on color and turbidity (n=8).

The results also showed that total suspended iron concentration, turbidity and color in water samples were significantly lower (p-values<0.05) in the presence of chlorine compared with the non-chlorinated samples. For example, at a chloride concentration of 10 mg/L, the concentration of total suspended iron decreased from 4.36 ± 0.38 mg/L in the non-chlorinated bottles (10Cl) to 3.42±0.43 mg/L in the chlorinated bottles (10Cl+Cl_2) (p-value=0.00031). The same trend was observed at higher concentrations of chloride. This shows that chlorine itself reduced the total suspended iron concentration, turbidity and color in water samples. It was again hypothesized that in the presence of chlorine larger iron particles were formed, which settled faster and resulted in lower concentrations of suspended iron particles, color and turbidity in the stagnant water. Moreover, in contact

with chlorine, soluble ferrous ions were oxidized to particulate ferric ions, which readily precipitated on the bottom of the bottles (Wang et al. 2012).

4.4.3 Particle Analysis

4.4.3.1. Settled Iron Particles

Visual comparison of the collected iron particles presented in Figure 4.3 supported the hypothesis stated in section 4.4.2 that larger iron particles were released from surface of cast iron coupons with increasing chloride concentration, which settled faster and resulted in lower concentrations of suspended iron particles, color and turbidity in the stagnant conditions tested in this experiment.

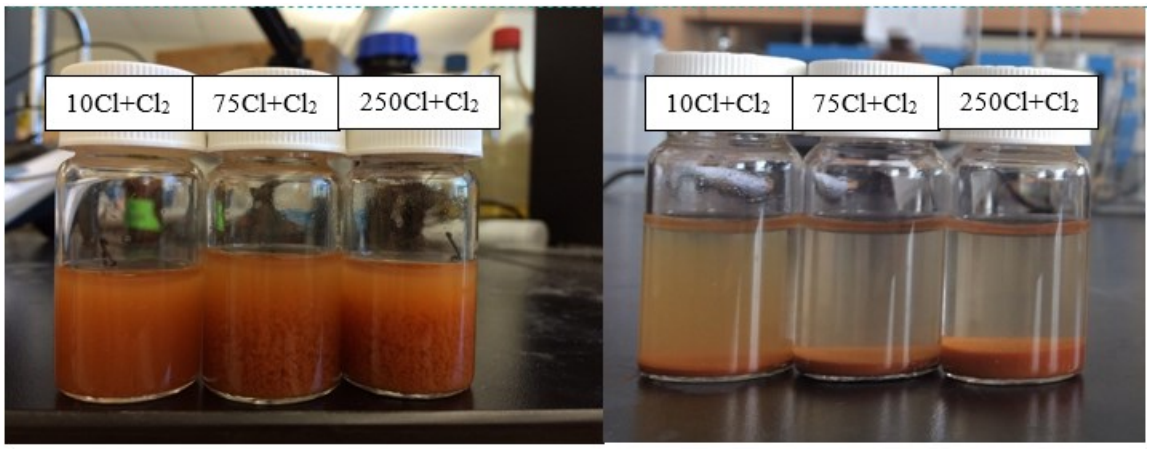

Figure 4.3 Visual appearance of settleable iron particles collected from test bottles with different chloride concentrations after 1 minute (left) and 15 minutes (right) settling time.

Visual comparison of the iron particles collected from chlorinated and non-chlorinated test bottles (Figure 4.4) revealed that in test bottles with chloride concentration of 75 and 250 mg/L, increased amounts of iron particles detached and settled out from the surfaces of cast iron coupons as compared to test bottle with chloride concentration of 10 mg/L. It must be

noted here that this conclusion is purely based on visual comparison and the differences between the test bottles were also quantified using a Micro-Flow Imaging (MFI™) system (Section 4.4.3.3).

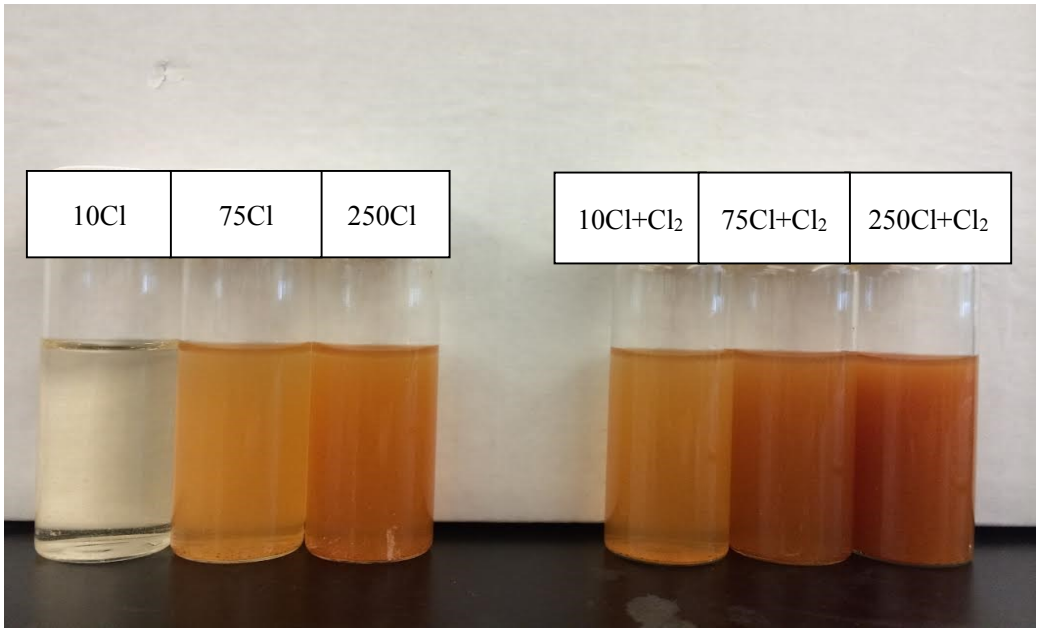

Figure 4.4 Visual appearance of iron particles collected from non-chlorinated (left) and chlorinated (right) bottles (resuspended in 40-mL glass vials).

Figure 4.4 also shows that there were greater amounts of iron particles detached and settled out from the surface of cast iron coupons in the chlorinated bottles. A possible explanation for this observation is that in presence of chlorine, soluble ferrous iron ions are oxidized to ferric iron particles following the reactions in Equations 4.3 and 4.4 (Wang et al. 2012), which readily precipitate depending on their size and density. This is also in accordance with the iron release results, in which, the concentration of total suspended iron decreased when bottles were spiked with chlorine.

$$6Fe^{2+} + 3ClO^{-} + 3H_2O \leftrightarrow 2Fe(OH)_3 + 4Fe^{3+} + 3Cl^{-} \quad (4.3)$$

$$2Fe^{2+} + HClO + H^{+} \leftrightarrow 2Fe^{3+} + Cl^{-} + H_2O \quad (4.4)$$

It should be noted that these reactions are pH-dependent. Chlorine rapidly hydrolyzes in water to form hypochlorous acid (HClO), which in turn forms hypochlorite ion (OCl^-) (Droste 1997). Between pH 6.5 and 8.5, the dissociation reaction is incomplete, and both hypochlorous acid and hypochlorite ion are present as the primary oxidizing agents in water, although hypochlorite has a lower oxidizing potential. Below a pH of approximately 7.6, HClO dominates and at pH levels above 7.6, chlorine primarily occurs in the form of OCl^- (Water 2009). As the pH of the water used in this experiment was below 7.6, the reaction in Equation 4.4 likely governed the oxidation of ferrous ions.

4.4.3.2 Particle Size Analysis

Analysis of particle samples collected from the test bottles at the end of exposure weeks 5 to 8 showed that there was significantly (p-values<0.05) higher number of particles per milliliter of sample with rising chloride concentrations, e.g., in the sample collected from 10Cl test bottle, there were $3.3x10^4 \pm 1.7x10^4$ particles/mL versus $4.1x10^5 \pm 1.8x10^5$ and $7.4x10^5 \pm 2.2x10^5$ particles/mL in 75Cl and 250Cl test bottles, respectively (Table 4.2). Also, samples collected from chlorinated bottles contained more individual particles than the samples collected from non-chlorinated bottles.

Table 4.2 Average particle size and particle concentration of settled particles (n=8)

	10Cl	**75Cl**	**250Cl**	**10Cl+Cl_2**	**75Cl+Cl_2**	**250Cl+Cl_2**
Average Particle Size (µm)	6.1±1.4	14.3±8.6	30.2±9.2	15.2±9.0	30.6±11.5	65.5±17.2
Particle Concentration (particles/mL)	$3.3x10^4$ ± $1.7x10^4$	$4.1x10^5$ ± $1.8x10^5$	$7.4x10^5$ ± $2.2x10^5$	$5.0x10^5$ ± $2.0x10^5$	$8.0x10^5$ ± $3.1x10^5$	$1.3x10^6$ ± $2.8x10^5$

Particle size analysis of the settleable iron particles showed that the higher chloride concentration test water resulted in larger particle sizes of the settled solids. For example, as the concentration of chloride in water increased from 10 to 250 mg/L, the average particle size of the settled iron corrosion products rose significantly from 6.1±1.4 µm to 30.2±9.2 µm in the non-chlorinated bottles (p-value=0.0001). Moreover, the average particle size was significantly greater in the chlorinated bottles compared to non-chlorinated bottles (p-values<0.05) (Table 4.2), demonstrating that the presence of chlorine resulted in larger iron particles released from the surface of cast iron coupons. These results support the hypotheses stated earlier that in the presence of both higher chloride levels and chlorine disinfection, larger iron particles were formed and released, which settled faster and resulted in lower concentrations of suspended iron particles in the stagnant water conditions simulated in this experiment. It should however, be noted that the settled particles reduce the capacity of the pipes in drinking water distribution systems. In addition, when stagnation period ends, the large settled particles will resuspend in the flowing water and cause water discoloration, which is often the most cited consumer complaint at many utilities.

These results were also confirmed by calculation of total amount of particulate iron release from cast iron coupons exposed to different conditions. Results (Table 4.3) showed that the total amount of particulate iron released from the coupons increased with increasing chloride concentrations in both the non-chlorinated and chlorine-disinfected test bottles. In the non-chlorinated bottles, for example, total particulate iron concentrations increased from 0.02 g/L in 10Cl test bottles to 36.3 g/L in 250Cl test bottles. The results also showed that total particulate iron concentrations increased substantially in chlorinated bottles compared to non-chlorinated bottles. For example, total particulate iron release was found to be 36.3 g/L in 250Cl test bottles, while 250Cl+Cl_2 test bottles contained a substantially higher concentration of 650.35 g/L.

Table 4.3 Total particulate iron release

	10Cl	**75Cl**	**250Cl**	**10Cl+Cl_2**	**75Cl+Cl_2**	**250Cl+Cl_2**
Total Particulate Iron Conc. (g/L)	0.02	2.14	36.30	3.13	40.81	650.35

4.4.3.3 Particle Imaging

MFI™ images of the particles collected from the test bottles at the end of Week 8 showed that the bottles with chloride concentration of 250 mg/L, in either presence or absence of chlorine, contained the largest particles and the most aggregation of the particles followed by chloride concentration of 75 mg/L and then 10 mg/L (Figure 4.5).

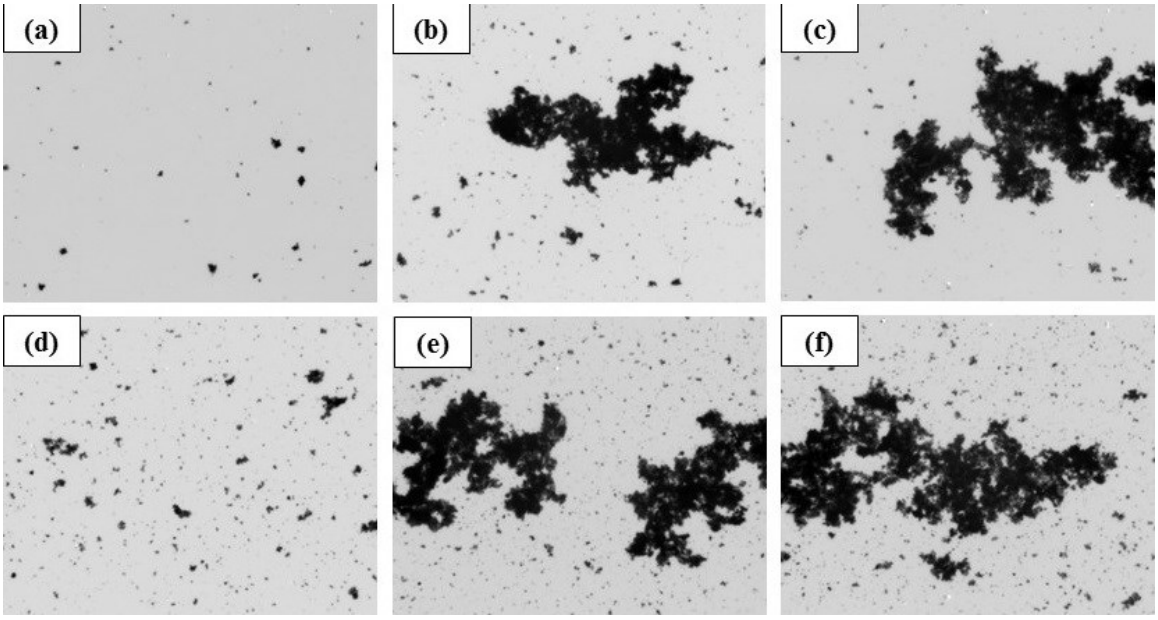

Figure 4.5 Image of iron particles in (a) 10Cl, (b) 75Cl and (c) 250Cl bottles. Image of iron particles in (d) 10Cl+Cl_2, (e) 75Cl+Cl_2 and (f) 250Cl+Cl_2 bottles.

Comparison of the solid samples collected from the non-chlorinated and chlorinated test bottles visually demonstrates that there were more individual particles and larger particle sizes in the samples collected from chlorinated bottles compared to non-chlorinated test bottles. Figure 4.5 also shows that the iron particles formed in presence of chlorine were more porous and less dense than iron particles formed in absence of chlorine under the same conditions, which is attributed to the rapid oxidation rate of Fe^{2+} in presence of chlorine (Burlingame et al. 2006).

4.5 Corrosion Rate

Figure 4.6 shows that the corrosion rate increased with an increase in chloride concentration. This observation is in accordance with the results of other studies that looked at iron corrosion rates in variable chloride concentrated waters (Liu et al. 2013, Zhang et al. 2014). It is possible that once a pit is formed on the metal surface due to metal

dissolution, the solution inside it is isolated from the bulk environment and becomes increasingly corrosive over time. The high corrosion rate in the pit produces an excess of positively charged metal cations (Fe^{2+}). The positive charge inside the pits attracts negative ions of chloride (Cl^-) from the bulk water to maintain electroneutrality and to complete the electrical circuit of the corrosion cell. This results in an increase in acidity of the solution inside the pits, which can be the reason for higher corrosion rates in the presence of higher chloride concentrations (Lytle et al. 2005, Burlingame et al. 2006).

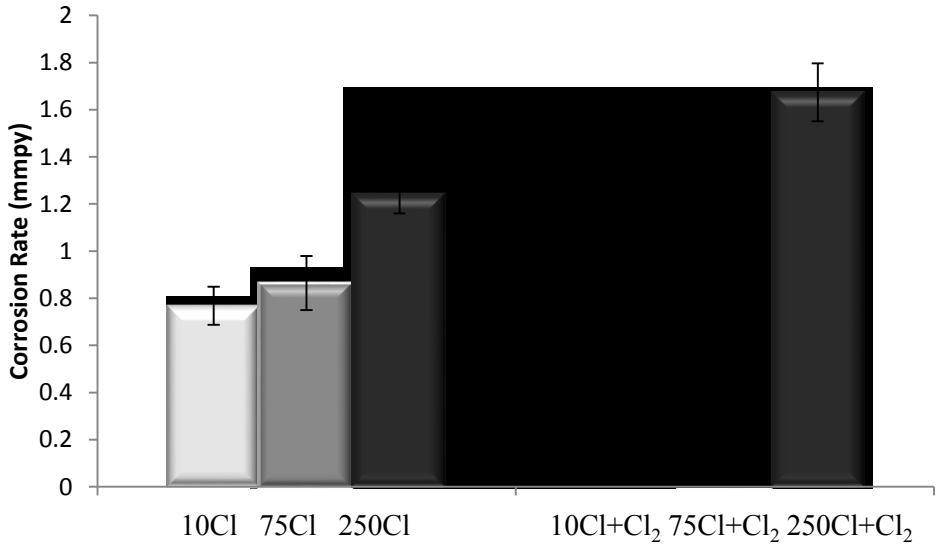

Figure 4.6 Corrosion rate of cast iron coupons under different water conditions (n=2).

Comparing chlorinated and non-chlorinated bottles, there were no differences in corrosion rates between the bottles containing water with chloride concentrations of 10 ($10Cl+Cl_2$) and 75 mg/L ($75Cl+Cl_2$). However, there was a relatively notable increase in the corrosion rate of cast iron coupons exposed to free chlorine in the presence of a chloride concentration of 250 mg/L ($250Cl+Cl_2$) compared to non-chlorinated bottles (250Cl). For

example, in the non-chlorinated bottles there was a 1-fold increase in corrosion rate when the chloride concentration increased from 10 mg/L to 250 mg/L, while in the presence of chlorine there was a 2-fold increase in corrosion rate with the same change in chloride concentration from 10 mg/L to 250 mg/L. In agreement with the model proposed by (Sarin et al. 2004a), the migration of negative ions of chloride (Cl^-) from bulk water, which was discussed earlier, increases the porosity of the oxide layer formed on the surface of coupons. As a result, it would be easier for chlorine to diffuse to the metal surface, thereby promoting dissolution of the metal and higher corrosion rates.

4.6 Characterization of Corrosion Scale

4.6.1 XRD

The XRD patterns of the corrosion scales on the surface of the cast iron coupons placed in non-chlorinated and chlorinated bottles at different concentrations of chloride are shown in Figure 4.7(a) and 4.7(b), respectively. Since the minor peaks were weak, only the major peaks were identified. Results revealed that goethite (α-FeOOH), maghemite (α-Fe_2O_3), lepidocrocite (γ-FeOOH) and siderite ($FeCO_3$) were the main crystalline phases found in all of the iron corrosion scales. This result was in agreement with the previous studies conducted on iron corrosion scales (Sarin et al. 2004b, Teng et al. 2008, Wang et al. 2012). However, more peaks of lepidocrocite with higher intensity appeared with an increase in chloride concentration, indicating the crystalline growth of γ-FeOOH.

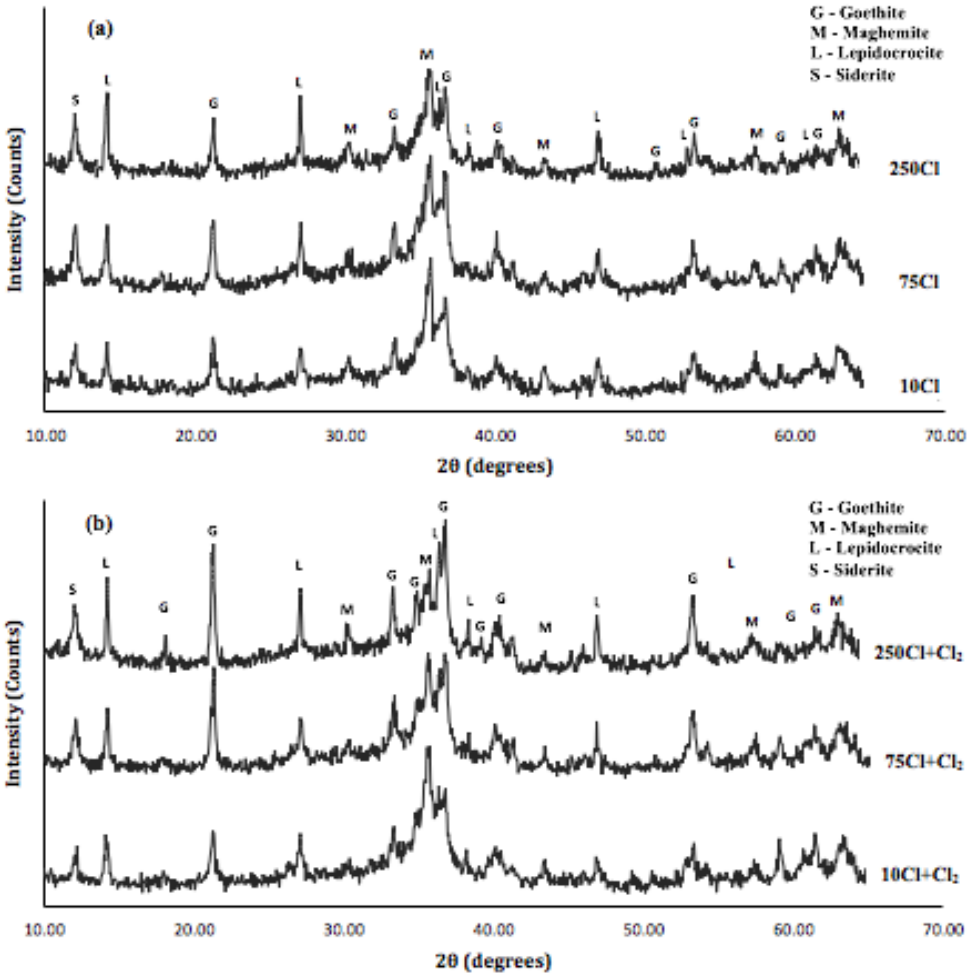

Figure 4.7 XRD patterns of iron corrosion products on surface of coupons exposed to (a) non-chlorinated and (b) chlorinated bottles with different chloride concentrations.

Chloride is believed to promote formation of lepidocrocite (Taylor 1984). It has been previously reported to be characteristic of loose and porous corrosion scale, and its presence is likely to play a role in increasing the iron release by increasing the porosity of the scale (Gerke et al. 2008, Liu et al. 2013). The same trend was observed in XRD patterns of the corrosion products in the presence of chlorine disinfection. In addition, results showed that the formation of goethite and lepidocrocite was clearly enhanced by the addition of chlorine. As can be seen in Figure 4.7(b), the intensities of goethite and

lepidocrocite peaks were higher in presence of chlorine than those in non-chlorinated conditions.

4.6.2 SEM

Figure 4.8 shows the SEM images of iron corrosion products on the surface of the test coupons exposed to the different test waters. In the presence of chloride concentration of 10 mg/L (10Cl and 10Cl+Cl_2), a dense and compact oxide layer with spherical particles was the dominant morphology of corroding iron surfaces (Figure 4.8(a) and 4.8(d)). At the chloride concentration of 75 mg/L (75Cl and 75Cl+Cl_2) (Figure 4.8(b) and 4.8(e)), a porous layer with a mixture of pseudo-hexagonal and sharp edged rod-like structures dominated. At the highest chloride concentration of 250 mg/L (250Cl and 250Cl+Cl_2), the surface of corroding iron was shown to be comprised primarily of porous and highly crystalline structures (Figure 4.8(c) and 4.8(f)).

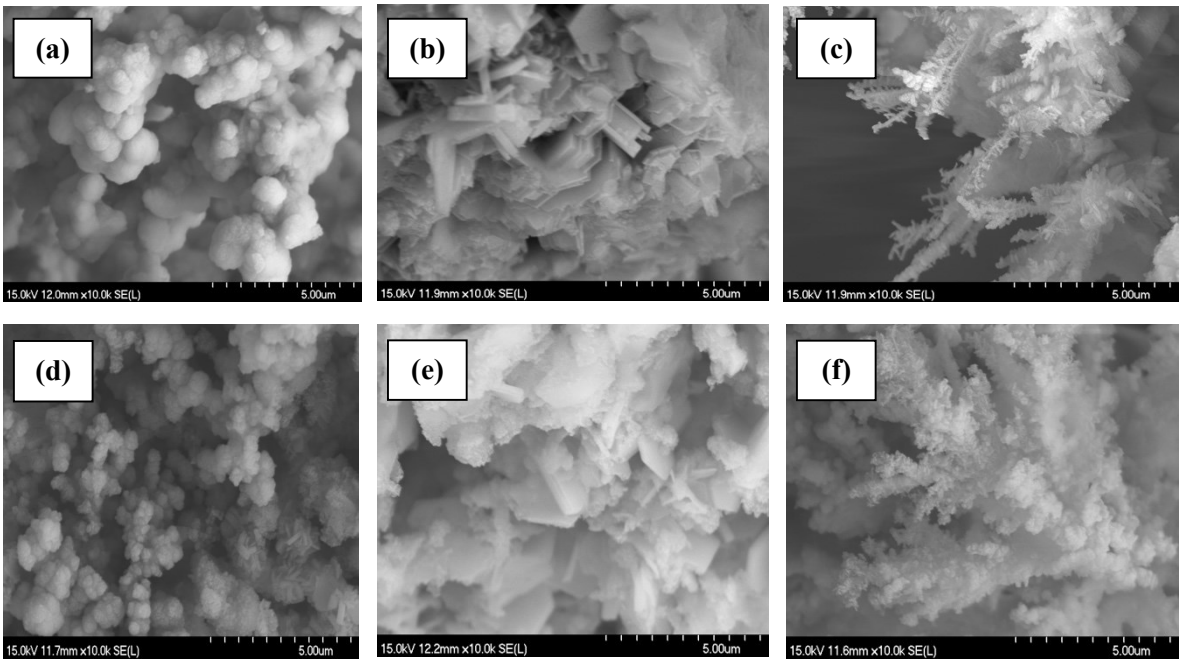

Figure 4.8 SEM images of iron corrosion products on surface of coupons exposed to (a) 10Cl, (b) 75Cl and (c) 250Cl bottles. SEM images of iron corrosion products on surface of coupons exposed to (d) 10Cl+Cl_2, (e) 75Cl+Cl_2 and (f) 250Cl+Cl_2 bottles.

Overall, the SEM images demonstrated that with increase in chloride concentration more crystalline and porous scales were formed on the surface of the metal. This promoted the diffusion of ferrous ions (Fe^{2+}) from the metal-scale interface to the bulk water. Moreover, more crystalline iron oxides like lepidocrocite, which are less corrosion protective and can be reduced more easily than others (Sarin et al. 2004a) were formed at increased concentrations of chloride. These iron oxides serve as a source of ferrous iron that can be released into the bulk water. As a result, higher amount of soluble ferrous iron ions is available to react with chlorine and settle out as ferric iron particles. On the other hand, diffusion of chlorine to the metal surface is easier through the porous scales, which promotes dissolution of the metal and results higher corrosion rates. This is in accordance with the results of settled iron particles and corrosion rate.

Comparison of the surface of coupons taken from non-chlorinated and chlorinated bottles showed that chlorine did not cause any significant change on the morphology of corrosion products on the surface of cast iron coupons.

4.7 Characterization of Cast Iron Biofilm Communities

Quantification of the *16S rRNA* gene copy numbers from the bacterial biofilm communities that had developed on the cast iron coupons after 8 weeks showed that community size depended on chlorination and increasing chloride concentration (Figure 4.9(a)). For the non-chlorinated biofilm, increasing chloride concentrations from 10 (10Cl) to 250 mg/L (250Cl) caused a nearly 2-log reduction from 7.86 Log_{10} *16S rRNA* copies/cm^2 to 6.07 Log_{10} *16S rRNA* copies/cm^2, respectively. The chlorinated biofilm populations ranged from 5.76 Log_{10} *16S rRNA* copies/cm^2 at a chloride concentration of 10 mg/L (10Cl+Cl_2) to 3.11 Log_{10} *16S rRNA* copies/cm^2 at a chloride concentration of 250 mg/L (250Cl+Cl_2), indicating that the chlorination combined with elevated chloride concentrations inhibited biofilm development and likely also diminished the putative biological component of the observed iron corrosion. Chlorination alone resulted in a 2-log reduction in the biofilm population.

Looking at the structure of the microbial communities, five bacterial phyla were present in all biofilms including the dominant *Proteobacteria* (accounting for 70-96%) that was mainly represented by three classes (*Alphaproteobacteria*, *Betaproteobacteria*, and *Gammaproteobacteria*). The phyla *Firmicutes*, *Fusobacteria*, *Actinobacteria*, and *Bacteroidetes* were also identified in all cast iron biofilms. Analyses of the class level taxonomic profile of biofilms revealed notable differences between the non-chlorinated

and chlorinated biofilms with minor differences occurring among the three different chloride concentrations (Figure 4.9(b)). In non-chlorinated bottles, *Betaproteobacteria* dominated with relative abundances of 65.5% to 77.4% followed by *Alphaproteobacteria* (4.3-27.3%) and *Gammaproteobacteria* (2.9-11.8%). Other minor classes were *Actinobacteria* (1.0-3.2%), *Bacilli* (0.7-2.5%), *Fusobacteria* (0.56-1.5%), and *Clostridia* (0.07-0.41%). However, in the chlorinated bottles, *Gammaproteobacteria* became the most abundant class (35.4-41.8%), while comparatively, the relative abundances of *Alphaproteobacteria* (2.5-13.2%), *Betaproteobacteria* (23.5-31.2%) and *Actinobacteria* (0.59% - 2.6%) decreased. Chlorination also increased the relative abundances of *Bacilli* (11-15.5%), *Clostridia* (0.78-2.5%) and *Fusobacteria* (5.6-12.6%). When the chloride concentration rose from 10 mg/L to 250 mg/L in both non-chlorinated and chlorinated bottles, the proportions of *Betaproteobacteria*, *Gammaproteobacteria*, *Bacilli*, *Actinobacteria* and *Clostridia* increased while *Alphaproteobacteria* and *Fusobacteria* decreased. The PCoA plot, seen in Figure 4.9(c), confirmed these trends and shows that 89.7% of the variation in microbial diversity depended on chlorination while a smaller difference (5.62% variation explained) was observed between the chloride concentrations. Among groups of bacteria potentially involved with iron corrosion, the relative abundances of the corrosion inhibitory NRB *Hyphomicrobium* (<0.01-0.10%), *Sphingomonas* (0.16-1.35%), and *Acinetobacter* (<0.01-7.5%) increased in the non-chlorinated bottles with rising chloride levels. However, when the chloride concentrations rose in the chlorinated bottles these NRBs fell below 0.01%. If present, *Hyphomicrobium* has been shown to inhibit corrosion by redox cycling of iron to increase the precipitation of iron oxides and formation of passivating Fe_3O_4 on cast iron pipes in drinking water distribution systems

subjected to UV/Cl_2 disinfection (Zhu et al. 2014). Microbial siderophores, including those produced by *Sphingomonas* and *Acinetobacter*, capture the iron thereby inhibiting the dissolution of iron and iron corrosion (Little et al. 2007, Zhu et al. 2014). Members of IRB including *Clostridium, Pseudomonas* and *Rhodobacter* (Sun et al. 2014, Zhu et al. 2014) were also detected. Both *Clostridium* and *Pseudomonas* increased as chloride concentrations went from 10 mg/L to 250 mg/L. *Clostridium*, which can inhibit corrosion (Sun et al. 2014), increased from 0.05% to 0.27% in the non-chlorinated bottles and from 0.52% to 1.9% in the chlorinated bottles. *Pseudomonas* spp., which can contribute to the corrosion of steel (Abdolahi et al. 2015), followed the similar pattern; however, its initial relative abundance at lowest chloride level (10 mg/L) increased with rising chloride concentrations in both non-chlorinated (1.23-2.3%) and chlorinated bottles (16.7-24.6%). In contrast, *Rhodobacter* decreased from 2.89% to 0.44% when the chloride concentrations increased in the non-chlorinated bottles and was not detected in the chlorinated bottles. It was concluded that, while the biofilm contained bacteria with possible impacts on corrosion, the community size decreased to levels as low as 3.1 Log_{10} *16S rRNA* copies/cm^2 in the chlorinated water with 250 mg/L chloride, rendering it unlikely that the microbes contribute to the observed corrosion under conditions tested in this experiment.

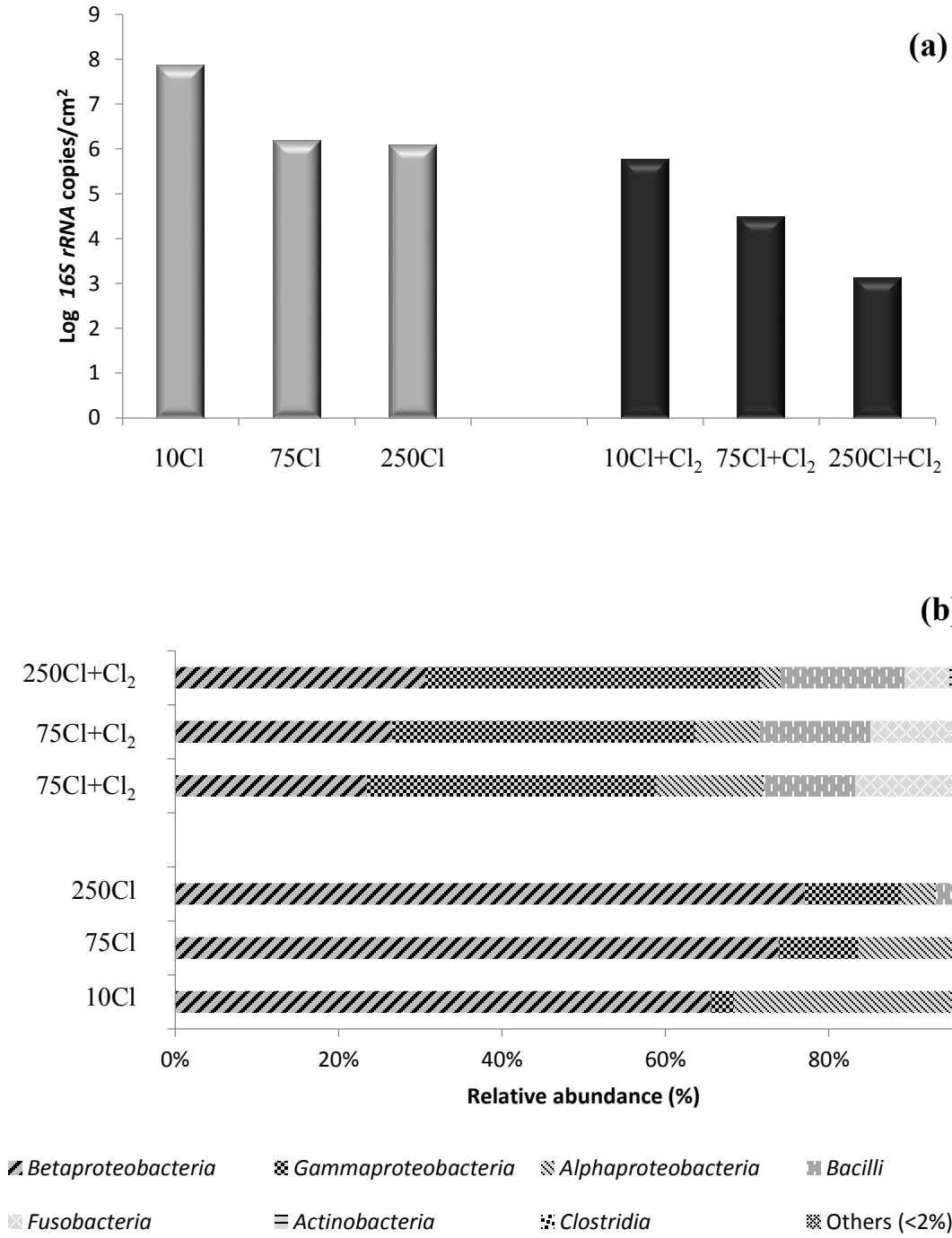
(a)
Log 16S rRNA copies/cm²
9
8
7
6
5
4
3
2
1
0
10Cl
75Cl
250Cl
10Cl+Cl2
75Cl+Cl2
250Cl+Cl2
(b)
250Cl+Cl2
75Cl+Cl2
75Cl+Cl2
250Cl
75Cl
10Cl
0%
20%
40%
60%
80%
100%
Relative abundance (%)
Betaproteobacteria
Gammaproteobacteria
Alphaproteobacteria
Bacilli
Fusobacteria
Actinobacteria
Clostridia
Others (<2%)

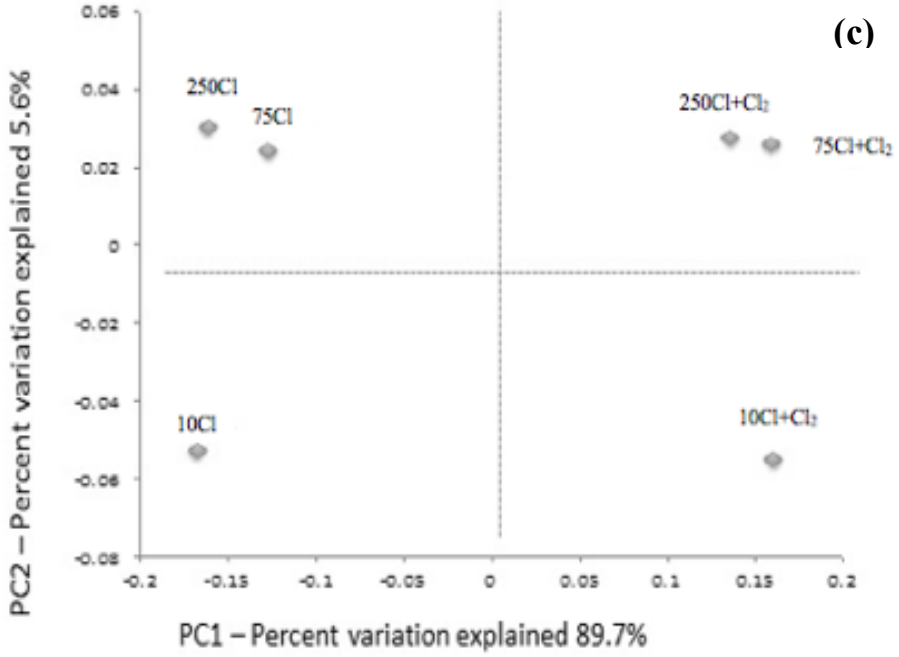

Figure 4.9 Size and diversity of the bacterial biofilm communities on cast iron coupons exposed to different chlorination and chloride levels for 8 weeks. (a) Community size as 16S rRNA gene copy numbers/cm^2 (n=1), (b) Relative abundance of bacterial classes and (c) Principal coordinate analysis (PCoA) of bacterial community diversity in relation to the different treatments.

4.8 Conclusion

This study looked at the effect of varying chloride concentrations in conjunction with chlorine disinfection on iron corrosion particles and water quality in cast iron drinking water distribution systems. The results revealed that

1. There were combined effects of these two water parameters on the properties of iron corrosion particles and water quality in drinking water distribution system.
2. In the presence of both elevated chloride concentration and chlorine disinfection, larger iron particles were formed and released from the surface of cast iron coupons, which settled faster and resulted in lower concentrations of total suspended and

dissolved iron concentration, color and turbidity in the stagnant water conditions simulated in this experiment.

3. The formation of goethite and lepidocrocite was enhanced by the addition of chlorine.
4. In the presence of elevated chloride concentration, more crystalline and porous scales were formed on the surface of cast iron coupons, which promoted the iron corrosion and release. However, chlorine disinfection did not cause any significant change on the morphology of corrosion products on the surface of cast iron coupons.
5. Bacterial biofilm population decreased with chlorination and increasing chloride concentrations and were unlikely to impact the observed corrosion.

Chapter 5 Effect of Different Corrosion Control Strategies on the Properties of Iron Corrosion Products and Water Quality in Chlorinated Distribution Systems in Presence of Varying Chloride Concentrations

5.1 Abstract

Corrosion control is a major challenge and cost for many water utilities worldwide. The purpose of this study was to evaluate the effectiveness of two different corrosion control strategies (orthophosphate addition and pH adjustment) on iron corrosion and release from cast iron coupons in the presence of high chloride concentrations in conjunction with chlorine disinfection. It also investigated the structures and morphologies of resulting iron corrosion products. An 8-week bench-scale experiment was conducted with two new cast iron coupons placed in 1-L amber glass bottles containing model water with different concentrations of chloride (10, 75 and 250 mg/L), and maintained chlorine residuals between 0.2 and 1.0 mg/L. Two commonly used corrosion control approaches in the presence of a chlorine residual were compared in this study: (a) pH 7.5 with orthophosphate (2 mg/L) corrosion inhibitor or (b) pH adjustment to 9.2. Key findings from this study were that both these approaches reduced the chlorine demand, although to a lesser extent in orthophosphate systems. Orthophosphate addition and pH adjustment made the iron particles' zeta potential more negative and decreased their particle size, which in turn increased turbidity and average total suspended iron in the stagnant water. The results also showed that both corrosion control strategies lowered the corrosion rate of cast iron coupons, with the orthophosphate addition being more efficient than pH adjustment to 9.2. More corrosion protective and dense oxide layers were formed with addition of

orthophosphate and pH adjustment to 9.2; however, these observed differences were not significant at the high chloride concentration of 250 mg/L. Although the biofilm population was increased by adding orthophosphate and decreased by pH adjustment to 9.2, the overall population remained low due to chlorine disinfection and increased chloride concentrations therefore the biofilm was unlikely to contribute to the observed cast iron corrosion under these conditions.

Keywords Iron release, Corrosion control, Orthophosphate, pH, Corrosion scale, High chloride concentration, Iron corrosion particles, Biofilm population.

5.2 Introduction

Water discoloration due to iron corrosion is the largest cause of consumer complaints (Husband and Boxall 2011). The colored water contains suspended particulate iron that can originate from the source water or from distribution system materials such as cast iron water mains. The release of iron from cast iron pipes in water distribution systems is a complex process including corrosion, redox reactions, precipitation, dissolution, solid phase reactions and microbiological activities. Corrosion reactions produce ferrous ions (Fe^{2+}), which either dissolve in the water or deposit as a scale on the surface of corroded metal. The released Fe^{2+} ion in the bulk water may be oxidized into ferric ions (Fe^{3+}), which forms particles and contributes to color and turbidity in water. Iron corrosion scales may also dissolve and contribute to the amount of iron release (Sarin et al. 2004a). According to previous studies, different corrosion products are formed on iron surfaces under different conditions. Typical iron corrosion products found in iron corrosion scales include goethite (α-FeOOH), lepidocrocite (γ-FeOOH), magnetite (Fe_3O_4), maghemite (α-Fe_2O_3), hematite

(Fe_2O_3), ferrous hydroxide ($Fe(OH)_2$), ferric hydroxide ($Fe(OH)_3$), ferrihydrite ($5Fe_2O_{3.9}H_2O$), siderite ($FeCO_3$) and calcite ($CaCO_3$) (Sarin et al. 2004b, Wang et al. 2012). The exact composition and structure of these corrosion products depends on and can vary based on water quality parameters, water flow regimes and seasonal temperature changes (Chun et al. 2005). Colored water problems can be reduced by controlling corrosion, properties of the iron particles and iron release from corrosion scales (Lytle et al. 2005). Corrosion and/or metal release in drinking water distribution systems may be controlled by two common approaches: (1) addition of a corrosion inhibitor and/or (2) pH adjustment.

The addition of phosphate-based chemicals such as orthophosphate has been reported to be effective in controlling iron corrosion and release (Maddison et al. 2001, Lytle and Snoeyink 2002, Sarin et al. 2003, Lytle et al. 2005, Alshehri et al. 2009, Mi et al. 2016). Orthophosphate inhibitors promote the formation of a protective impervious layer on the surface of cast iron, which in turn makes the iron surface less available to react with corrosive water (Singley 1994, Sarin et al. 2004b). It has been suggested that orthophosphates form insoluble phosphates in the corrosion scale that decrease the permeability of the scale, thereby reducing the iron release (Sarin et al. 2003, Ebrahimi Mehr et al. 2004, Lytle et al. 2005). However, there are contradictory results in the research literature. Studies conducted by McNeill and Edwards (2000), and Zhang and Andrews (2011) showed that addition of phosphate-based corrosion inhibitors has no effect or a detrimental effect on iron release under stagnant and low flow conditions. Previous studies (Lytle and Snoeyink 2002, Lytle et al. 2005, Rahman and Gagnon 2014) also evaluated the effects of phosphate-based corrosion inhibitors on iron release and properties of the iron suspensions. They concluded that phosphate changed the properties of iron particles and

reduced color and turbidity of the resulting iron suspensions.

Raising the water pH protects pipes by decreasing the solubility of pipe materials and corrosion products, thereby decreasing the corrosion rate and metal concentrations at the tap (Maddison et al. 2001, Zhang et al. 2014, Mi et al. 2016). Previous studies (Lasheen et al. 2008) showed that in pH values less than 5 iron corrodes rapidly, while pH values higher than 9 may decrease corrosion rates. Sarin et al. (2003) reported that increasing pH from 7.6 to 9.5 could reduce the amount of iron released to water from more than 1.5 mg/L to less than 0.3 mg/L over a period of few months. Investigation of the effect of pH adjustment on iron release and properties of the iron suspensions revealed that stability of the iron suspensions increased as pH of the solutions increased (Lytle et al. 2004).

Both corrosion control strategies can potentially affect the microbial biofilm communities in the distribution system. Phosphate-based compounds used as corrosion inhibitors in drinking water distribution systems are nutrients for bacterial growth. Some studies showed that addition of phosphate stimulates bacterial regrowth in biofilm or in bulk water (Szewzyk et al. 2000, Appenzeller et al. 2001, Appenzeller et al. 2002, Gouider et al. 2009, Jang et al. 2012). Increasing pH used as a common corrosion control strategy can reduce the biofilm growth in drinking water distribution systems (Meckes et al. 1999).

Chloride can be present in drinking water from various sources. High chloride concentrations are believed to accelerate the corrosion of cast iron and its release to the water by promoting formation of porous and less protective corrosion scales (Taylor 1984, Sarin et al. 2004a, Sarin et al. 2004b, Liu et al. 2013, Chapter 4). Some researchers investigated the effects of control measures on iron release with blending of different water sources containing high chloride concentrations (Lytle et al. 2005, Alshehri et al. 2009,

Zhang et al. 2014, Mi et al. 2016). However, little information is available about the mechanism and impact of variable chloride concentrations on effectiveness of the corrosion control practices. In addition, the effect of corrosion inhibitors on the properties of the iron corrosion products and iron suspensions in presence of high chloride concentration is lacking.

The purpose of this study was to evaluate the influence of different corrosion control strategies (orthophosphate addition and pH adjustment) on iron corrosion and release from corroding iron surfaces in the presence of high chloride concentrations in chlorinated systems, and to investigate the structures and morphologies of resulting iron corrosion products and particles. An additional goal was to investigate how biofilm populations responded to these two corrosion control strategies (orthophosphate addition and pH adjustment) in the presence of variable chloride concentrations in chlorinated systems.

5.3 Materials and Methods

5.3.1 Experimental Design

An 8-week bench-scale fill-and-dump experiment was conducted to examine the impact of two different corrosion control treatments on iron release from cast iron coupons in model waters with chloride concentrations of 10, 75 and 250 mg/L concentrations of chloride with maintained chlorine residual between 0.2 and 1.0 mg/L. Two different corrosion control treatments were compared in this study: (a) pH 7.5 with orthophosphate (2 mg/L) corrosion inhibitor or (b) pH 9.2. A 0.1 M phosphoric acid (H_3PO_4) solution was used to provide the phosphate dose, and pH adjustment to the desired level was performed using a 1 N sodium hydroxide (NaOH) solution. pH levels were maintained constant at least 15 minutes before

the start of the experiment.

The source water used in this experiment was taken from the filter effluent of Halifax Water's J.D. Kline Water Supply Plant (prior to final disinfection, pH adjustment and corrosion inhibitor addition), and then spiked with chloride, free chlorine, orthophosphate and sodium hydroxide to produce the test waters.

The experiments were conducted using nine 1-L amber glass bottles (Figure 5.1) in parallel with an additional 9 bottles run in parallel as duplicates. The reaction bottles were made chlorine demand-free before use by soaking in a concentrated sodium hypochlorite solution of 300 mg/L for 24 hours prior to the test. Afterwards, the bottles were rinsed thoroughly three times with deionized water and dried at 100 °C overnight. All the bottles were chlorinated to achieve an initial chlorine residual of 1 mg/L using a chlorine stock solution of 1000 mg/L prepared by a 5-6% aqueous sodium hypochlorite (NaOCl) solution (Fisher Scientific, USA). Free chlorine residuals were monitored on a daily basis and the bottles were boosted with required chlorine dose to maintain the target free chlorine residuals between 0.2 and 1 mg/L.

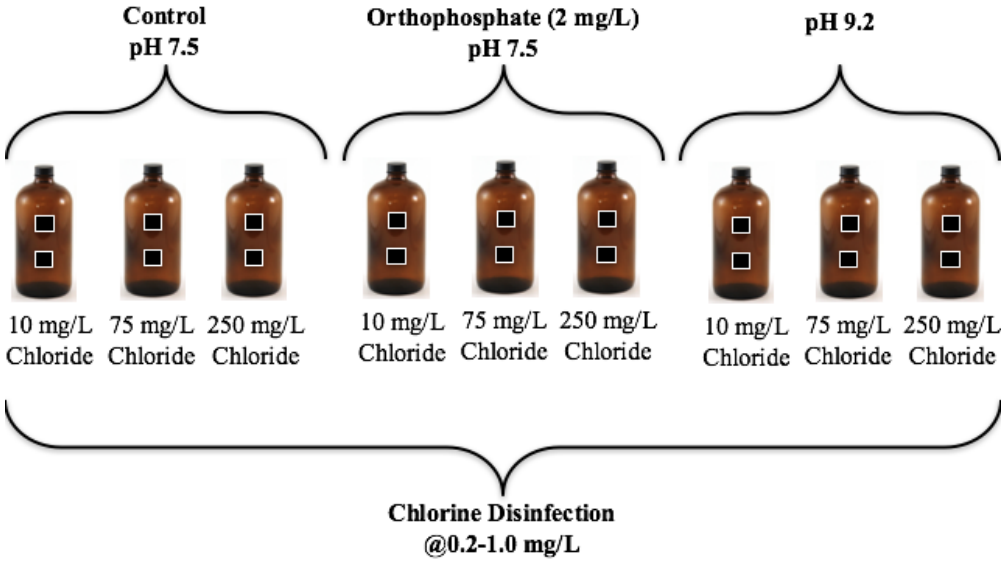

Figure 5.1 Schematic of experimental design.

Two new iron coupons (with dimensions of 1.0 cm x 1.0 cm x 0.5 cm), one with a predetermined weight for corrosion rate measurement and the other designated for biofilm and morphological analyses, were placed in each bottle using nylon line. New coupons were used in this experiment to minimize any impacts from service age. The bottles were capped and kept in the dark to simulate the dark environment in distribution system. The test bottles were kept at room temperature and gently agitated for 5 rotations on a daily basis after addition of chlorine to mix the water, and then allowed to sit for a 24-hour stagnation period. Care was taken to avoid disturbing the coupon surfaces and settled particles. At the end of each week, all of the water in the bottles were decanted and replaced with fresh 1.0 L of model water to simulate the intermittent water flow environment in the actual pipes in water distribution system. Before decanting the water, samples were taken and prepared for analysis of total and dissolved iron concentrations, DOC, pH, temperature and turbidity.

Size analysis and images of settled iron particles were analyzed using a Micro-Flow Imaging (MFI) system (Brightwell Technologies Inc., Ottawa, ON). To collect settled iron particles, bottles were inverted gently two times and a 30 mL sample was collected using a wide mouth pipette and resuspended in 40-mL glass vials.

5.3.2 Determination of Corrosion Rate and Corrosion By-products Characteristics

At the end of week 8, the two iron coupons were removed from each bottle. The biofilm was harvested from one side of one of the coupons (see section 5.3.4) and then the coupons were dried under vacuum condition (to avoid altering the crystalline composition of corrosion scales under the atmosphere) for one day at room temperature. The oxidation products were removed from the surface of the coupons following methodology presented elsewhere (Liy et al. 2013). These coupons were then rinsed with deionized water, wiped, air-dried for a day and weighed to determine the weight loss and corrosion rate over the experiment (ASTM G31-72).

The corrosion scales were scraped from the surface of other selected coupons with a clean utility knife to be analyzed for their morphology and composition using Scanning Electron Microscopy (SEM, Hitachi S-4700, Japan) and X-ray diffraction (XRD, Siemens D500). XRD analysis used CuKα radiation (λ=1.54 Å) at a scanning range of 2θ=10-70º, tube voltage of 35 kV, and tube current of 30 mA.

5.3.3 Water Quality Analysis

Free chlorine was measured on a daily basis using the DPD colorimetric method at a wavelength of 530 nm using a DR5000 UV-Visible spectrophotometer (HACH Co.,

Loveland, Colorado). Before every water exchange, samples were taken to measure the total suspended iron concentration using an Inductively Coupled Plasma-Mass Spectroscopy (ICP-MS) instrument (Thermo Fisher Scientific, MA, USA). Two drops of concentrated nitric acid were added and the samples were refrigerated at 4ºC until analysis was performed. General water quality parameters including DOC, pH, temperature and turbidity were also measured on a weekly basis. Samples for DOC analysis were passed through a 0.45 μm polysulfone membrane filter and analyzed using a TOC-V CHP analyzer (Shimadzu Corporation, Kyoto, Japan). pH and temperature of samples were measured using a pH meter (CyberScan pH 6000). A HACH 2100 AN Turbidimeter was used to measure the turbidity in water samples. Zeta potential of the samples was measured using Zetasizer Nano (Malvern Instruments Ltd., UK).

5.3.4 Extraction of DNA from Coupon Biofilms

At the end of Week 8, the biofilm formed by the naturally occurring microbiota on one coupon from each treatment was harvested by scraping with a sterile spatula and transferred into 10 mL of sterile phosphate-buffered saline (pH 7.0) in a 50 mL sterile test tube. Following centrifugation at 3200 x *g* for 15 minutes, the supernatant was discarded. The resulting cell pellet was resuspended using the residual liquid (250 μL) and subjected to genomic DNA extraction using the MO BIO PowerSoil DNA isolation kit (MO BIO Laboratories, Carlsbad, CA, USA) according to manufacturer's instructions. DNA concentrations were then quantified with a QuantiFluor@ ds DNA kit (Promega Corporation, Madison, WI, USA) and a Quantus Fluorometer (Promega) and ranged from 0.02-0.15 ng/μL. All DNA samples were stored at -20°C until further analysis.

5.3.5 *16S rRNA* Copy Number in Biofilms

To determine the size of the biofilm population, the bacterial *16S rRNA* genes copy numbers were detected using a quantitative polymerase chain reaction (qPCR) assay with primer set BACT 2 (Suzuki et al. 2000). The qPCR amplification was conducted on a Bio-Rad CFX96 Touch Real-Time PCR system (Bio-Rad, Hercules, CA, USA). Each reaction (20-µL volumes) consisted of 4.0 µL of template DNA, 4.4 µL of sterile and nuclease-free water (Fisher Scientific), 0.8 µL of each primer (10 µM), and 10 µL of Power SYBR Green PCR master mix (Applied Biosystems, Life Technologies, Canada) using the following thermocycler program: 10 minutes initial denaturation at 95 °C, followed by 40 cycles of 15 seconds (s) denaturation at 94 °C, 30 s annealing at 55 °C, and 30 s extension at 72 °C. In order to confirm the presence of the *16S rRNA* gene PCR amplicon, a melt curve analysis was performed and the melting temperature of the PCR amplicon is 80.7 °C ± 0.4 °C.

A plasmid construct containing the partial region of bacterial *16S rRNA* gene was a generous gift from Dr. Yost (University of Regina, personal communication) and used to create a standard curve (10-fold serial dilutions, 10^1 to 10^8 copies/µL) to enable quantification of *16S rRNA* copy numbers. Each standard, sample, and non-template control was run with two technical replicates. Between the replicates, the difference of the threshold cycle (Ct) value was less than 0.5. The efficiency of qPCR assay was 102%, with an R^2 value of 0.999. The limit of detection (LOD) is 10^3 copies/cm^2 coupon. The limit of quantification (LOQ) for the *16S rRNA* gene is 10^2 copies/µL. Quantity of *16S rRNA* gene numbers was reported as $\log_{10}$ gene copies/cm^2 of cast iron coupon area.

5.3.6 Data Analysis

Statistical analysis was conducted to identify any significant differences between the average values for the water quality parameters measured. Statistical procedures followed an analysis of variance (ANOVA) test at a significance level of 95%. Error bars included in figures, and ± values throughout the manuscript represent one standard deviation from the mean.

5.4 Results and Discussion

5.4.1 Characterization of Corrosion Scale

5.4.1.1 XRD

The XRD patterns of the corrosion scales scraped from the surface of the cast iron coupons in the presence of different corrosion control strategies and the control system at chloride concentration of 75 mg/L are shown in Figure 5.2. Results revealed that goethite (α-FeOOH), magnetite (Fe_3O_4), lepidocrocite (γ-FeOOH) and siderite ($FeCO_3$) were the main crystalline phases identified in all of the iron corrosion scales, in agreement with the results reported by other researchers (Sarin et al. 2004b, Teng et al. 2008, Echeverría et al. 2009, Wang et al. 2012). Results showed that intensity of magnetite peaks increased over goethite and lepidocrocite peaks in orthophosphate and pH 9.2 systems compared to control system. The same trend was observed at other concentrations of chloride (10 mg/L and 250 mg/L) and the XRD patterns are presented in Appendix A.

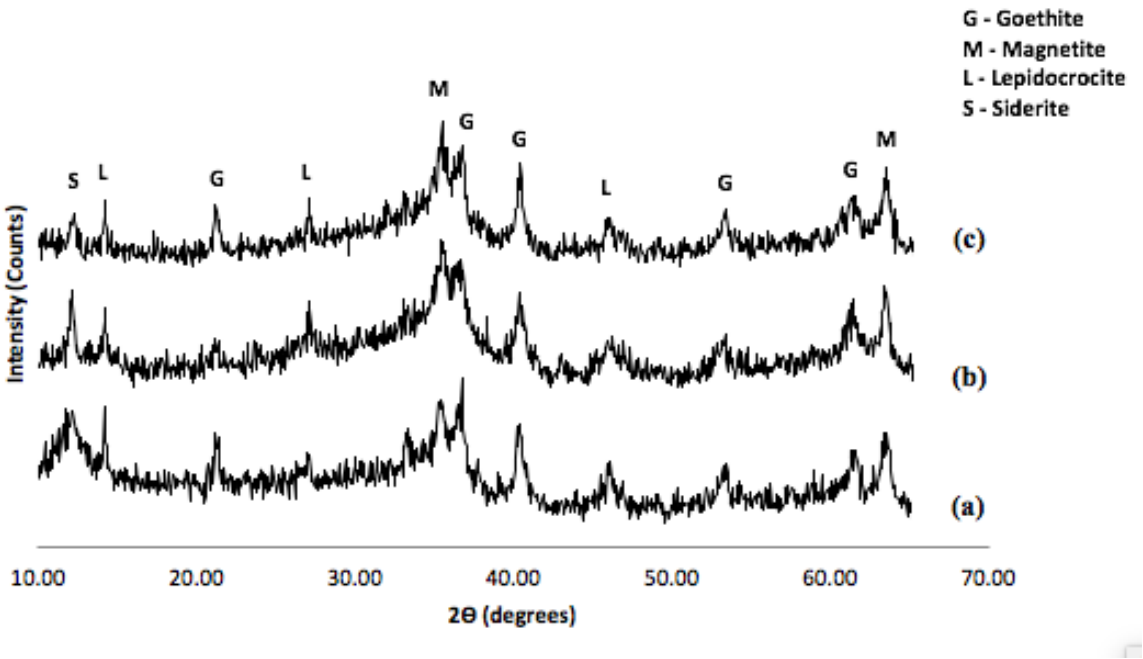

Figure 5.2 XRD patterns of iron corrosion products on surface of coupons exposed to (a) control, (b) orthophosphate and (c) pH 9.2 systems at chloride concentration of 75 mg/L.

The formation of Fe_3O_4 is favored at pH values above 8 (Cornell and Schwertmann 2003) and it has been reported previously to be thermodynamically stable and less likely to dissolve. Moreover, iron corrosion scales with a high percentage of magnetite have usually shown dense and good corrosion protective properties. No phosphate-containing solids were identified on the surface of cast iron coupons in orthophosphate system by XRD. An explanation can be that phosphate corrosion inhibitors may have formed an amorphous or semi-amorphous film on the surface of cast iron coupons, acting as a barrier between the metal surface and the water in contact with it (Zhang and Andrews 2011).

5.4.1.2 SEM

Iron corrosion surfaces were further characterized by SEM. Figure 5.3 shows the representative images obtained from SEM analysis of iron corrosion products on the

surface of the test coupons exposed to different treatments at a chloride concentration of 75 mg/L. The oxide layer formed on the surface of coupons exposed to all treatments showed structural similarities (a mixture of pseudo-hexagonal and spherical particles structures). However, more densely shaped particles with less crystalline morphologies appeared on the surface of coupons exposed to orthophosphate (Figure 5.3(b)) or pH 9.2 (Figure 5.3(c)) systems indicating formation of a protective layer. The oxide layer formed on the surface of coupons in the control system (Figure 5.3(a)) was more irregular and open than for the other systems.

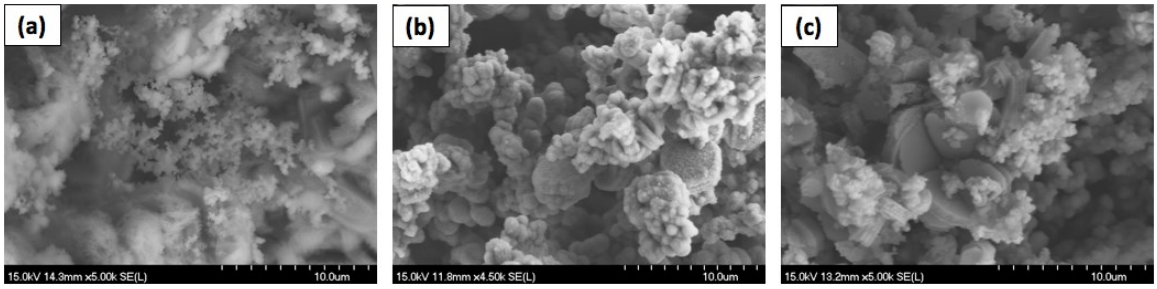

Figure 5.3 SEM images of iron corrosion products on surface of coupons exposed to (a) control, (b) orthophosphate and (c) pH 9.2 systems at chloride concentration of 75 mg/L.

5.4.2 Chlorine Demand

As mentioned before free chlorine residuals were measured on a daily basis in both duplicate bottles and the bottles were boosted with required chlorine dose to maintain the target free chlorine residuals between 0.2 and 1 mg/L. Average daily chlorine dosages for exposure weeks 5 to 8 in both duplicate bottles (Figure 5.4) showed that, regardless of treatment, a higher chlorine dose was required to maintain the target free chlorine residual in presence of higher chloride concentration, which was in agreement with the previous studies (Zhang et al. 2008, Sharafimasooleh et al. 2015).

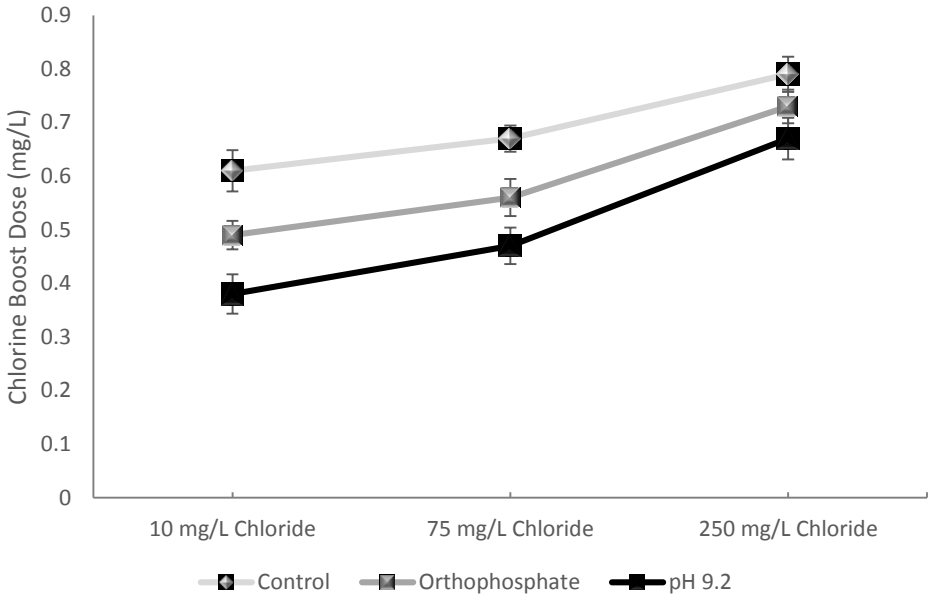

Figure 5.4 Average chlorine boost dose in presence of different treatments (n=8).

Results showed that there was higher chlorine demand in the control system compared to orthophosphate and pH 9.2 systems, showing that both approaches were able to minimize the chlorine demand, although to a lesser extent at chloride concentration of 250 mg/L. However, chlorine demand was relatively higher in orthophosphate system compared to pH 9.2 systems. Lower chlorine demand in the presence of orthophosphate compared to the control system is likely attributed to the formation of the protective scale on the surface of cast iron coupons observed in SEM results, thereby making the iron surface less available to react with chlorine. Formation of protective scale could also decrease the release of iron corrosion products, which readily react with oxidizing agents like chlorine. Decreasing the solubility of corrosion products and formation of denser ferric phases on the surface of cast iron coupons could be the reason for lower chlorine demand at pH 9.2 system. Low solubility could limit dissolution and release of ferrous iron products to react with chlorine (Sarin et al. 2003, Sarin et al. 2004a), thereby decreasing the chlorine

consumption.

5.4.3 Corrosion Rate

Figure 5.5 shows the corrosion rates calculated from the weight loss of the cast iron coupons under different water conditions at the end of the 8-week experiment. Regardless of the treatment process, the corrosion rates were higher in the presence of higher concentrations of chloride, with chloride concentration of 250 mg/L resulting the highest corrosion rates. This observation was in agreement with the results of previous chapter (Chapter 4) conducted on the effect of variable chloride concentrations on iron corrosion and its release from corroding cast iron coupons. The investigation by Liu et al. (2013) on the effect of blending desalinated water with conventionally treated surface water on iron corrosion and release from iron surfaces, also revealed that the increase of desalinated water ratio in the blend (increase in chloride concentration) was accompanied by a steady increase of iron loss rate due to corrosion.

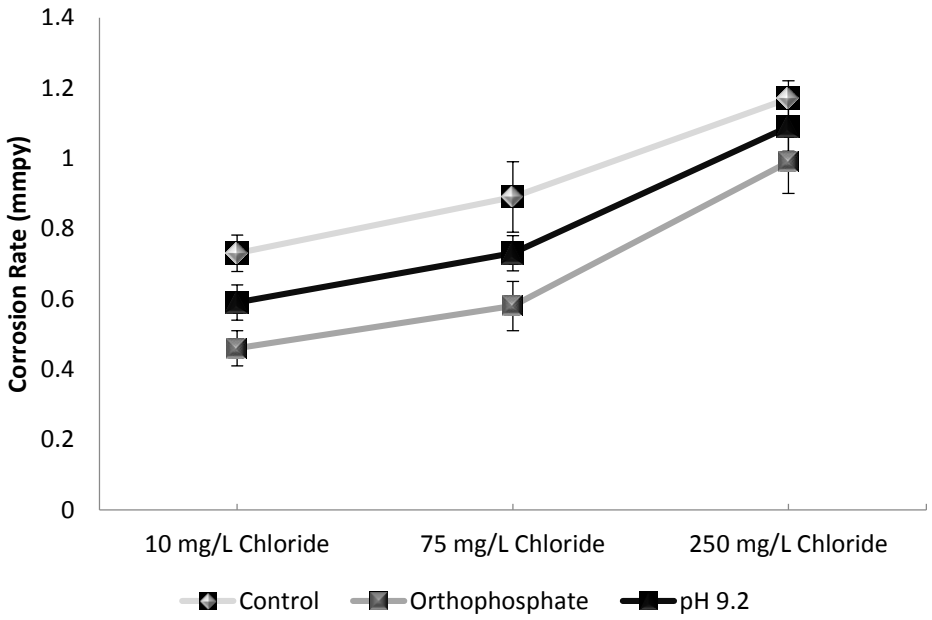

Figure 5.5 Corrosion rate of cast iron coupons under different water conditions (n=2).

Corrosion rates were higher in the control system compared to pH 9.2 and orthophosphate systems, with orthophosphate treatment resulting in the lowest corrosion rate. This indicates both corrosion control strategies were able to decrease corrosion of the test cast iron coupons and orthophosphate was more effective than pH adjustment to 9.2. For example, at a chloride concentration of 75 mg/L, the corrosion rate increased from 0.58±0.07 mm/y to 0.73±0.05 and 0.89±0.1 mm/y in orthophosphate, pH 9.2 and control systems, respectively. Referring to SEM results presented earlier, the formation of an impervious protective layer on the surface of cast iron coupons could act as a barrier between the corroding iron and the water and likely led to lower corrosion rates in presence of orthophosphate. A dense oxide layer (corrosion scale) could limit migration and diffuse of corrosive constituents of the water to the metal surface, thereby preventing dissolution of the metal and resulting lower corrosion rates. Raising the pH of the water could decrease

the corrosion rates by decreasing the solubility of the metal and corrosion products formed on its surface.

The results also showed that at chloride concentration of 250 mg/L these differences were less pronounced, showing that high chloride concentrations interfered with the inhibiting action of the corrosion control strategies used in this experiment and reduced their effectiveness. According to previous studies (Sarin et al. 2004a, Liu et al. 2013, Chapter 4), high chloride concentrations increased the porosity of the oxide layer formed on the surface of cast iron coupons. As a result, it was easier for corrosive elements in the water (e.g. chlorine in this experiment) to diffuse to the iron surface, thereby promoting dissolution of the iron and resulting higher corrosion rates. Chloride is believed to promote formation of lepidocrocite (Taylor 1984, Chapter 4). It has been previously reported to be characteristic of loose and porous corrosion scale, and its presence is likely to play a role in increasing the iron release by increasing the porosity of the scale (Gerke et al. 2008, Liu et al. 2013). These results are in agreement with the results of the characterization of the corrosion scales formed on the surface of cast iron coupons in this study.

5.4.4 Iron Release from Corroding Iron Surfaces

The results of average total suspended iron concentrations released from the test coupons in both duplicate bottles from exposure weeks 5 to 8 are presented in Figure 5.6. The experimental results showed that the total suspended iron concentrations in the water decreased significantly (p-values<0.05) with increasing chloride concentrations in all treatments. For example, in the orthophosphate system, total suspended iron concentrations were 5.4±0.63 mg/L in test bottles with chloride concentration of 10 mg/L, while the total

suspended iron concentrations in test bottles with chloride concentration of 75 mg/L and 250 mg/L were 3.1±0.75 and 1.8±0.5 mg/L, respectively. This was in accordance with the results of previous studies (Liu et al. 2013, Chapter 4), which showed that in presence of elevated chloride concentrations larger iron particles were formed and released from the surface of cast iron coupons. Larger particles settled more rapidly under stagnant conditions and resulted in lower iron concentrations in the stagnant bulk water. The results of turbidity measurements (Figure 5.7) showed similar trend of lower turbidity measurements in the test bottles that were operated at elevated chloride concentrations.

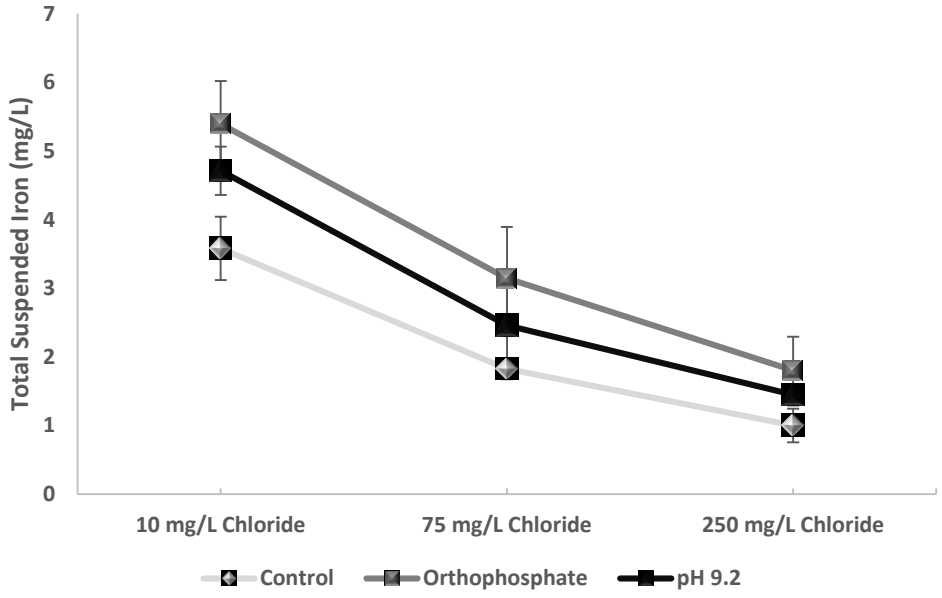

Figure 5.6 Effect of different treatments on total suspended iron concentration (n=8).

Average total suspended iron differed between treatment processes, with the orthophosphate system showing the highest concentration followed by pH 9.2 and then the control system (Figure 5.6). At chloride concentration of 75 mg/L, the concentration of total suspended iron decreased from 3.1±0.75 mg/L in the orthophosphate system to

2.5±0.65 and 1.8±0.15 mg/L in the pH 9.2 and control systems, respectively. The same trend was observed at other concentrations of chloride (10 mg/L and 250 mg/L), although the observed differences were not significant at chloride concentration of 250 mg/L (p-values>0.05). The results of the turbidity measurements presented in Figure 5.7 were also in accordance with these observations.

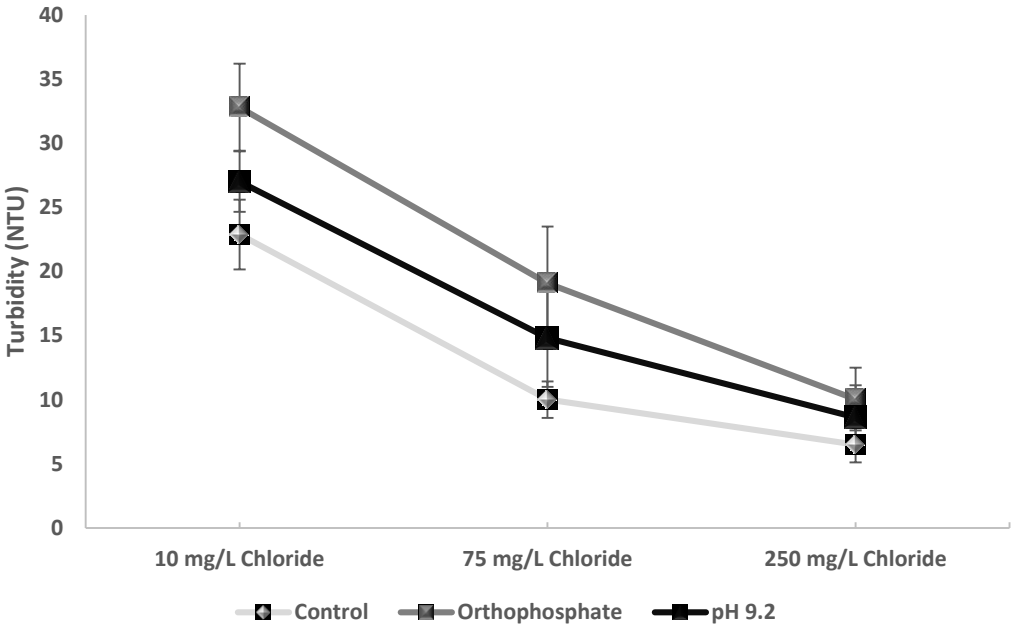

Figure 5.7 Effect of different treatments on turbidity (n=8).

It was hypothesized that smaller iron particles were formed and released from the surface of cast iron coupons with orthophosphate addition and pH adjustment compared to the control system. Small iron particles remained suspended in the bulk water in the stagnant water condition simulated in this experiment and resulted higher concentrations of total suspended iron and turbidity. To test the hypothesis, settled iron particles were collected from the bottles with different treatments and were analyzed using a MFI™ system.

5.4.5 Particle Analysis

5.4.5.1 Particle Size Analysis

Size analysis, concentration, and images of settled iron particles collected from the test bottles were analyzed using a MFI™ system. Results (Table 5.1) showed that, regardless of treatment process, there was significantly (p-values<0.05) higher number of iron particles per milliliter of sample with increasing chloride concentration. For example, in the orthophosphate system, there were $9.1x10^3 \pm 2.0x10^3$ particles/mL at chloride concentrations of 10 mg/L versus $1.8x10^4 \pm 6.8x10^3$ and $5.2x10^5 \pm 2.4x10^5$ particles/mL at chloride concentrations of 75 and 250 mg/L, respectively. The results also showed that larger iron particles were formed and released from the surface of corroding coupons in presence of higher chloride concentration in all treatments, e.g. in orthophosphate system, as the concentration of chloride in water increased from 10 to 250 mg/L, the average particle size of the settled iron particles significantly increased (p-value=0.002) from 4.1±2.7 μm to 30.2±9.4 μm. These results were in agreement with the results of previous chapter (Chapter 4) conducted on the effect of variable chloride concentrations on iron corrosion and its release from corroding cast iron coupons.

Table 5.1 Average particle size and particle concentration of settled particles (n=8)

	Control			Orthophosphate			pH 9.2		
Chloride Conc. (mg/L)	**10**	**75**	**250**	**10**	**75**	**250**	**10**	**75**	**250**
Average Particle Size (µm)	12.2 ±6.5	23.6 ±8.2	46.5 ±11.4	4.1 ±2.7	12.3 ±8.1	30.2 ±9.4	7.57 ±2.8	18.91 ±6.6	39.23 ±12.3
Particle Conc. (#/mL)	$4.3x10^5$ $\pm1.8x10^5$	$8.2x10^5$ $\pm2.8x10^5$	$1.2x10^6$ $\pm6.5x10^5$	$9.1x10^3$ $\pm2.0x10^3$	$1.8x10^4$ $\pm6.8x10^3$	$5.2x10^5$ $\pm2.4x10^5$	$1.2x10^4$ $\pm7.2x10^3$	$5.1x10^5$ $\pm1.2x10^5$	$9.4x10^5$ $\pm1.4x10^5$

Results showed that there was a higher number of iron particles per mL of sample in control system followed by pH 9.2 and then orthophosphate systems. As can be seen in Table 5.1, at chloride concentration of 250 mg/L, there were $1.2x10^6$, $9.4x10^5$ and $5.2x10^5$ particles/mL of sample taken from control, pH 9.2 and orthophosphate systems, respectively. The results showed that although there were higher concentrations of suspended iron in pH 9.2 and orthophosphate systems (Figure 5.6), there were smaller amounts of iron particles detached and settled out from the surface of cast iron coupons with these treatments, indicating that both approaches were able to reduce iron release from corroding iron surfaces compared to the control system. These observations are likely attributed to the formation of a protective scale on the surface of cast iron coupons in pH 9.2 and orthophosphate systems (observed in XRD and SEM analysis results). Formation of the protective scale reduced the rate at which ferrous ions diffused out, and limited dissolution and release of ferrous iron products to react with chlorine, resulting in ferric iron particles that readily precipitate.

The particle size analysis of settled iron particles also showed that smaller iron particles were formed in the orthophosphate system compared to pH 9.2 and control systems. At chloride concentration of 250 mg/L, the average particle size of the settled iron corrosion products increased from 30.2 μm to 39.23 and 46.5 μm in samples taken from the orthophosphate, pH 9.2 and control systems, respectively. These observations support the hypothesis stated earlier that smaller iron particles were formed and released from the surface of coupons with addition of orthophosphate compared to pH 9.2 and control systems. The decrease in particle size with addition of orthophosphate and increase in pH could be attributed to a decrease in zeta potentials in presence of these treatments, which

would decrease particle-particle interactions. In other words, addition of orthophosphate and increase in pH made the zeta potential more negative and reduced interactions between iron particles by strong electrostatic charge repulsion, decreased particle size and increased iron suspension stability (Lytle et al. 2004, Rahman and Gagnon 2014). At chloride concentration of 75 mg/L zeta potential measurements of the water samples were found to be more negative with addition of orthophosphate (-29.7±1.3 mV) and pH adjustment to a lesser extent (-21.8±1.6 mV), compared to that measured in control system (-17.5±0.3 mV). Discrete and stable particles would likely not settle out during the stagnation time due to their small particle sizes and could be the reason for higher concentration of total suspended iron concentrations in the bulk water as observed in Figure 5.6.

5.4.5.2 Particle Imaging

Figure 5.8 presents MFI™ images of the particles collected from the test bottles with chloride concentrations of 250 mg/L in control, orthophosphate and pH 9.2 systems. Comparison of the solid samples visually demonstrated that there were less individual particles with smaller particle sizes in the samples collected from the test bottles in orthophosphate treatment (Figure 5.8(b)) followed by pH 9.2 treatment (Figure 5.8(c)) and control test bottles (Figure 5.8(a)), respectively. This observation was in agreement with the results of particle size analysis presented in section 5.4.5.1. MFI™ images of the particles collected from test bottles with chloride concentrations of 10 and 75 mg/L showed the same trend and were not presented here.

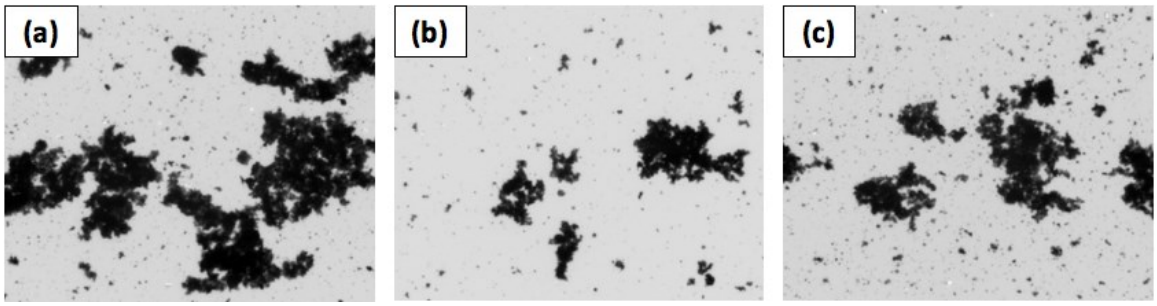

Figure 5.8 Images of the iron particles collected from the test bottles with chloride concentration of 250 mg/L in (a) control, (b) orthophosphate and (c) pH 9.2 systems.

5.4.6 Cast Iron Biofilm Population

The qPCR results are presented in Figure 5.9. It can be seen that similar to findings in the previous chapter, when chloride concentration was increased, the biofilm population decreased regardless of orthophosphate addition or pH adjustment. The biofilm populations ranged from 4.86 Log_{10} *16S rRNA* copies/cm^2 at a chloride concentration of 10 mg/L to 4.65 Log_{10} *16S rRNA* copies/cm^2 at a chloride concentration of 250 mg/L, indicating that the elevated chloride concentrations under the chlorine condition inhibited biofilm growth and likely also reduced the putative microbial activity that could contribute to the observed iron corrosion in the control group.

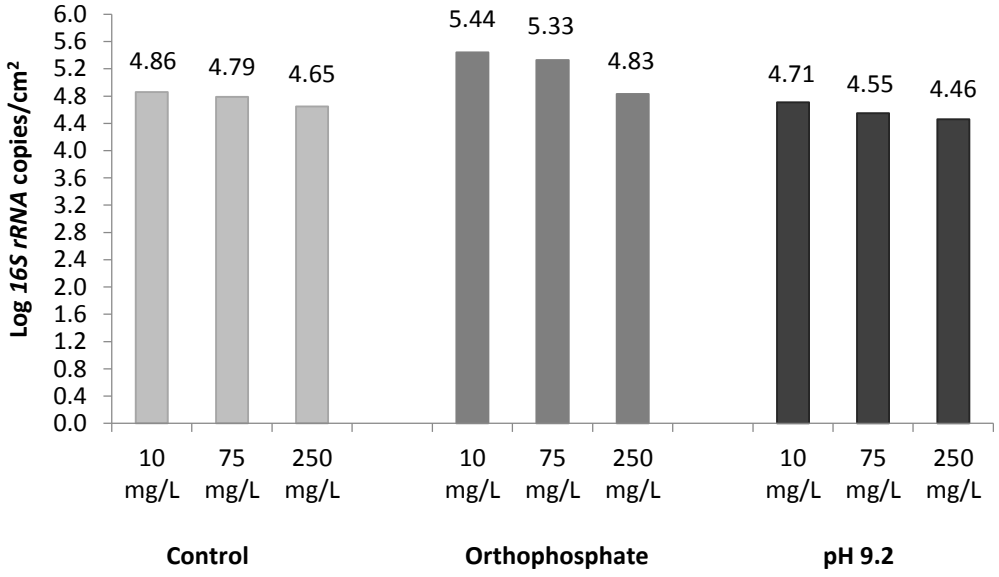

Figure 5.9 The biofilm population as *16S rRNA* gene copy numbers/cm^2 on cast iron coupons exposed to different treatments for 8 weeks (n=1).

The qPCR results show that biofilm population increased by adding orthophosphate at 2 mg/L and decreased when pH was adjusted to 9.2 in comparison with the population in control groups (pH 7.5). When chloride concentrations were at 10, 75 and 250 mg/L, the addition of orthophosphate caused the biofilm population to increase by approximately 0.6, 0.5 and 0.2 Log_{10} *16S rRNA* gene copies/cm^2, respectively. Previous studies showed that phosphate addition (ranging from 10 μg/L to 5 mg/L) promoted bacterial growth in drinking water distribution systems (Miettinen et al. 1997, Sathasivan et al. 1997, Jang et al. 2012). When pH was adjusted from 7.5 to 9.2, the biofilm population was reduced by approximately 0.2 Log_{10} *16S rRNA* gene copies/cm^2 regardless of the level of chloride concentrations, indicating that pH at 9.2 is likely to reduce the biofilm population by providing an aggressive environment for microbial regrowth (Meckes et al. 1999). These observations can also be the cause of chlorine demand results. The addition of orthophosphate as a key nutrient for bacterial growth could promote biofilm formation and

increase the diversity of biofilms grown on cast iron coupons, which in turn increases the resistance of biofilms to chlorine (Simões et al. 2010, Jang et al. 2012), thereby increasing chlorine demand. Lower chlorine demand at pH 9.2 could also be attributed to bacterial growth inhibition at high pH values.

5.5 Conclusion

This study looked at the effectiveness of two commonly used corrosion control approaches (orthophosphate addition and pH adjustment) on the properties of iron corrosion products and water quality in cast iron drinking water distribution systems in presence of varying chloride concentrations. The results revealed that

1. Both approaches were able to reduce chlorine demand, although to a lesser extent in orthophosphate systems.
2. Orthophosphate addition and pH adjustment, (to a lesser extent), made zeta potential more negative, and decreased particle size of iron particles, thereby increasing turbidity and average total suspended iron concentrations in the stagnant water conditions in this study.
3. Both corrosion control strategies were able to reduce corrosion rate of cast iron coupons while addition of orthophosphate was more effective than pH adjustment to 9.2.
4. The formation of magnetite was enhanced over goethite and lepidocrocite on the surface of cast iron coupons using both approaches, which was indicative of formation of dense and corrosion protective scales.

5. The observed trends were less pronounced with increasing chloride concentrations. Increases in the chloride concentration interfered with inhibiting action of the corrosion control strategies and reduced their effectiveness by promoting formation of porous and less corrosion-protective oxide layers, which in turn increased iron corrosion and its release.
6. Rising chloride concentrations also increased the average particle size of the settleable iron particles. The large particles have a greater tendency to settle out in the distribution system pipes, thereby reduce the hydraulic capacity of pipelines in drinking water distribution systems.
7. Orthophosphate addition caused a slight increase of biofilm populations while increasing pH reduced the biofilm population regardless of different levels of chloride concentrations. The low biofilm populations observed in all treatment conditions were unlikely to contribute majorly to the observed iron corrosion.

Chapter 6 Impact of high chloride concentrations on effectiveness of different corrosion control strategies on iron release from corroded cast iron pipes

6.1 Abstract

Iron release from corroded iron pipes is the principal cause of "coloured water" problems in drinking water distribution systems. A 4-month bench-scale study using a fill and dump procedure was performed using old corroded cast iron pipe sections harvested from a local distribution system to investigate the effectiveness of common corrosion control strategies on iron release in presence of high concentrations of chloride. The corrosion control methods investigated were pH adjustment, alkalinity addition and orthophosphate addition. Results showed that, in general, the presence of high concentrations of chloride limited iron sequestration by corrosion control strategies tested in this study. Addition of orthophosphate did not apparently have beneficial effects on iron release for the conditions tested in this study, since no significant mitigation of iron was observed. Elevating the pH of the water to 9.2 was found to effectively control iron release; however, this effect was less profound at high chloride concentration. Alkalinity addition had the largest impact on reducing average iron release and was considered as the preferred corrosion control strategy in the presence of high chloride concentrations and lengthy stagnation times (extremities of distribution system).

Keywords High chloride concentration, Iron release, Orthophosphate addition, pH adjustment, Corrosion scale, Corrosion control, Corroded iron pipes, High alkalinity

6.2 Introduction

Red water occurrence due to iron corrosion in drinking water distribution systems is one of the most prominent causes of consumer complaints (Husband and Boxall 2011). Red water events occur when iron corrosion particles are released to the bulk water. The secondary drinking water guideline for iron is recommended as 0.3 mg/L by the U.S. Environmental Protection Agency (U.S. EPA 2008). The Canadian drinking water quality guideline for iron is an Aesthetic Objective (AO) of less than or equal to 0.3 mg/L (Health Canada 2014). Presence of iron in concentrations greater than 0.3 mg/L in drinking water can be the reason for unpleasant metallic taste and rusty colour. In addition to an unpleasant appearance, red water creates stains in sinks, fixtures, laundry and toilets. Iron in drinking water poses no direct threat to human health, but there are some significant health concerns that are related to iron corrosion in drinking water distribution systems including disinfectant loss (Al-Jasser 2007, Zhang et al. 2008, Sharafimasooleh et al. 2015), bacterial re-growth (McNeill and Edwards 2001, Chowdhury 2012) and also adsorption and release of toxic trace metals such as lead and arsenic, which can cause adverse health effects (Lytle et al. 2010, Peng and Korshin 2011, Trueman and Gagnon 2016).

The corrosion deposits on the surface of old iron pipes may dissolve and contribute to the amount of iron release (Lytle et al. 2004, Sarin et al. 2004a, Benson et al. 2012). The iron corrosion scales have a complex morphology that consists of: (1) a corroded floor, (2) a porous interior, (3) a dense shell-like layer and (4) a top surface layer (Sarin et al. 2001, Sarin et al. 2004b, Lytle et al. 2005, Benson et al. 2012). The corroded floor, which is the corroded metal surface beneath the corrosion scale, is the source of iron that is presented in the corrosion scales. The porous interior of the scale is made up of different

morphologies and structures. A study conducted by Sarin et al. (2001) showed the presence of a high concentration of ferrous iron in this region of the scale, which is present either as solids, or as dissolved iron in water inside the scale pores and cavities. As corrosion continues and scale is developed, a dense shell-like layer covers the porous interior of the corrosion scale. Previous studies conducted by Sarin et al. (2001, 2004b) showed that the shell-like layer is predominantly composed of oxidized species such as magnetite and goethite. This layer prevents flow of oxidants to the pipe surface, and separates them from the oxidizable ferrous ions and solids inside the scale. However, ions may continue to pass through the shell-like layer to maintain electroneutrality. On the top of the shell-like layer (at the scale-water interface), particles are loosely held as a layer, which is in contact with the water and is greatly influenced by water quality. Iron oxides such as lepidocrocite and amorphous ferric hydroxide as well as the precipitates of silicates, phosphates and carbonates may be present in this layer (Sarin et al. 2001). Different iron corrosion products have been shown to form under different conditions, and the exact composition and structure of iron corrosion scales and the rates of iron release strongly depends on the water quality as well as the flow conditions (Sarin et al. 2004a, Chun et al. 2005, Wang et al. 2012).

Chloride can be present in drinking water from various sources. When a source water with high concentrations of chloride enters a drinking water distribution system that contains large amounts of iron pipes, pronounced chemical differences between these waters can affect the stability of the pre-existing iron corrosion scales and result in iron release. High chloride concentrations are believed to accelerate the corrosion of cast iron and its release to the water by promoting formation of porous and less protective corrosion scales. In

addition, chloride ions promote formation of iron oxides (i.e., lepidocrocite) that are less stable against reduction, thereby promoting dissolution of the corrosion scale and higher iron release (more red water events) (Taylor 1984, Sarin et al. 2004a, Sarin et al. 2004b, Liu et al. 2013).

The objective of this study was to test whether common corrosion control strategies (pH adjustment, alkalinity addition and orthophosphate addition) can counteract the possible corrosive effect of high chloride concentrations on iron release from corroded cast iron pipes in drinking water distribution systems. The chloride concentration of 250 mg/L was used to represent the upper limit for the aesthetic objective (AO) for chloride concentrations outlined in the *Canadian Drinking Water Quality Guidelines* (Health Canada 2014) and to model worst-case scenario in terms of elevated chloride concentrations in cast iron systems.

6.3 Materials and methods

6.3.1 Experimental Design

The experiment involved a 4-month bench-scale fill and dump procedure using eight sections of corroded cast iron pipe in parallel (vertical position), with different water compositions (Figure 6.2) to reflect alternative treatments. A pipe section excavated from a local distribution system (with corrosion scale on its surfaces) was used in this study (Figure 6.1).

Figure 6.1 Harvested pipe section from a local distribution system.

The pipe section had received constant exposure to city water until disconnected from service. The pipe sections were approximately 15.2 cm in diameter and were cut into 10 cm-long sections. About 5 cm of their effective inside diameter was lost to corrosion scales. One end of the pipe sections was sealed and the other end was covered with a plastic plate to ensure reduced interaction with the outside environment.

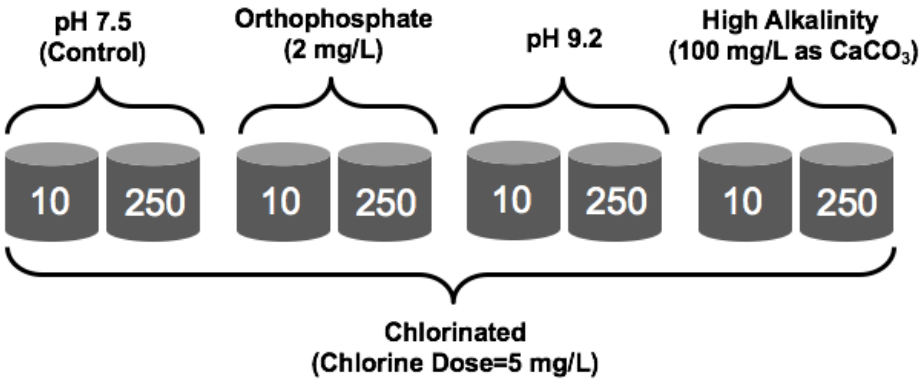

Figure 6.2 Schematic of experimental design.

The source water used in this experiment was taken from the filter effluent of Halifax

Water's J.D. Kline Water Supply Plant (prior to final disinfection, pH adjustment and corrosion inhibitor addition). Water quality parameters were measured once the water was delivered to the lab at the beginning of each week. A summary of source water quality characteristics can be found in Table 6.1.

Table 6.1 Summary of source water characteristics

Water Quality Parameter	Value
Temperature (°C)	18 ± 0.5
pH	5.5 ± 0.1
Chloride (mg/L)	9.2 ± 0.9
Sulfate (mg/L)	8.3 ± 0.3
Alkalinity (mg/L as $CaCO_3$)	5.5 ± 0.2
TOC (mg/L)	1.5 ± 0.4
Total Iron (mg/L)	<0.01

At the beginning of the experiment, the pH of the source water was adjusted to 7.5 and it was spiked with a chlorine dose of 5 mg/L. All pipes were fed with this water every day using pumps at slow rate to stabilize the pipe sections (stabilization phase). At the end of stabilization phase (60 days into the experiment), the water in pipe sections was switched to test waters, each having an alternative treatment option (treatment phase). The same water used in the stabilization phase was spiked with chloride, orthophosphate, sodium hydroxide and sodium bicarbonate to produce the test waters in treatment phase as shown in Figure 6.1. Sodium chloride (NaCl) salt was added to achieve the chloride concentration of 250 mg/L. A 0.1 M phosphoric acid (H_3PO_4) solution was used to provide the phosphate dose, and pH adjustment to the desired level was performed using a 1 N sodium hydroxide

(NaOH) solution. pH levels were maintained constant at least 15 minutes before the start of the experiment. A 50 g/L stock solution of sodium bicarbonate ($NaHCO_3$) was used to increase the alkalinity of the source water to 100 mg/L as $CaCO_3$. After sitting undisturbed for either 1, 2, or 4 days, all the water in the pipe sections was decanted and immediately replaced with fresh test water using pumps at a slow rate three times per week (every Tuesday, Wednesday and Friday). Before every water exchange (in both stabilization and treatment phases), water in each pipe section was gently stirred using a cleaned glass rod and water samples were collected to measure the total iron concentration, color and turbidity. Dissolved oxygen (DO), free chlorine concentration, pH and temperature of the water in each pipe section were also measured. Caution was exercised not to damage the corrosion scales during mixing or sampling water for analysis.

6.3.2 Water Quality Analysis

Free chlorine residuals were measured at the end of each 1, 2, or 4-day stagnation period using the DPD colorimetric method at a wavelength of 530 nm using a DR5000 UV-Visible spectrophotometer (HACH Co., Loveland, Colorado). Total iron concentrations were measured using an Inductively Coupled Plasma-Mass Spectroscopy (ICP-MS) instrument (Thermo Fisher Scientific, MA, USA). Two drops of concentrated nitric acid were added and the samples were refrigerated at 4ºC until analysis was performed. DO was measured using a DO meter (VWR, SP5OD, SympHony, Thermo Orion, USA) with a DO probe (VWR, SympHony, Thermo Orion, UK). Color and phosphate concentration were measured by a DR5000 UV-Visible spectrophotometer (HACH Co., Loveland, Colorado). Samples for DOC analysis were passed through a 0.45 µm polysulfone membrane filter

and analyzed using a TOC-V CHP analyzer (Shimadzu Corporation, Kyoto, Japan). pH and temperature of samples were measured using a pH meter (CyberScan pH 6000). A HACH 2100 AN Turbidimeter were used to measure the turbidity in water samples. Alkalinity was measured using an automatic titrator (T50-Mettler Toledo).

6.3.3 Data Analysis

Statistical comparisons were done using an analysis of variance (ANOVA) test at a significance level of 95%, using Microsoft Excel® 2016 to identify any significant differences between the average values for the water quality parameters measured before and after treatments. Error bars included in figures, and ± values throughout the manuscript represent one standard deviation.

6.4 Results and Discussion

6.4.1 Stabilization Phase

As mentioned before, at the stabilization phase all pipe sections were fed with the modified source water (pH adjusted to 7.5 and spiked with a chlorine dose of 5 mg/L), and the water was sampled and renewed every day (1-day stagnation). At the beginning of the stabilization phase, pH and alkalinity varied considerably for a period of time, but then stabilized at the end of stabilization phase (day 60). Although the pipe sections were geometrically identical and were removed from one continuous section of the distribution system, the concentration of total iron at the end of stabilization phase was not the same for all pipe sections and ranged from 1.9 mg/L to about 11.4 mg/L (p-values<0.05). However, consistent iron release was observed in each pipe after approximately 60 days,

indicating that stabilization of the pipe sections was achieved. Different stabilization time was required in this study compared to other studies conducting iron release from corroded iron pipes, which ranged in time from 3 days to four months (Sarin et al. 2003, Mi et al. 2016). This could be attributed to the differences in feed water characteristics, pipe materials and also diameter of the pipe sections, resulting in different iron surface area exposed to the water.

6.4.2 Treatment Phase

Similar to the stabilization phase, chlorine was added to all pipe sections with an initial dose of 5.1±0.2 mg/L and the concentration of free chlorine residuals were measured at the end of each stagnation time. Results showed that only after 1-day stagnation time residual chlorine was detected in the effluent of the pipe sections used in this study, and it was not detectable after 2- and 4-day stagnation period, which was expected. It has been previously established that chlorine as an oxidizing agent reacts with iron corrosion products, which results in free chlorine loss in the distribution system (Frateur et al. 1999, Hallam et al. 2002, Sarin et. al. 2004 a, b, Mutoti et al. 2007, Rand et al. 2013, Sharafimasooleh et al. 2015). Since iron release had stabilized during stabilization phase (1-day stagnation), data were categorized according to stagnation time and average iron release from 1-day stagnation was used in this section to evaluate the effect of different treatments. Data from 2- and 4-day stagnation times was used to evaluate the effect of stagnation time on iron release from pipe sections in presence of different treatments (see section 6.4.3).

It is useful to compare iron release data from pipes before and after treatment at each water quality. The percent change in iron release was calculated for each condition as follows:

$$\%\text{Change} = \frac{\text{Fe}_{\text{Treatment}} - \text{Fe}_{\text{Stabilization}}}{\text{Fe}_{\text{Stabilization}}} \times 100 \qquad (6.1)$$

Thus, positive numbers indicate an increase in iron concentration (a detrimental effect), whereas negative numbers indicate a decrease in iron (a beneficial effect). Results of percent change in total iron release are presented in figure 6.3 and are discussed in the following sections.

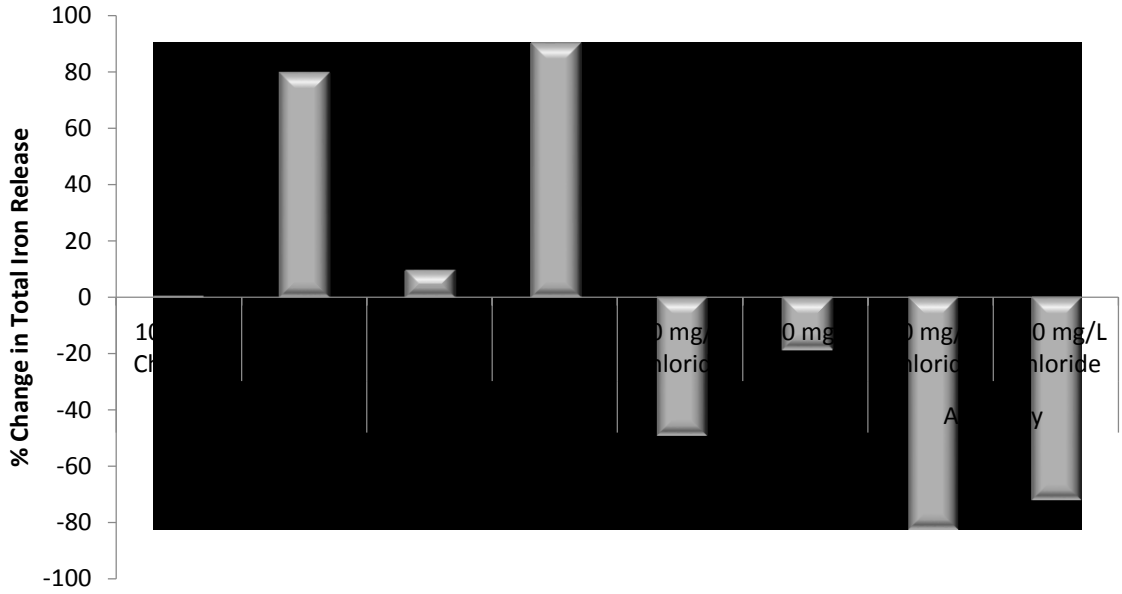

Figure 6.3 Percent change in total iron release in pipe sections in different conditions.

6.4.2.1 Effect of High Chloride Concentration

In order to evaluate the effect of chloride concentration on iron release from corroded iron pipes in the presence of chlorine disinfection, chloride concentration was increased to 250 mg/L in the feed water of one pipe section after the stabilization phase without further treatment. Another pipe section continued to receive the same water as in stabilization

phase (chloride concentration of 10 mg/L), also without corrosion treatment. These two pipe sections then served as controls for corrosion control treatments. Results in Figure 6.3 showed that the iron concentration increased only about 0.5% and did not vary significantly (p-value=0.96) in the pipe section with chloride concentration of 10 mg/L over the course of the treatment phase, indicating stabilization was successfully achieved. In contrast, the pipe section with chloride concentration of 250 mg/L significantly increased total iron release (p-value=0.01) from 4.1±1.6 mg/L during stabilization to more than 7.4±1.4 mg/L during treatment phase, and had a detrimental effect on total iron release (about 80% increase in iron).

Results also showed that changes in apparent color and turbidity corresponded directly to changes in total iron. Apparent color averaged 185±14.2 Pt-Co units at the end of stabilization phase and decreased slightly to 169±12.9 Pt-Co units in the effluent of the pipe section with chloride concentration of 10 mg/L during the treatment phase. Turbidity values averaged 20.8±1.4 NTU and decreased slightly to 18.5±2.8 NTU. Statistical analysis, however, showed that the observed reduction in apparent color and turbidity were not significant (p-values>0.05). In the 250 mg/L chloride pipe section, apparent color increased significantly from 110±15.6 Pt-Co to 196±22.0 Pt-Co (p-value=0.02) and turbidity increased significantly from 12.5±2.1 NTU to 21.7±3.3 NTU (p-value=0.02) during treatment phase when the chloride concentration was increased.

In agreement with the iron release models proposed in previous studies (Sarin et al. 2004b, Benson et al. 2012), high concentrations of chloride could diffuse and damage the dense shell-like layer of iron scale, thereby increasing the iron release. The porous interior of the corrosion scale serves as a reservoir for ferrous iron ions, which attract negative ions of

chloride from the bulk water to maintain electroneutrality and to complete the electrical circuit of the corrosion cell (Burlingame et al. 2006). Therefore, the rate of chloride diffusion to the porous interior increases with an increase in chloride concentration, resulting in an increase in acidity of the solution inside the porous interior that promotes ferrous iron production and its release. Additionally, an increase in ferrous iron in the porous interior will drive the penetration of iron from the pipe surface into the bulk water and break down the dense shell-like layer, thereby resulting in an increase in iron release. Moreover, high concentrations of chloride can enhance dissolution of the corrosion deposits on the pipe wall by promoting formation of unstable iron oxides such as lepidocrocite that in turn leads to iron release (Taylor 1984, Sarin et al. 2004b, Liu et al. 2013, Chapter 4).

6.4.2.2. Effect of Orthophosphate

As mentioned before, orthophosphate was added in the feed water of two pipe sections at the end of stabilization phase to determine whether it is effective in controlling iron release in presence of high chloride concentrations in drinking water distribution systems. As can be seen in Figure 6.3, at a chloride concentration of 10 mg/L, there was a 10% increase in iron release from 11.4±1.4 mg/L to 12.5±1.6 mg/L after addition of orthophosphate, but statistical analysis indicated this was not significant (p-value=0.29). At a chloride concentration of 250 mg/L, iron concentration increased significantly (p-value=0.02) from 3.4±0.7 mg/L to 6.4±1.3 mg/L (about 90% increase in iron).

Similar to iron results, at chloride concentration of 10 mg/L, apparent color increased from 232±17.3 Pt-Co units to 258±11.5 Pt-Co units with addition of orthophosphate to the feed

water. Turbidity increased from 37.2±6.5 NTU to 40.8±9.2 NTU. These observed differences were not significant (p-values>0.05). At a chloride concentration of 250 mg/L, apparent color increased significantly from 96.4±14.4 Pt-Co units to 175.3±22.3 Pt-Co units (p-value=0.04), as did turbidity from the average value of 12.0±2.3 NTU to 23.0±1.8 NTU (p-value=0.03).

Comparing iron release in the control pipe sections with iron release in the pipe sections that received orthophosphate treatment at chloride concentration of 10 and 250 mg/L showed that addition of orthophosphate did not apparently have beneficial effects on iron release for the conditions tested in this study, since no significant sequestration of iron was observed. This is in accordance with results of McNeill and Edwards (2000), and Zhang and Andrews (2011) indicating that addition of phosphate-based corrosion inhibitors either increased iron release or had no effect on iron corrosion and release under stagnant and low flow conditions. Higher increase in iron release in presence of high chloride concentration of 250 mg/L could be attributed to detrimental effect of chloride ions on iron release.

The results of total iron released to the water (data included for all stagnation times) as a function of phosphate residual are presented in Figure 6.4. The results showed a large variation in phosphate consumption. Phosphate can either adsorb on the corroded walls of pipe sections or precipitate as iron phosphate compounds in the corrosion scale (Sarin et al. 2003). There was no correlation between residual phosphate and the amount of iron released at either chloride concentration of 10 mg/L (R^2=0.04) or chloride concentration of

250 mg/L (R^2=0.09).

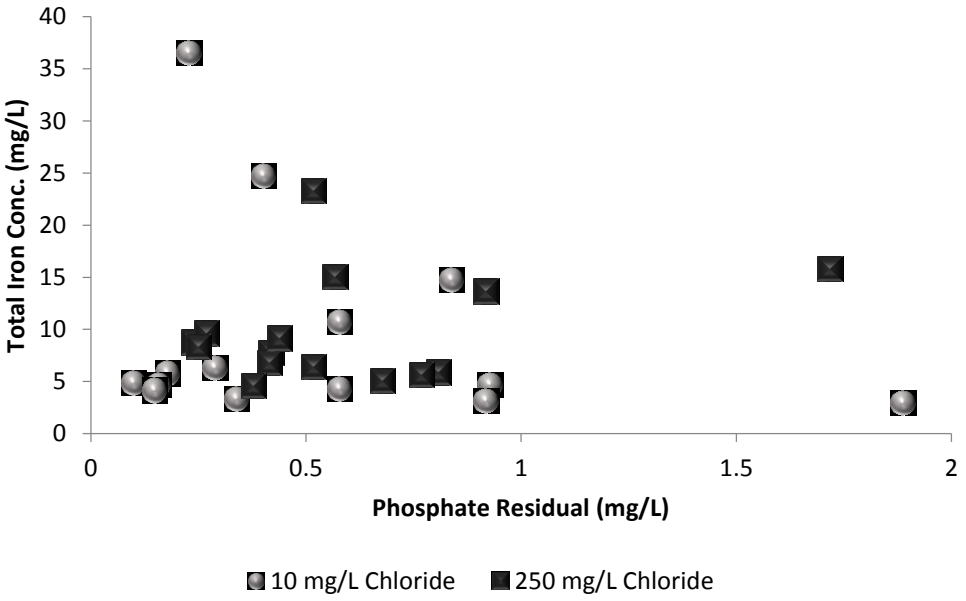

Figure 6.4 Total iron released as a function of residual phosphate.

6.4.2.3. Effect of pH

Initial pH was increased from 7.5 to 9.2 in two pipe sections with chloride concentration of 10 and 250 mg/L to explore its efficiency as a common corrosion control strategy to control iron release from corroded iron pipes in drinking water distribution systems containing high concentrations of chloride. In general, results showed that iron concentration decreased with increase in pH (Figure 6.3). In the pipe sections with chloride concentration of 10 mg/L, the average total iron concentration decreased about 50% from 4.5±0.6 mg/L to 2.3±0.3 mg/L after increasing pH to 9.2 (p-value=0.001). At chloride concentration of 250 mg/L average total iron concentration decreased about 18% from 3.3±0.4 mg/L to 2.7±0.5 mg/L after increasing pH to 9.2. The statistical analysis, however,

did not show any significant difference between iron release at stabilization and treatment phase (p-value=0.08). It should also be mentioned that pH adjustment with NaOH increased alkalinity of the test water from 5.5 ± 0.1 to about 23.2 ± 1.5 mg/L as $CaCO_3$ that could have beneficial effects on mitigating iron release from the pipe section.

At a chloride concentration of 10 mg/L, apparent color decreased significantly from 117±12.8 Pt-Co units to 65.3±12.7 Pt-Co units after increasing the pH to 9.2 (p-value=0.002). Turbidity also decreased from 15.5±4.1 NTU to 7.8±1.6 with increase in pH (p-value=0.03). At a chloride concentration of 250 mg/L, the increase in pH decreased the apparent color significantly from 85±9.2 Pt-Co units to 66.3±7.5 Pt-Co units (p-value=0.001). Turbidity also decreased significantly from 11.1±0.9 NTU to 8.5±1.1 NTU after increasing pH to 9.2 (p-value=0.01).

Sarin et al. (2003) suggested that an increase in pH decreases the solubility of ferrous solids (ferrous hydroxide and siderite) in the scale, thereby reducing the amount of iron release. It has also been proposed that more porous ferrous phases form at lower pH, whereas a higher pH results in formation of denser ferric phases, which are less likely to dissolve, and if precipitated in the scale can make the scale less porous. Formation of a denser scale structure limits the rate of migration of ions through the scales, and thereby lowers the corrosion rate and iron release rate (Sarin et al. 2003, Sarin et al. 2004b).

6.4.2.4. Effect of Alkalinity

Alkalinity was increased to 100 mg/L as $CaCO_3$ in the feed water of two pipe sections containing chloride concentrations of 10 and 250 mg/L by addition of sodium bicarbonate ($NaHCO_3$). As shown in Figure 6.3, at a chloride concentration of 10 mg/L, average iron

concentration decreased about 82% from 1.9±0.8 mg/L to 0.3±0.06 mg/L after increasing the alkalinity at the end of stabilization phase (p-value=0.005). Comparing with the control pipe section that received feed water with alkalinity of 19±0.5 mg/L as $CaCO_3$, results showed that increasing alkalinity could significantly decrease the release of iron from corroded cast iron pipe section. Raising the alkalinity to 100 mg/L produced a 70% reduction in total iron release at chloride concentration of 250 mg/L, as iron concentration decreased significantly from 3.2±0.3 mg/L to 0.9±0.2 mg/L (p-value=9.5E-6). In general, in this study, iron release decreased with increase in alkalinity in either low or high chloride concentrations. However, this effect was less profound at chloride concentration of 250 mg/L, indicating that high chloride concentrations interfered with inhibiting action of increasing alkalinity and reduced its effectiveness.

The results of apparent color and turbidity measurements showed a similar trend of lower turbidity and apparent color in presence of either low or high chloride concentrations with increase in alkalinity. Apparent color decreased significantly from 62.44±9.6 Pt-Co units to 16.5±5.5 Pt-Co units at chloride concentration of 10 mg/L (p-value=0.001). Turbidity also decreased significantly from 7.3±2.3 NTU to 1.3±0.7 NTU with increase in alkalinity to 100 mg/L as $CaCO_3$ (p-value=0.003). At a chloride concentration of 250 mg/L, with increase in alkalinity of the feed waters, apparent color and turbidity decreased significantly from 83.2±7.5 Pt-Co units to 37.0±6.3 Pt-Co units (p-value=0.04), and from 10.2±2.5 NTU to 5.2±1.5 NTU (p-value=0.02), respectively.

It is suggested that the link between alkalinity and iron release is related to the dissolution of carbonate containing iron phases such as siderite ($FeCO_3$) within the scale. Lower iron

corrosion rates and iron concentrations in distribution systems have been associated with higher alkalinity due to the formation of the less soluble siderite species (Sarin et al., 2003). Higher alkalinity in the water may also minimize pH variations due to its higher buffer capacity. Minimization of local pH variations has been shown to promote formation of a denser scale structure on the surface of the pipe, thereby decreasing the release of iron and the chance for red water events to occur (Sarin et al. 2004b, Imran et al. 2005).

6.4.3 Effect of Stagnation Time

The effect of stagnation time on iron release from corroded pipe sections at varying conditions was investigated by comparing iron concentrations at different stagnation times (1-day, 2-day and 4-day) to simulate the dead-end sections (i.e. worst-case scenario) of a distribution system. Results showed that in general, average iron concentration increased with longer stagnation time for all the treatment conditions (Figure 6.5). Average iron release was not significantly different between 1- and 2-day stagnation time in any water condition with chloride concentration of 10 mg/L (p-values>0.05). At a chloride concentration of 250 mg/L, average iron release was significantly different between 1- and 2-day stagnation time in all water conditions (p-values<0.05) with the exception of the condition with high alkalinity (p-value=0.29). A chloride concentration of 250 mg/L resulted in increased iron concentration in the bulk water with increased stagnation time. Increasing alkalinity to 100 mg/L as $CaCO_3$, mitigated more iron release and performed better than other corrosion control strategies in presence of high concentrations of chloride.

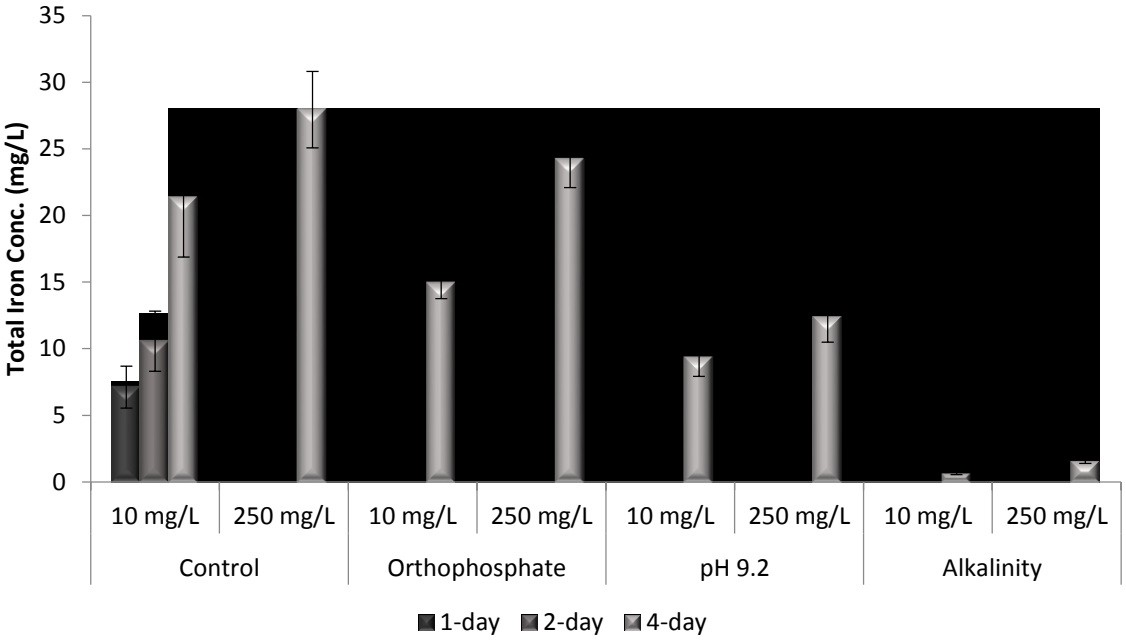

Figure 6.5 Iron release with stagnation time for all water conditions (n=6 for each stagnation time).

Average iron release was significantly higher after 4-day stagnation time compared to 1- and 2-day stagnation times in most water conditions (p-values<0.05). However, at 100 mg/L as $CaCO_3$ alkalinity, average iron concentrations were not significantly different after 4-day stagnation time (p-values>0.05) in presence of either low or high chloride concentrations. Therefore, increasing alkalinity had beneficial impacts on mitigating iron release despite an increase in stagnation time.

During the experiment, free chlorine and dissolved oxygen (DO) concentrations were measured. As mentioned before, chlorine was added to the feed water of all pipe sections with an initial concentration of 5.1±0.2 mg/L. Results showed that free chlorine residuals were not detectable with prolonged periods of stagnation. For example, in the control pipe section with chloride concentration of 10 mg/L, after 1-day stagnation time, residual chlorine was averaged 0.67±0.5 mg/L in the effluent of the pipe section and it was non-

detectable after 2- and 4-day stagnation period. The initial DO values averaged 10.3±0.2 mg/L between all pipe sections, while it decreased with stagnation time. For example, after 4-day stagnation period the final DO concentration decreased from 10.4±0.8 mg/L to 5.2±1.2 mg/L in the control pipe section with chloride concentration of 10 mg/L. Also, the ferrous iron concentration increased from 0.09±0.01 mg/L to 0.2±0.04 mg/L after 4-day stagnation period in the same pipe section. Stagnation of the water leads to decrease in amount of oxidants (e.g. oxygen and free chlorine) next to the scale, which produces conditions that favors formation of ferrous species. This provides greater opportunity for iron release via dissolution of the outer layer of the corrosion scale. In addition, the lack of a dense layer on the corrosion scale provides no barrier for the migration of ferrous species from the porous core of the scale to the bulk water, or restricting diffusion of anions from the bulk water to the core of the scale (Sarin et al. 2004b, Burlingame et al. 2006, Benson et al. 2012).

Results also showed that the increase in iron release was higher in control and orthophosphate conditions compared to pH 9.2 and high alkalinity conditions with time (Figure 6.5). For example, at a chloride concentration of 250 mg/L, average iron concentration increased by approximately 166% in the control pipe section and 127% in the pipe section with pH 9.2 from 2-day to 4-day stagnation time.

As previously mentioned, NaOH was added to increase the pH of the source water to either 7.5 or 9.2. In the control pipe section at a chloride concentration of 250 mg/L and after a 4-day stagnation time, pH decreased on average from an initial value of 7.8±0.1 to 7.04±0.2. In pH 9.2 pipe section, pH dropped from an initial value of 9.3±0.1 to 7.43±0.2. Despite pH drop, the pH of test waters with initial pH 9.2 remained significantly higher

than initial pH 7.5 water conditions. At high alkalinity conditions, pH values did not experience significant variations due to the high buffering capacity of the water. The consistently higher pH in water conditions with alkalinity addition and pH 9.2 could explain why iron release was less in high alkalinity and pH 9.2 conditions compared to control and orthophosphate conditions with time.

6.5 Conclusion

The objective of this study was to evaluate the effectiveness of common corrosion control strategies (pH adjustment, alkalinity addition and orthophosphate addition) on iron release from corroded cast iron pipes in drinking water distribution systems in presence of high chloride concentrations. Based on the results of this study, the following conclusions could be drawn.

1. Addition of 2 mg/L orthophosphate was not beneficial for controlling iron release during long stagnation conditions in presence of either low or high chloride concentrations.
2. pH adjustment to 9.2 was found to effectively control iron release. This effect was less profound at a chloride concentration of 250 mg/L.
3. Increasing alkalinity to 100 mg/L as $CaCO_3$ mitigated iron release and performed better than other corrosion control strategies in the presence of high concentrations of chloride.
4. Changes in apparent color and turbidity corresponded directly to changes in total iron resulting from water chemistry adjustments.
5. Average iron concentration increased significantly with longer stagnation time for

all of the treatment conditions at chloride concentration of 250 mg/L, except for the condition with high alkalinity.

Chapter 7 Conclusions and Recommendations

7.1 Research Summary

Chapter 3 investigated the potential impacts of elevated chloride concentrations in finished water on disinfection efficacy, microbial regrowth and metal release, using annular reactors (ARs) as the model drinking water distribution systems containing cast iron or polycarbonate pipe materials. The results showed that elevated chloride concentrations did not have a significant impact on microbial regrowth in terms of bulk or biofilm HPCs in either the polycarbonate or cast iron ARs. Higher chlorine dosages were required to achieve target free chlorine residuals in ARs received higher concentrations of chloride in the cast iron systems. However, in polycarbonate systems, similar doses of chlorine were required to achieve the target free chlorine residual in both ARs operated at chloride concentration of 10 and 75 mg/L. Metal release results showed that chloride concentration of 75 mg/L resulted in spikes in total iron concentration after chlorine disinfection was initiated. Results showed that total iron concentrations decreased back to the initial levels after a few days. Further investigation into the metal release in the presence of higher chloride concentration of 250 mg/L showed that there was higher iron release in the effluent of the ARs that persisted through disinfection trial. It was hypothesized that in the presence of high concentrations of chloride, porous and less corrosion-protective surface phases were formed on the surface of cast iron coupons, which resulted in higher chlorine demand and were not able to inhibit further iron release.

To test this hypothesis, an 8-week bench-scale fill and dump experiment (**Chapter 4**) was designed. Results showed that elevated concentrations of chloride in conjunction with

chlorine disinfection increased the corrosion rate and also the iron release from cast iron coupons, which was in accordance with the results of AR studies (Chapter 3). Analysis of the corrosion products formed on the surface of cast iron coupons confirmed that these effects were due to the enhanced formation of crystalline phases such as lepidocrocite in presence of elevated concentrations of chloride in conjunction with chlorine disinfection. Lepidocrocite has been previously reported to be characteristic of loose and porous corrosion scale (Liu et al. 2013, Gerke et al. 2008), which was also confirmed by surface analysis of the coupons. Lepidocrocite also can be reduced easily and serve as a source of ferrous iron that can be released into the bulk water, which in turn increases the chlorine demand and iron release. Another interesting result was that increase in chloride concentration enhanced formation and release of larger iron particles from the surface of cast iron coupons. Analysis of the biofilms formed on the surface of cast iron coupons showed that biofilm microbial populations decreased with chlorination and increasing chloride concentrations and were unlikely to contribute to the observed corrosion under conditions tested in this study.

The next step (**Chapter 5**) was to investigate the effectiveness of different corrosion control strategies (orthophosphate addition and pH adjustment) on iron corrosion and release from corroding iron surfaces in the presence of elevated chloride concentrations in chlorinated systems. Results of this 8-week bench-scale fill and dump experiment showed that both approaches were able to reduce chlorine demand, corrosion rate and also iron release from cast iron coupons. Analysis of the composition and morphology of the corrosion scales formed on the surface of cast iron coupons showed that intensity of

magnetite peaks increased over goethite and lepidocrocite peaks in the presence of corrosion control strategies. Magnetite has been previously reported to be thermodynamically stable and less likely to dissolve. Moreover, iron corrosion scales with a high percentage of magnetite have usually shown dense and good corrosion protective properties, which was also confirmed by surface analysis of the coupons. However, the observed differences were less pronounced in presence of elevated concentrations of chloride, in which more peaks of lepidocrocite with higher intensity appeared. This was in accordance with the results of Chapter 4, which revealed that chloride promotes formation of lepidocrocite phases. It can be concluded that increase in chloride concentrations interfered with inhibiting action of the corrosion control strategies used in this experiment and reduced their effectiveness. The results also showed that orthophosphate addition and pH adjustment decreased particle size of released iron particles from the surface of cast iron coupons. However, larger iron particles were formed with increase in chloride concentration in all treatments, which was in agreement with the results of Chapter 4. The results of the investigation on how the biofilm population responded to these two corrosion control strategies in the presence of variable chloride concentrations in chlorinated systems showed that although the biofilm population was increased by adding orthophosphate and decreased by pH adjustment to 9.2, the overall population remained low due to chlorine disinfection and increased chloride concentrations (in agreement with Chapter 4); therefore the biofilm was unlikely to contribute to the observed cast iron corrosion under conditions tested in this study.

Results of a 4-month bench-scale fill and dump experiment (**Chapter 6**) to investigate the effectiveness of common corrosion control strategies on iron release from old corroded cast iron pipe sections harvested from a local distribution system receiving water with high chloride concentrations showed that the effectiveness of corrosion control methods investigated was diminished in presence of high concentrations of chloride. Addition of orthophosphate did not show any beneficial effects on iron release for the conditions tested in this study, which was in contrast with its beneficial effects observed in Chapter 5. A potential explanation is that iron release was considered as the product of the iron matrix with virgin cast iron coupons used in Chapter 5, in which formation of a protective oxide layer on the surface of the coupons with orthophosphate addition provided a barrier between the bulk water and the iron surface and thereby decreased the corrosion rate and iron release. However, corrosion scales on the surface of old corroded pipe sections were considered as the source of iron release, which could be destroyed under stagnant conditions in Chapter 6 and increased the iron release. pH adjustment to 9.2 was beneficial in controlling iron release, although to a lesser extent at high chloride concentrations. With orthophosphate addition and pH adjustment not being beneficial in controlling iron release in presence of high chloride concentrations, alkalinity addition was also tested in this experiment in addition to conditions tested in chapter 5. Results showed that increasing the alkalinity of the test water had the largest impact on reducing average iron release and was considered as the preferred corrosion control strategy in presence of high chloride concentrations and lengthy stagnation times (extremities of distribution system).

7.2 Conclusions

The main purpose of this research work was to determine the effect of elevated chloride concentrations on cast iron corrosion and water quality in drinking water distribution systems, which was investigated through the completion of the following specific research objectives:

1. To determine if elevated concentrations of chloride in finished water have negative effects on disinfection efficacy and microbial regrowth in drinking water distribution systems. With respect to this objective, this research showed that:
    - Elevated chloride concentrations in treated water did not have a significant effect on disinfection efficacy of chlorine in controlling bulk and biofilm HPC bacteria.
    - Elevated chloride concentrations did not have a significant impact on microbial regrowth in terms of bulk or biofilm HPCs.
    - Higher chlorine dosages were required to achieve target free chlorine residuals in presence of higher concentrations of chloride in the cast iron systems.

2. To examine the effect of variable chloride concentrations on iron corrosion and its release from corroding iron surfaces in chlorinated systems, and to investigate the structures and morphologies of resulting iron corrosion products. The results showed that:

- Elevated concentrations of chloride in conjunction with chlorine disinfection increased the corrosion rate and also the iron release from cast iron surfaces.
- Formation of porous and less corrosion-protective phases such as lepidocrocite was enhanced in presence of elevated concentrations of chloride in conjunction with chlorine disinfection.
- Increase in chloride concentration enhanced formation and release of larger iron particles from the surface of cast iron coupons in chlorinated systems.

3. To evaluate the influence of common corrosion control strategies (orthophosphate addition and pH adjustment to 9.2) on iron corrosion and release from corroding cast iron surfaces in the presence of high chloride concentrations in chlorinated systems, and to investigate the structures and morphologies of resulting iron corrosion products. With respect to this objective, this research showed that:
    - Although both approaches were able to reduce chlorine demand, corrosion rate and also iron release from cast iron coupons, increase in chloride concentration interfered with their inhibiting action and reduced their effectiveness.
    - Orthophosphate addition and pH adjustment made the zeta potential of the released iron particles more negative and decreased their particle size. However, the average particle size of the settleable iron particles increased with increase in chloride concentration.

4. To test whether common corrosion control strategies can counteract the possible corrosive effect of high chloride concentrations on iron release from corroded cast iron pipes in drinking water distribution systems. The results showed that:
    - Addition of orthophosphate was not beneficial for controlling iron release from corroded cast iron pipes in presence of either low or high chloride concentrations during long stagnation conditions tested in this study.
    - pH adjustment to 9.2 effectively controlled iron release, however, to a lesser extent at high chloride concentration.
    - Increasing alkalinity to 100 mg/L as $CaCO_3$ mitigated iron release and performed better than other corrosion control strategies in the presence of high concentrations of chloride.

5. To examine the size and characteristics of bacterial biofilm communities formed on the cast iron surfaces to determine if the microbes contributed to the corrosion of cast iron under the conditions tested in this research. Results showed that:
    - Although the biofilm population was increased by adding orthophosphate and decreased by pH adjustment to 9.2, the overall population of bacterial biofilm decreased and remained low due to chlorine disinfection and increased chloride concentrations and were unlikely to contribute to the observed cast iron corrosion in this study.

7.3 Recommendations for Future Research

Based on the findings of this research, there are several recommendations for future research works.

- The experiments conducted in this project were all at bench-scale. It is recommended that pilot-scale experiments, such as pipe-loop configuration, be conducted to confirm the bench-scale findings. Further studies are needed to be investigated at flow conditions to better mimic the flow-through conditions in distribution systems. This would also allow for exploration of the role of different mixing or intermittency regimes on the corrosion of cast iron pipes and resulting corrosion by-products in distribution systems receiving the test waters used in the current study.
- The findings of this study showed that higher concentration of chloride in presence of cast iron led to high chlorine demands. Addition of high chlorine dosage leads to a further increase in the formation of disinfection by-products (DBPs), which are harmful to human health. Thus, future research works should be designed to evaluate the effects of high chloride concentrations on the DBP formation potential.
- Since pH adjustment and orthophosphate addition as common corrosion control strategies were not significantly beneficial in mitigating iron release from cast iron in the presence of high chloride concentrations, more research is required on use of alternative corrosion inhibitors such as blend of different phosphate inhibitors. Experiments should also be designed to elucidate the potential synergistic effect of different corrosion control strategies in waters with high concentrations of chloride.

- Alkalinity addition was shown to be beneficial in reducing iron release from corroded cast iron pipe sections by producing a dense protective layer on the corrosion scale. Bench-scale experiments could be designed with virgin cast iron coupons to understand the mechanism of impact of alkalinity addition on the properties of the iron corrosion products and iron suspensions in presence of high chloride concentration.
- The results of this study are limited to the cast iron pipe materials. However, different pipe materials such as lead and copper are in use in distribution systems and premise plumbing. Increase in chloride concentration could increase corrosion of lead and copper by increasing chloride to sulfate mass ratio (CSMR). Thus, further research into effect of high chloride concentrations in water in contact with these pipe materials is recommended.
- Further studies should be undertaken to observe how conditions tested in this research affects biofilm population and community structure at the full scale under real drinking water operating conditions.

References

Abdolahi, A., Hamzah, E., Ibrahim, Z., & Hashim, S. (2015). "Localised corrosion of mild steel in presence of Pseudomonas aeruginosa biofilm." Corrosion Engineering, Science and Technology, 50(7), 538-546.

Al-Jasser, A. O. (2007). "Chlorine decay in drinking-water transmission and distribution systems: Pipe service age effect." Water Research, 41(2), 387-396.

Allen, M. J., Edberg, S. C., and Reasoner, D. J. (2004). "Heterotrophic plate count bacteria – what is their significance in drinking water?" International Journal of Food Microbiology, 92 (3), 265–274.

Alshehri, A. A., Duranceau, S. J., Taylor, J. S., & Stone, E. D. (2009). "Investigating iron release in distribution systems with blend variations of source waters and phosphate inhibitors." Desalination and Water Treatment, 8(1-3), 211-220.

American Public Health Association (APHA), American Water Works Association & Water Environment Federation. (2012). Standard methods for the examination of water and wastewater, 22nd Edition.

Anderson, L., and Walsh M.E. (2012). "Evaluation of temperature impacts on drinking water treatment efficacy of magnetic ion exchange and enhanced coagulation." Journal of Water Supply: Research & Technology – AQUA, 61(7), 403-412.

Appenzeller, B. M. R., Batté, M., Mathieu, L., Block, J. C., Lahoussine, V., Cavard, J., & Gatel, D. (2001). "Effect of adding phosphate to drinking water on bacterial growth in slightly and highly corroded pipes." Water Research, 35(4), 1100-1105.

Appenzeller, B. M., Duval, Y. B., Thomas, F., & Block, J. C. (2002). "Influence of phosphate on bacterial adhesion onto iron oxyhydroxide in drinking water." Environmental Science & Technology, 36(4), 646-652.

AWWA, (1999). Water Quality and Treatment. Fifth edition McGraw- Hill, New York.

Benson, A. S., Dietrich, A. M., & Gallagher, D. L. (2012). "Evaluation of iron release models for water distribution systems." Critical Reviews in Environmental Science and Technology, 42(1), 44-97.

Bolto, B., Dixon, D., Eldridge, R., King, S., and Linge, K. (2002). "Removal of natural organic matter by ion exchange." Water Research, 36(20), 5057-5065.

Boyer, T. H., and Singer, P. C. (2007). "Stoichiometry of removal of natural organic matter by ion exchange." Environmental Science & Technology, 42(2), 608-613.

Burlingame, G. A., Lytle, D. A., & Snoeyink, V. L. (2006). "Why Red Water? Understanding Iron Release in Distribution Systems." Opflow, 32(12), 12-16.

Bursill, D. (2001). "Drinking water treatment-understanding the processes and meeting the challenges." Water Science and Technology-Water Supply-, 1(1), 1-8.

Camper, A. K. (1995). "Factors influencing biofilm growth in drinking water distribution systems." (Doctoral dissertation, Montana State University--Bozeman).

Camper, A. K. (1996). "Factors limiting microbial growth in the distribution system laboratory and pilot-scale experiments." AWWAR.

Camper, A. K., Brastrup, K., Sandvig, A., Clement, J., Spencer, C., and Capuzzi, A. J. (2003). "Effect of distribution system materials on bacterial regrowth." Journal of American Water Works Association, 95(7), 107-121.

Caporaso, J. G., Bittinger, K., Bushman, F. D., DeSantis, T. Z., Andersen, G. L., & Knight, R. (2010a). "PyNAST: a flexible tool for aligning sequences to a template alignment." Bioinformatics, 26(2), 266-267.

Caporaso, J. G., Kuczynski, J., Stombaugh, J., Bittinger, K., Bushman, F. D., Costello, E. K., ... & Huttley, G. A. (2010b). "QIIME allows analysis of high-throughput community sequencing data." Nature methods, 7(5), 335-336.

Cantwell, R. (2005). "Impact of chlorine dioxide on transmission, treatment, and distribution system performance." American Water Works Association.

Chowdhury, S. (2012). "Heterotrophic bacteria in drinking water distribution system: a review." Environmental Monitoring and Assessment, 184(10), 6087-6137.

Chun, C. L., Hozalski, R. M., & Arnold, W. A. (2005). "Degradation of drinking water disinfection byproducts by synthetic goethite and magnetite." Environmental Science & Technology, 39(21), 8525-8532.

Claesson, M. J., O'Sullivan, O., Wang, Q., Nikkilä, J., Marchesi, J. R., Smidt, H., ... & O'Toole, P. W. (2009). "Comparative analysis of pyrosequencing and a phylogenetic microarray for exploring microbial community structures in the human distal intestine." PloS one, 4(8), e6669.

Comeau, A. M., Li, W. K., Tremblay, J. É., Carmack, E. C., & Lovejoy, C. (2011). "Arctic Ocean microbial community structure before and after the 2007 record sea ice minimum." PLoS One, 6(11), e27492.

Cornell, R. M., & Schwertmann, U. (2003). "The iron oxides: structure, properties, reactions, occurrences and uses." John Wiley & Sons.

Crittenden, J. C., Trussell, R. R., Hand, D. W., Howe, K. J., & Tchobanoglous, G. (2012). "MWH's water treatment: principles and design." John Wiley & Sons.

Deshommes, E., Laroche, L., Nour, S., Cartier, C., & Prévost, M. (2010). "Source and occurrence of particulate lead in tap water." Water Research, 44(12), 3734-3744.

Droste, R. L. (1997). "Theory and practice of water and wastewater treatment." John Wiley & Sons Incorporated.

Dykstra, T. S., O'Leary, K. C., Chauret, C., Andrews, R. C., and Gagnon, G. A. (2007). "Impact of UV disinfection on biological stability in distribution systems." Journal of Environmental Engineering & Science, 6:147-155.

Ebrahimi Mehr, M., Shahrabi, T., & Hosseini, M. G. (2004). "Determination of suitable corrosion inhibitor formulation for a potable water supply." Anti-Corrosion Methods and Materials, 51(6), 399-405.

Echeverría, F., Castaño, J. G., Arroyave, C., Peñuela, G., Ramírez, A., & Morató, J. (2009). "Characterization of deposits formed in a water distribution system/caracterizacion de depositos formados en un sistema de distribucion de agua potable." Ingeniare: Revista Chilena de Ingenieria, 17(2), 275.

Edgar, R. C. (2013). "UPARSE: highly accurate OTU sequences from microbial amplicon reads." Nature methods, 10(10), 996-998.

Eisnor, J. D., & Gagnon, G. A. (2004). "Impact of secondary disinfection on corrosion in a model water distribution system." Journal of Water Supply: Research and Technology-AQUA, 53(7), 441-452.

Essink, G. H. O. (2001). "Salt water intrusion in a three-dimensional groundwater system in the Netherlands: a numerical study." Transport in porous media, 43(1), 137-158.

Frateur, I., Deslouis, C., Kiene, L., Levi, Y., and Tribollet, B. (1999). "Free chlorine consumption induced by cast iron corrosion in drinking water distribution systems." Water Research, 33(8), 1781-1790.

Gagnon, G. A., O'Leary, K. C., Volk, C. J., Chauret, C., Stover, L., and Andrews, R. C. (2004). "Comparative analysis of chlorine dioxide, free chlorine and chloramines on bacterial water quality in model distribution systems." Journal of Environmental Engineering, 130(11), 1269-1279.

Gagnon, G. A., Rand, J. L., O'leary, K. C., Rygel, A. C., Chauret, C., and Andrews, R. C. (2005). "Disinfectant efficacy of chlorite and chlorine dioxide in drinking water biofilms." Water Research, 39(9), 1809-1817.

Gedge, G. (1993). “Corrosion of cast Iron in potable water service.” The Institute of Materials, Corrosion and Related Aspects of Materials for Potable Water Supplies(UK), 1993, 18-28.

Gerke, T. L., Maynard, J. B., Schock, M. R., & Lytle, D. L. (2008). “Physiochemical characterization of five iron tubercles from a single drinking water distribution system: Possible new insights on their formation and growth.” Corrosion Science, 50(7), 2030-2039.

Gouider, M., Bouzid, J., Sayadi, S., & Montiel, A. (2009). “Impact of orthophosphate addition on biofilm development in drinking water distribution systems.” Journal of Hazardous Materials, 167(1), 1198-1202.

Greenlee, L. F., Lawler, D. F., Freeman, B. D., Marrot, B., & Moulin, P. (2009). “Reverse osmosis desalination: water sources, technology, and today's challenges.” Water Research, 43(9), 2317-2348.

Hallam, N. B., West, J. R., Forster, C. F., Powell, J. C., and Spencer, I. (2002). “The decay of chlorine associated with the pipe wall in water distribution systems.” Water Research, 36(14), 3479-3488.

Health Canada, (2014) “Guidelines for Canadian drinking water quality summary table.”

Heijman, S. G. J., Van Paassen, A. M., Van der Meer, W. G. J., and Hopman, R. (1999). “Adsorptive removal of natural organic matter during drinking water treatment.” Water Science and Technology, 40(9), 183-190.

Husband, P. S., & Boxall, J. B. (2011). “Asset deterioration and discolouration in water distribution systems.” Water Research, 45(1), 113-124.

Hwang, B. F., Magnus, P., and Jaakkola, J. J. (2002). “Risk of specific birth defects in relation to chlorination and the amount of natural organic matter in the water supply.” American Journal of Epidemiology, 156(4), 374-382.

Imran, S. A., Dietz, J. D., Mutoti, G., Taylor, J. S., Randall, A. A., & Cooper, C. D. (2005). “Red water release in drinking water distribution systems.” Journal of American Water Works Association, 97(9), 93-100.

InfraGuide (2001). “Developing a water distribution system renewal plan.” Ottawa, Ontario, Canada.

Ishii, S. K., & Boyer, T. H. (2011). “Evaluating the secondary effects of magnetic ion exchange: focus on corrosion potential in the distribution system.” Desalination, 274(1), 31-38.

Jang, H. J., Choi, Y. J., Ro, H. M., & Ka, J. O. (2012). "Effects of phosphate addition on biofilm bacterial communities and water quality in annular reactors equipped with stainless steel and ductile cast iron pipes." The Journal of Microbiology, 50(1), 17-28.

Lasheen, M. R., Sharaby, C. M., El-Kholy, N. G., Elsherif, I. Y., & El-Wakeel, S. T. (2008). "Factors influencing lead and iron release from some Egyptian drinking water pipes." Journal of Hazardous Materials, 160(2), 675-680.

LeChevallier, M. W., Cawthon, C. D., and Lee, R. G. (1988). "Inactivation of biofilm bacteria." Applied and Environmental Microbiology, 54(10), 2492-2499.

Le Puil, M., Chang, Y. C., & Randall, A. A. BIOSTABILITY OF MEMBRANE-TREATED FINISHED WATERS IN DISTRIBUTION SYSTEM: STUDY AT PILOT-SCALE.

Li, X., Wang, H., Hu, X., Hu, C., & Liao, L. (2016). "Characteristics of corrosion sales and biofilm in aged pipe distribution systems with switching water source." Engineering Failure Analysis, 60, 166-175.

Little, B., Lee, J., & Ray, R. (2007). "A review of 'green'strategies to prevent or mitigate microbiologically influenced corrosion." Biofouling, 23(2), 87-97.

Liu, H., Schonberger, K. D., Peng, C. Y., Ferguson, J. F., Desormeaux, E., Meyerhofer, P., ... & Korshin, G. V. (2013). "Effects of blending of desalinated and conventionally treated surface water on iron corrosion and its release from corroding surfaces and pre-existing scales.' Water Research, 47(11), 3817-3826.

Liu, R., Yu, Z., Zhang, H., Yang, M., Shi, B., & Liu, X. (2012). "Diversity of bacteria and mycobacteria in biofilms of two urban drinking water distribution systems." Canadian Journal of Microbiology, 58(3), 261-270.

Lytle, D. A., & Snoeyink, V. L. (2002). "Effect of ortho-and polyphosphates on the properties of iron particles and suspensions." Journal of American Water Works Association, 94(10), 87-99.

Lytle, D. A., Magnuson, M. L., & Snoeyink, V. L. (2004). "Effect of oxidants on the properties of Fe (III) particles and suspensions formed from the oxidation of Fe (II)." Journal of American Water Works Association, 96(8), 112-124.

Lytle, D. A., Sarin, P., & Snoeyink, V. L. (2005). "The effect of chloride and orthophosphate on the release of iron from a cast iron pipe section." Journal of Water Supply: Research and Technology-AQUA, 54(5), 267-281.

Lytle, D. A., Sorg, T. J., Muhlen, C., & Wang, L. (2010). "Particulate arsenic release in a drinking water distribution system." Journal of American Water Works Association, 102(3), 87.

Maddison, L. A., Gagnon, G. A., & Eisnor, J. D. (2001). "Corrosion control strategies for the Halifax regional distribution system." Canadian Journal of Civil Engineering, 28(2), 305-313.

McNeill, L. S., & Edwards, M. (2000). "Phosphate inhibitors and red water in stagnant iron pipes." Journal of Environmental Engineering, 126(12), 1096-1102.

McNeill, L. S., & Edwards, M. (2001). "Iron pipe corrosion in distribution systems." Journal of American Water Works Association, 93(7), 88-100.

Meckes, M. C., Haught, R. C., Dosani, M., Clark, R. M., & Sivaganesan, M. (1999). "Effect of pH adjustments on biofilm in a simulated water distribution system." In Proceedings of the American Water Works Association Water Quality Technology Conference (Vol. 31). American Water Works Association.

Mi, Z., Zhang, X., & Chen, C. (2016). "Iron release in drinking water distribution systems by feeding desalinated seawater: characteristics and control." Desalination and Water Treatment, 57(21), 9728-9735.

Miettinen, I. T., Vartiainen, T., & Martikainen, P. J. (1997). "Phosphorus and bacterial growth in drinking water." Applied and Environmental Microbiology, 63(8), 3242-3245.

Murphy, H. M., Payne, S. J., and Gagnon, G. A. (2008). "Sequential UV-and chlorine-based disinfection to mitigate Escherichia coli in drinking water biofilms." Water Research, 42(8), 2083-2092.

Mutoti, G., Dietz, J. D., Arevalo, J., and Taylor, J. S. (2007). "Combined chlorine dissipation: Pipe material, water quality, and hydraulic effects." Journal of American Water Works Association, 99(10), 96.

Niquette, P., Servais, P., and Savoir, R. (2000). "Impacts of pipe materials on densities of fixed bacterial biomass in a drinking water distribution system." Water Research, 34(6), 1952-1956.

Novotny, E. V., Murphy, D., and Stefan, H. G. (2008). "Increase of urban lake salinity by road deicing salt." Science of the Total Environment, 406(1), 131-144.

Ollos, P. J., Huck, P. M., and Slawson, R. M. (2003). "Factors affecting biofilm accumulation in model distribution systems." Journal of American Water Works Association, 95(1), 87-97.

Pavlov, D., Wet, C. M., Grabow, W. O., and Ehlers, M. M. (2004). "Potentially pathogenic features of heterotrophic plate count bacteria isolated from treated and untreated drinking water." International Journal of Food Microbiology, 92 (3), 275–287.

Peng, C. Y., & Korshin, G. V. (2011). "Speciation of trace inorganic contaminants in corrosion scales and deposits formed in drinking water distribution systems." Water Research, 45(17), 5553-5563.

Price, M. N., Dehal, P. S., & Arkin, A. P. (2010). "FastTree 2–approximately maximum-likelihood trees for large alignments." PloS one, 5(3), e9490.

Rahman, M. S., & Gagnon, G. A. (2014). "Bench-scale evaluation of drinking water treatment parameters on iron particles and water quality." Water Research, 48, 137-147.

Rand, J. L., Hofmann, R., Alam, M. Z. B., Chauret, C., Cantwell, R., Andrews, R. C., and Gagnon, G. A. (2007). "A field study evaluation for mitigating biofouling with chlorine dioxide or chlorine integrated with UV disinfection." Water Research, 41(9), 1939-1948.

Rand, J. L., Sharafimasooleh, M., and Walsh, M. E. (2013). "Effect of water hardness and pipe material on enhanced disinfection with UV light and chlorine." Journal of Water Supply: Research & Technology-AQUA, 62(7).

Reuter, C. (2000). Saline solutions: the quest for fresh water. Environmental Health Perspectives 108 (2), A78-A80.

Sarin, P., Snoeyink, V. L., Bebee, J., Kriven, W. M., & Clement, J. A. (2001). "Physico-chemical characteristics of corrosion scales in old iron pipes." Water Research, 35(12), 2961-2969.

Sarin, P., Clement, J. A., Snoeyink, V. L., & Kriven, W. M. (2003). "Iron release from corroded, unlined cast-iron pipe." Journal of American Water Works Association, 95(11), 85-96.

Sarin, P., Snoeyink, V. L., Bebee, J., Jim, K. K., Beckett, M. A., Kriven, W. M., & Clement, J. A. (2004a). "Iron release from corroded iron pipes in drinking water distribution systems: effect of dissolved oxygen." Water Research, 38(5), 1259-1269.

Sarin, P., Snoeyink, V. L., Lytle, D. A., & Kriven, W. M. (2004b). "Iron corrosion scales: model for scale growth, iron release, and colored water formation." Journal of Environmental Engineering, 130(4), 364-373.

Sartory, P. D. (2004). "Heterotrophic plate count monitoring of treated drinking water in the UK: a useful operational tool." International Journal of Food Microbiology, 92, 297–306.

Sathasivan, A., Ohgaki, S., Yamamoto, K., & Kamiko, N. (1997). "Role of inorganic phosphorus in controlling regrowth in water distribution system." Water Science and Technology, 35(8), 37-44.

Sharafimasooleh, M., Rand, J. L., & Walsh, M. E. (2015). "Effect of High Chloride Concentrations on Microbial Regrowth in Drinking Water Distribution Systems." Journal of Environmental Engineering, 142(2), 04015061.

Sharp, R. R., Camper, A. K., Crippen, J. J., Schneider, O. D., and Leggiero, S. (2001). "Evaluation of drinking water biostability using biofilm methods." Journal of Environmental Engineering, 127(5), 403-410.

Shi, B., & Taylor, J. S. (2007). "Potential impact of enhanced coagulation on corrosion by-product release in a distribution system." Desalination, 208(1), 260-268.

Simões, L. C., Simoes, M., & Vieira, M. J. (2010). "Influence of the diversity of bacterial isolates from drinking water on resistance of biofilms to disinfection." Applied and Environmental Microbiology, 76(19), 6673-6679.

Singley, J. E. (1994). "Electrochemical nature of lead contamination." Journal of American Water Works Association, 86(7).

Spechler, R. M. (1994). "Saltwater intrusion and quality of water in the Floridan aquifer system, northeastern Florida." US Geological Survey.

Standard, A. S. T. M. (2004). "Standard practice for laboratory immersion corrosion testing of metals." American Society for Testing and Materials G31-72.

Sun, H., Shi, B., Bai, Y., & Wang, D. (2014). "Bacterial community of biofilms developed under different water supply conditions in a distribution system." Science of the Total Environment, 472, 99-107.

Suzuki, M. T., Taylor, L. T., & DeLong, E. F. (2000). "Quantitative analysis of small-subunit rRNA genes in mixed microbial populations via 5′-nuclease assays." Applied and Environmental Microbiology, 66(11), 4605-4614.

Szewzyk, U., Szewzyk, R., Manz, W., & Schleifer, K. H. (2000). "Microbiological safety of drinking water." Annual Reviews in Microbiology, 54(1), 81-127.

Taylor, R. M. (1984). "Influence of chloride on the formation of iron oxides from Fe (II) chloride. II. Effect of [Cl] on the formation of lepidocrocite and its crystallinity." Clays and Clay Minerals, 32(3), 175-180.

Teng, F., Guan, Y. T., & Zhu, W. P. (2008). "Effect of biofilm on cast iron pipe corrosion in drinking water distribution system: corrosion scales characterization and microbial community structure investigation." Corrosion Science, 50(10), 2816-2823.

Thunqvist, E. L. (2004). "Regional increase of mean chloride concentration in water due to the application of deicing salt." Science of the Total Environment, 325(1), 29-37.

Trueman, B. F., & Gagnon, G. A. (2016). "A new analytical approach to understanding nanoscale lead-iron interactions in drinking water distribution systems." Journal of Hazardous Materials, 311, 151-157.

USEPA (US Environmental Protection Agency). (1989). 40 CFR Parts 141 and 142. Drinking water; National primary drinking water regulations; Filtration, disinfection; turbidity, Giardia lamblia, viruses, Legionella, and heterotrophic bacteria; Final Rule. Federal Register, 54(124), 27486– 27541.

USEPA (US Environmental Protection Agency). (2008). Drinking water contaminants. Washington, DC: U.S. Environmental Protection Agency. Retrieved from http://www.epa.gov/safewater/contaminants/index.html

USEPA (US Environmental Protection Agency). (2010). Source water protection practices bulletin. Managing highway deicing to prevent contamination of drinking water. http://www.epa.gov/safewater/sourcewater/pubs/fs_swpp_deicinghighway.pdf.

Van der Kooij, D. (2003). "Biodegradable Compounds and Biofilm Formation in Water Treatment and Distribution." Sapporo: Hokkaido University Press.

Wang, Q., Garrity, G. M., Tiedje, J. M., & Cole, J. R. (2007). "Naive Bayesian classifier for rapid assignment of rRNA sequences into the new bacterial taxonomy." Applied and Environmental Microbiology, 73(16), 5261-5267.

Wang, H., Hu, C., Hu, X., Yang, M., & Qu, J. (2012). "Effects of disinfectant and biofilm on the corrosion of cast iron pipes in a reclaimed water distribution system." Water Research, 46(4), 1070-1078.

Wang, H., Hu, C., & Li, X. (2015). "Characterization of biofilm bacterial communities and cast iron corrosion in bench-scale reactors with chloraminated drinking water." Engineering Failure Analysis, 57, 423-433.

Water, G. E., (2009). Process Technologies. Handbook of Industrial Water Treatment.

WHO (World Health Organization). (2011). Guidelines for drinking-water quality (4th ed.). Geneva, Switzerland: WHO.

Willison, H., & Boyer, T. H. (2012). "Secondary effects of anion exchange on chloride, sulfate, and lead release: Systems approach to corrosion control." Water Research, 46(7), 2385-2394.

Zhang, Y., and Edwards, M. (2007). "Anticipating effects of water quality changes on iron corrosion and red water." Journal of Water Supply: Research & Technology— AQUA, 56(1), 55–68.

Zhang, Z., Stout, J. E., Victor, L. Y., & Vidic, R. (2008). “Effect of pipe corrosion scales on chlorine dioxide consumption in drinking water distribution systems.” Water Research, 42(1), 129-136.

Zhang, H., & Andrews, S. A. (2011). “Effects of phosphate-based corrosion inhibitors on the kinetics of chlorine degradation and haloacetic acid formation in contact with three metal materials.” Canadian Journal of Civil Engineering, 39(1), 44-54.

Zhang, X., Mi, Z., Wang, Y., Liu, S., Niu, Z., Lu, P., ... & Chen, C. (2014). “A red water occurrence in drinking water distribution systems caused by changes in water source in Beijing, China: mechanism analysis and control measures.” Frontiers of Environmental Science & Engineering, 8(3), 417-426.

Zhu, Y., Wang, H., Li, X., Hu, C., Yang, M., & Qu, J. (2014). “Characterization of biofilm and corrosion of cast iron pipes in drinking water distribution system with UV/Cl_2 disinfection.” Water Research, 60, 174-181.

Appendix A: XRD patterns of iron corrosion products on surface of coupons exposed to different treatments at chloride concentration of 10 and 250 mg/L

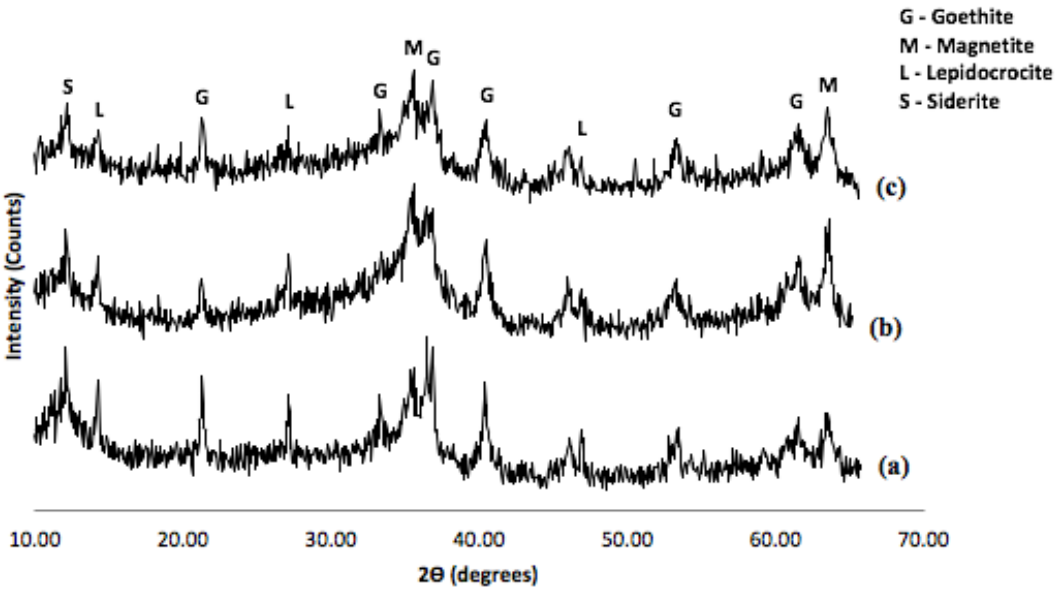

XRD patterns of iron corrosion products on surface of coupons exposed to (a) control, (b) orthophosphate and (c) pH 9.2 systems at chloride concentration of 10 mg/L.

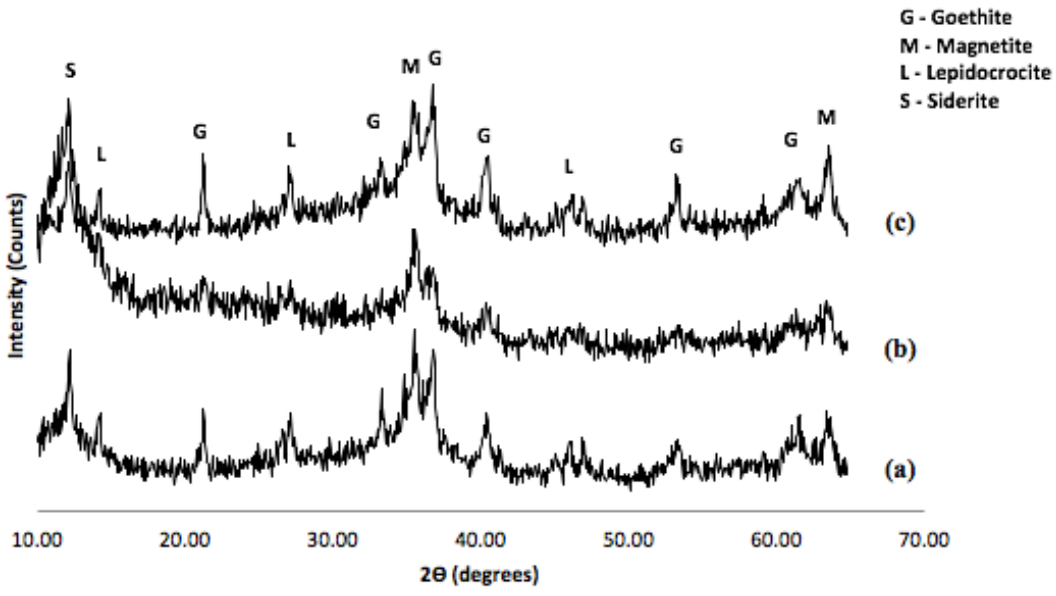

XRD patterns of iron corrosion products on surface of coupons exposed to (a) control, (b) orthophosphate and (c) pH 9.2 systems at chloride concentration of 250 mg/L.

Appendix B: Copyright Permissions

Chapter 3 (Journal of Environmental Engineering, ASCE)

Copyright Clearance Center RightsLink®

Home | Create Account | Help | Live Chat

ASCE AMERICAN SOCIETY OF CIVIL ENGINEERS

Title: Effect of High Chloride Concentrations on Microbial Regrowth in Drinking Water Distribution Systems

Author: Masoumeh Sharafimasooleh, Jennie L. Rand, Margaret E. Walsh

Publication: Journal of Environmental Engineering

Publisher: American Society of Civil Engineers

Date: 02/01/2016

Copyright © 2016, ASCE. All rights reserved.

LOGIN

If you're a copyright.com user, you can login to RightsLink using your copyright.com credentials. Already **a RightsLink user** or want to learn more?

Permissions Request

As an author of an ASCE journal article, you are permitted to reuse the accepted manuscript version of your article for your thesis or dissertation.

BACK | CLOSE WINDOW

Copyright © 2016 Copyright Clearance Center, Inc. All Rights Reserved. Privacy statement. Terms and Conditions.
Comments? We would like to hear from you. E-mail us at customercare@copyright.com